S P E C T R O S C O P I C S T U D I E S O F

M O L E C U L A R C O N F O R M A T I O N S

by

David A.C. Compton, C.Chem., MRIC

A thesis submitted during April, 1977 in part fulfilment of the requirements for a C.N.A.A. Ph.D. degree, describing work carried out jointly at :-

Kingston Polytechnic

and

The Polytechnic of Wales.

I N D E X

Acknowledgements

I would like to thank my Academic Supervisor, Dr. W.O. George, for his constant guidance and encouragement throughout this work. Also my gratitude is expressed to my Industrial Supervisor, Mr. W.F. Maddams for his helpful discussions and kindness.

My appreciation goes to all those in both polytechnics who gave help, including technicians and computer staff. I wish to thank especially Victor Mansell and Norman Morris for their help constructing the matrix isolation system, Dr. A. O'Keefe for his lucid discussions on thermodynamics and my wife Louise for typing this thesis.

My thanks are expressed to both Kingston Borough and Mid Glamorgan County Councils for providing assistantships, to Kingston Polytechnic and the Polytechnic of Wales for providing the facilities, and to B.P. Trading for additional funding for the work.

Abstract

The vibrational spectra of a series of diesters of fumaric and maleic acids and also of substituted butadienes have been investigated over a range of temperatures and phases. The effects on infrared and Raman spectra of altering the temperature and phase of these compounds (using matrix isolation techniques in some cases) have been interpreted in terms of conformational equilibria; table (1) summarises the results.

Low frequency vibrations have been assigned as torsions associated with either $C-CH_3$ or =C-C= bonds. The frequency of each torsion leads to a value for V_3 or V*, functions relating to the barrier height opposing internal rotation, shown in table (2).

In a number of cases sharp bands in the infrared spectra of gaseous substituted butadienes were associated with a series of side bands. In order to assign bands of this nature in chloroprene the isoelectronic compound acryloyl chloride was studied. A comparative analysis indicated that these bands are hot bands due to perturbation of fundamental vibrations by torsional modes. From the intensities of these bands torsional frequencies have been estimated in some cases.

Vibrational assignments are proposed in all cases. From these assignments values for the gas phase thermodynamic functions are calculated for the substituted butadienes over a range of temperatures, using statistical mechanics. Thermodynamic functions are also presented for the following additional compounds over a range of temperatures:- crotonaldehyde, acrolein, acryloyl fluoride, glyoxal and oxalyl chloride.

These results enable a better understanding of vibrational spectra and provide quantitative data which characterises conformational equilibria in these compounds in terms of thermodynamic equilibria.

Compound	ΔH^{θ} (KJ mol^{-1})	Low Energy Conformer	High Energy Conformer	Evidence for Equilibrium.
Dimethyl Fumarate	3.24 ± 0.77	trans, trans	trans, cis	Raman
Diethyl Fumarate	0.92 ± 0.12	trans, trans	trans, cis	Raman
Dibutyl Fumarate	1.66 ± 0.18	trans, trans	trans, cis	Raman
Dimethyl Maleate	-	cis, trans	-	-
Diethyl Maleate	-	cis, trans	-	-
Dibutyl Maleate	-	cis, trans	-	-
Butadiene	10.4	s-trans	s-cis	Thermodynamic
Isoprene	4.59 ± 0.16	s-trans	s-cis *	Raman
Cis-Pentadiene	-	s-trans	-	-
Trans-Pentadiene	-	s-trans	-	-
Chloroprene	8.8	s-trans	s-cis *	Thermodynamic
Acryloyl Chloride	2.51 +	s-trans	s-cis *	Infrared

Table (1)

* Assumed structure by comparison with other molecules.

\+ Value calculated by J.E. Katon and W.R. Feairheller, shown for comparison.

	V*	V_3
Butadiene	100.6	-
s-trans isoprene	143.2	11.33
s-cis ~~butadiene~~ isoprene		10.80
cis-pentadiene	133.4	10.38
trans-pentadiene	119.5	12.25
chloroprene	124.8	-

Table (2) ($kJ\ mol^{-1}$)

CHAPTER I

Introduction.

A. Introduction.

B. Compounds Studied.

C. Calculation of the Thermodynamic Differences Between Conformers by Variable Temperature Vibrational Spectroscopy.

D. The Interaction Between Vibrational and Rotational Energy.

E. Effect of the Population of Torsional Energy Levels on Vibrational Frequencies.

CHAPTER I

Introduction.

A. Introduction.

The purpose of this work is to investigate the possible conformational equilibria present in a range of conjugated compounds. The compounds studied include α,β - unsaturated carbonyl compounds and conjugated hydrocarbons. Various experimental techniques are used to study the structure and conformational behaviour of these compounds; including vibrational spectroscopy of samples at different temperatures over a range of pure phases or isolated in a low temperature inert matrix. Theoretical techniques used also include thermodynamics, calculation of the barriers to internal rotation between conformers and analysis of high resolution spectra of gaseous samples.

Before discussing the conformational analysis of the compounds studied, a brief review of the general subject is given in order to set the present work in context.

If two different three dimensional spatial arrangements of the atoms in a molecule are interconvertible merely by rotation about single bonds, they are called conformations or conformers. These conformers are rapidly interconvertible in the fluid phases and so are inseparable. In the early part of this century it was believed that rotation about a single bond was unhindered, which would result in an infinite number of equally possible conformers. However, in 1936 it was shown that calculations of the entropy and enthalpy of ethane by statistical mechanics were inconsistent with calorimetric

values. These differences were interpreted by postulating a barrier to rotation of about 13 KJ mol^{-1} As one methyl group rotates past the other the potential energy of the molecule reaches a maximum in an eclipsed conformation and falls to a minimum in a staggered conformation, these structures are depicted as (a) and (b) in diagram (1.1)

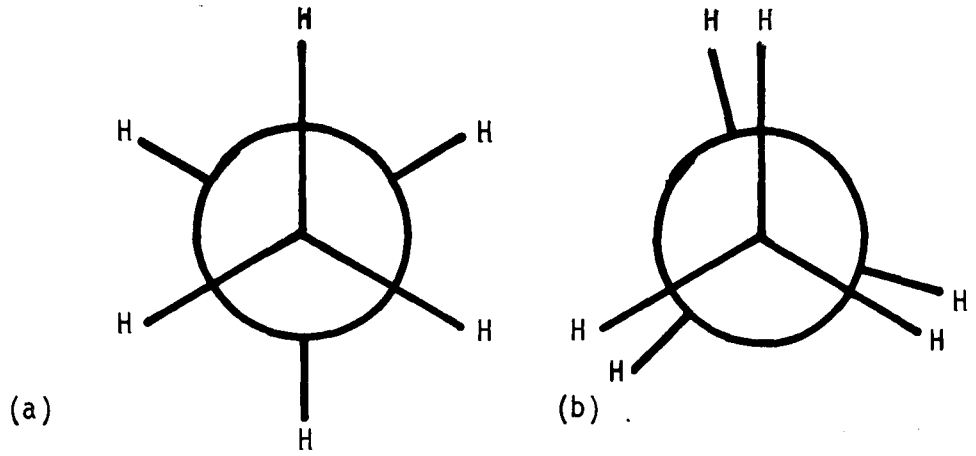

Diagram (1.1)
The staggered, (a), and eclipsed (b) conformers of ethane

The barrier hindering rotation about the C-C single bond in ethane is due to the difference in potential energy between the staggered and eclipsed forms. The variation in potential energy as the angle of torsion (dihedral angle) alters can be represented as a cosine function, as in diagram (1.2). In the case of ethane this results in a three-fold symmetric barrier, V_3 giving three equivalent minima.

At ordinary temperatures there is enough energy present for the molecule to be rapidly interconverting between conformers, although it spends most of its time at or near an energy minimum, in a prefered conformation.

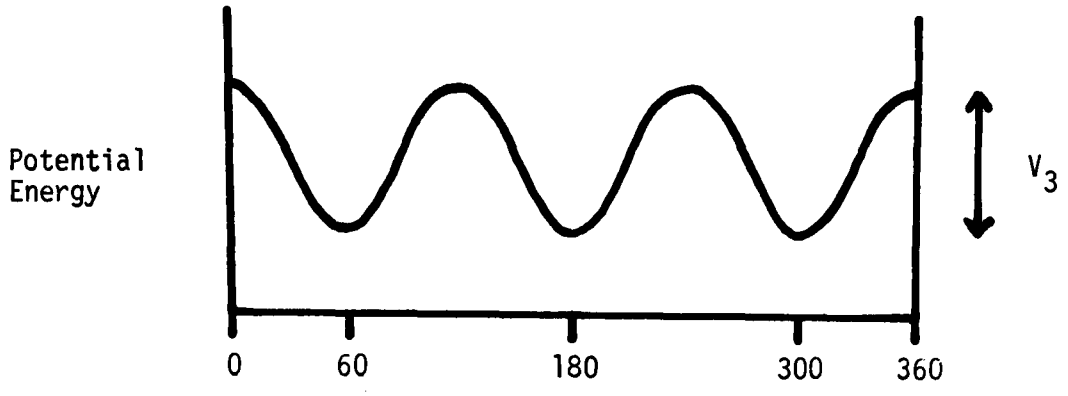

Diagram (1.2).
Variation of Potential Energy of Ethane During Internal Rotation

The potential energy function is not so simple for a system with lower symmetry. n-Butane, for example shows two different types of minimum and maximum, due to repulsion between the methyl group on one carbon and either the methyl group or hydrogens on the neighbouring carbon. The potential functions and various conformers of n-butane are depicted in diagram (1.3). An asymmetric function alters the free energy of each conformer and this results in an uneven population of the preferred conformations. The free energy change, ΔG^{θ}, on going from one conformer to another is given by (1.1),

$$\Delta G^{\theta} = - RT \ln K \qquad \ldots\ldots (1.1)$$

and so the population of different conformers depends on the temperature of the system. In general raising the temperature gives more molecules in a conformer of higher energy and lowering the temperature gives less. In the solid state normally only one conformer is present, which means that variable temperature vibrational spectroscopy is a useful method for studying conformational changes due to an asymmetric function.

Saturated Esters

In a saturated ester R^1COOR^2 there are two types of internal

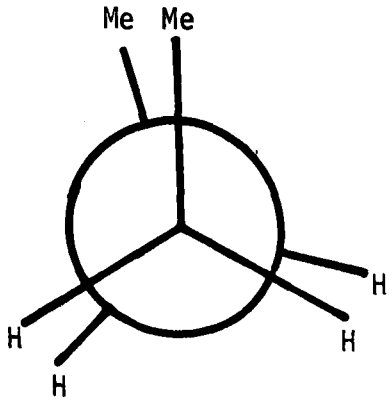

(a) Eclipsed (Me, Me)

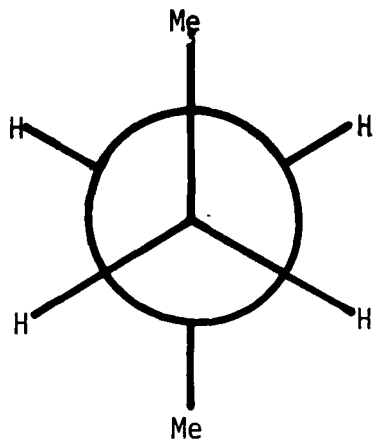

(b) Staggered (trans)

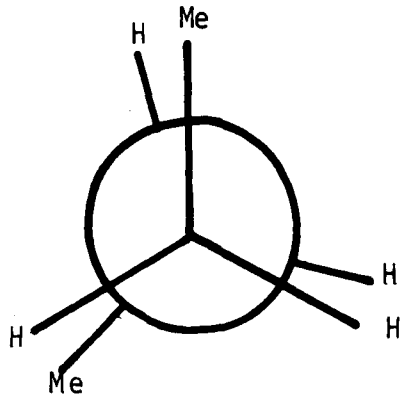

(c) Eclipsed (Me, H)

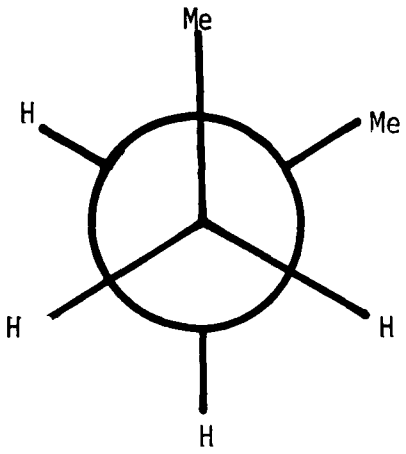

(d) Staggered (gauche)

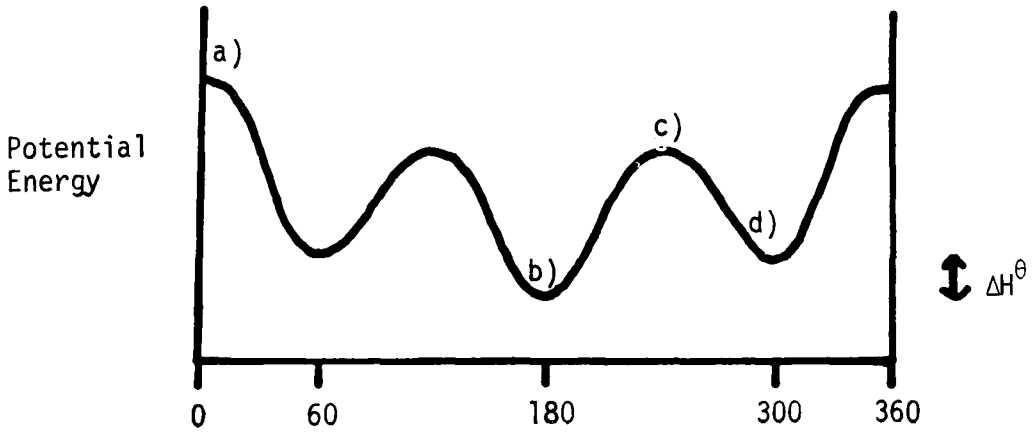

Diagram (1.3)
Variation of Potential Energy of n-Butane with Angle of Torsion

rotation available; these are internal rotation of the R groups and rotation about the CO-OR bond.

The possible rotation of the alkyl groups follows the same function as ethane when R = Me, and the same type as n-butane for longer R groups. Riveros and Wilson[2] gave the angle of rotation of the gauche conformer (b) relative to the s-trans conformer (a) in ethyl formate as 90^0, in diagram (1.4), using microwave spectroscopy. In chains longer than

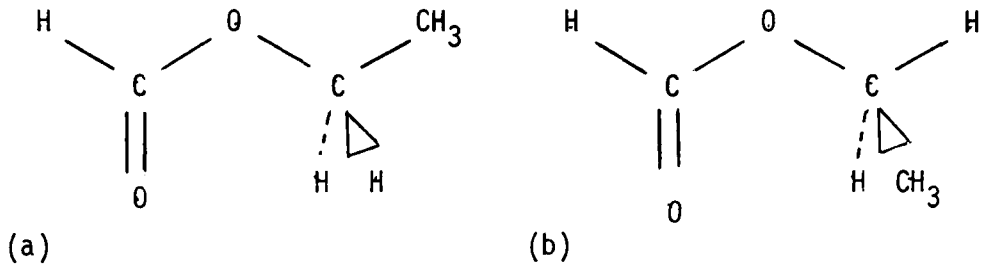

Diagram (1.4)
The s-trans (a) and gauche (b) conformers of ethyl formate[2].

methyl, internal rotation of the alkyl C-C bonds can occur but the analysis of the resulting spectra becomes very difficult. Evidence for internal rotation of the R^1 group of propionate and butyrate esters exists in the i.r. spectra of a series of these esters[3]. The extra enthalpy of the high energy gauche conformer, ΔH^θ, was found to be 364 ± 80 Jmol^{-1} for methyl propionate and 385 ± 113 Jmol^{-1} for n-butyrate. In subsequent work[4], evidence for existence of a high energy gauche conformer in the R^2 group of a series of esters was found using i.r. spectroscopy, and ΔH^θ calculated for ethyl acetate as 1320 ± 105 Jmol^{-1}.

The other rotation found in saturated esters is about the CO-OR bond. Normally the hybridisation of the ester oxygen is assumed to

be sp^3, but if this changes to sp^2 the non-hybrid p orbital can conjugate with the ester group if the molecule is planar.

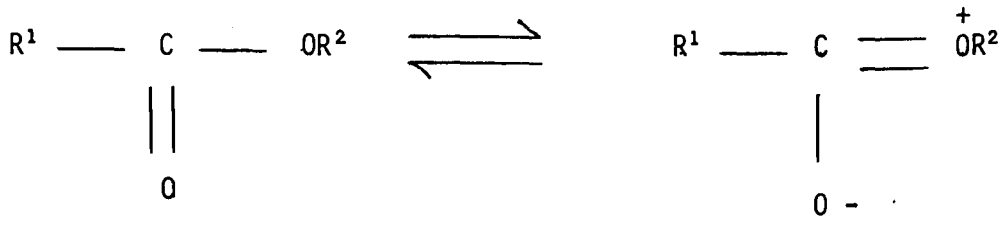

Possible rotation about the R^1CO-OR^2 bond is constricted by this conjugation to two possible conformers denoted s-trans (a) and s-cis (b). In the simplest ester, methyl formate microwave[5], i.r.[3,6-8] and ultrasonics[9] studies have all shown that the most stable conformer

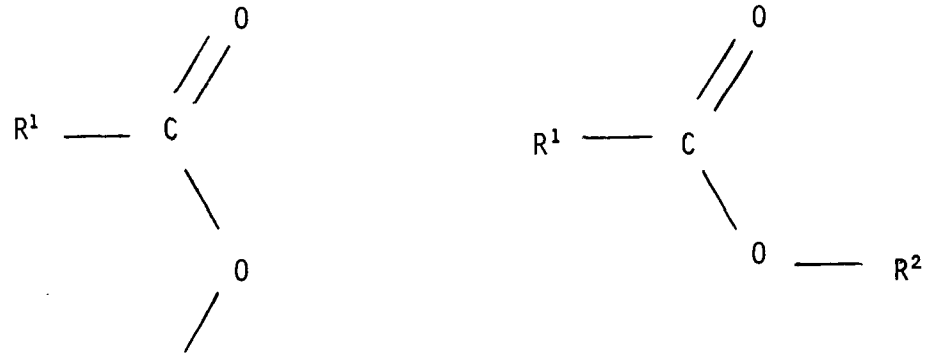

(a) s-trans (b) s-cis

Diagram (1.5)
The s-trans (a) and s-cis (b) conformers of saturated esters.

is s-cis.

The only evidence for the high energy s-trans conformer of methyl formate is the ultrasonic study[9], and a value of ΔH^{θ} given as 1670 J mol^{-1}. This result disagrees with an ab initio calculation[10] which gives ΔH^{θ} as 33 ± 13 KJ mol^{-1} and therefore explains why the s-trans conformer is not normally observed. Similarly studies on methyl acetate[5,7,11], vinyl formate[12] and other acetates and formate esters[7,13] indicate that these compounds exist exclusively or predominantly in the s-cis conformer. The presence of the s-trans form is only likely to be

appreciable, however, if the s-cis conformer is destabilised by bulky R^2 groups[8] such as t-butyl, 1,1-dimethyl propyl and triphenyl methyl, which interact sterically with the carbonyl group.

Conjugated Compounds

If an unsaturated compound has double bonds separated by a single bond then the compound is said to be conjugated. According to molecular orbital theory there are the same number of π molecular orbitals as individual non-hybrid p orbitals, and each atom (such as carbon, oxygen or nitrogen) contributes one p orbital as each atom is sp^2 hybridised. There are 4 molecular π orbitals in butadiene which must lie in a plane for minimum energy. The consequence of this argument is that butadiene has two possible planar stable conformers only, designated s-trans (a) and s-cis (b) by Mulliken[14], with the s-trans conformer the most stable. However it is possible that the high energy conformer may be about 30^0 skewed off s-cis (gauche) due to steric

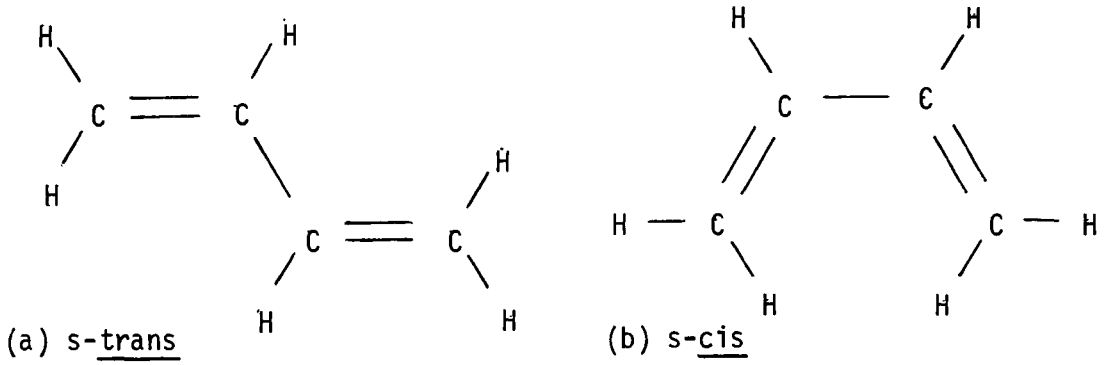

(a) s-trans (b) s-cis

Diagram (1.6)
The s-trans (a) and s-cis (b) conformers of Butadiene.

interactions between hydrogens close together only in the planar s-cis structure. Such skewing would still enable the normal conjugation to occur but minimise the steric interaction.

The predominance of the s-trans conformer of butadiene is well proven, notably by microwave[15,16], vibrational spectroscopy[17-21]

electron diffraction[22], chemical[23,24], thermodynamic[25] and theoretical[26,27] techniques. Evidence for the presence of a high energy conformer has been given in several works[23-25,28,29] but the structure of the high energy conformer (s-cis or gauche) could not be given. Evidence that an s-cis form is present has been put forward[21,26,30] but so has evidence that the structure is gauche[27,31,32].

Conjugated compounds isoelectronic to butadiene, acrolein and glyoxal have both been shown to exist predominantly in the s-trans conformer with a high energy s-cis conformer. E.A. Cherniak and C.C. Costain examined the microwave spectra of acrolein and ten isotopically substituted species[33] and assigned the structure as s-trans, but found no evidence of any high energy conformer. Electron diffraction[22], i.r.[18,34] dipole moment[35], and ultrasonic[36] studies all uphold this result, finding no evidence of the high energy conformer. L.A. Carreira examined the low frequency Raman spectrum of acrolein and assigned bands to torsional overtones of the s-cis conformer, and obtained the potential function associated with internal rotation.

Durig et.al. assigned the high energy conformer of glyoxal as s-cis using microwave spectroscopy[37], and also observed the s-cis torsion. High resolution visible spectroscopy[38] gave the same result using rotational spacing. The predominant conformer was assigned as s-trans by i.r. [18,39] and electron diffraction studies[22]

Substitutional butadienes which have been shown to exist predominantly in the s-trans conformation are isoprene[16,40,41], cis and trans - pentadienes[42], fluoroprene[43,44] chloroprene[45] 2,3-dichlorobutadiene[45], bromoprene[46] iodoprene[46] 2,3-dimethyl butadiene[16] other 2-alkyl butadienes[23] and 1,1-difluoro butadiene[47].

Evidence for the presence of a high energy conformer has been put forward only for isoprene[48,49], chloroprene[45], 2,3-dichlorobutadiene[50] and 2-alkyl butadienes[23], but no distinction can be made between an s-cis or gauche structure of the high energy form.

Various substituted butadienes have been shown to exist predominantly in the s-cis (or gauche) low energy formdue to steric hindrance between groups at the 2 and 4 positions of butadiene or other effects. These include hexafluorobutadiene[51], hexachlorobutadiene[45], 2-t-butylbutadiene[52], 2,3-di-t-butylbutadiene[53], 2,4-dimethylbutadiene[54], 2-chloro-4-methylbutadiene[54], 1,1,3-trichloro and 1,1,3-tribromobutadienes[46]. In general, again no distinction can be made between a low energy s-cis or gauche conformer, although hexafluorobutadiene has been shown[51] to be some 40^0 skewed of s-cis.

The compounds 1,1-dibromo-3-fluorobutadiene and 1,1-dichloro-3-fluorobutadiene[55] have been shown to exist predominantly in the s-trans conformer below room temperature and mainly in the gauche conformer above.

Substituted acrolein compounds (α,β - unsaturated carbonyl compounds) which have been shown to exist predominantly in the s-trans conformer are crotonaldehyde[34,56], acryloyl fluoride[57,58], acryloyl chloride[59-61], methyl vinyl ketone[34,62], ethylidene acetone[34,62], crotonoyl chloride[60] and methacryloyl chloride[60]. Of these compounds, evidence for a high energy conformer of crotonaldehyde[63], acryloyl chloride[61], methyl vinyl ketone[34], ethylidene acetone[34] and crotonoyl chloride[60] has been put forward, but the only compound for which structural information (microwave [54]) indicating the high energy conformer to be s-cis is acryloyl fluoride[57].

Acrylic acid has been shown to exist predominantly in the s-cis conformer[64], with the hydroxyl group cis to the carbonyl group. Methacryloyl chloride[60] exists only in the s-trans form.

Substituted glyoxal compounds known to exist in the s-trans conformer are oxalyl chloride[65] and oxalyl bromide[66]. Electron diffraction studies on both compounds indicate that the high energy conformers of both conformers are gauche.

Generally in the case of the substituted butadienes, numbered as in Diagram (1.7) bulky substituent groups in positions 3 and 4

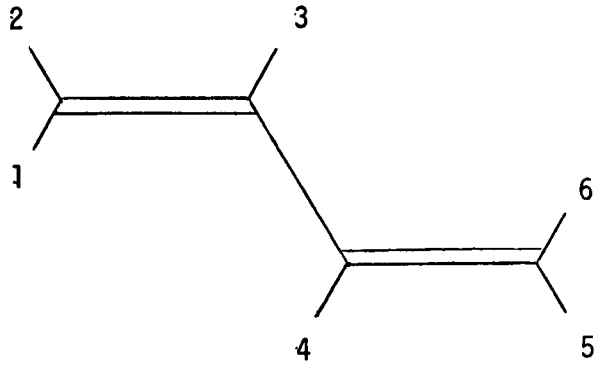

Diagram (1.7)
Numbering of Substituted Butadienes

destabilise the normally predominant s-trans conformer by steric interaction and often give significant or even major amounts of s-cis conformer, whereas bulky groups in positions 1 or 6 sterically interact with each other in the s-cis conformer and destabilise the conformer. A combination of these effects often leads to stabilisation of the gauche form, as in the hexafluorobutadiene, where the s-trans conformer is destabilised by fluorine-fluorine interaction, and so is the s-cis conformer.

The same principles apply to substituted acrolein and glyoxal compounds, if the change from a CH_2 group to an oxygen is taken into account.

B. Compounds Studied.

The following compounds were studied by experimental techniques; the normal common names given are used throughout this thesis, but the IUPAC names are given in brackets for reference here.

Methyl, ethyl and n-butyl esters of fumaric (trans - butenedioic) acid;

methyl,ethyl and n-butyl esters of maleic (cis - butenedioic) acid;

butadiene (buta-1,3-diene), isoprene (2-methylbuta-1,3-diene), cis and trans-pentadienes (penta-1,3-dienes);

chloroprene (2-chlorobuta-1,3-diene);

acryloyl chloride (propenoyl chloride).

The gas phase thermodynamic functions of the following compounds were also calculated over a range of temperatures by statistical mechanics;

crotonaldehyde (trans-but-2-enal), acrolein (propenal), glyoxal (ethanedial), acryloyl (propenoyl) fluoride,oxaloyl (ethanedioyl) chloride and bromide;

butadiene, isoprene, cis- and trans-pentadiene, chloroprene and acryloyl chloride.

α,β - Unsaturated Esters.

In these compounds (substituted acroleins) there exists the conformational activity due to conjugated portion of the molecule, as in acrolein, and that due to the ester group itself.

The predominant conformers of the conjugated portion of methyl - and ethyl - esters of crotonic and acrylic acids were all assigned[77] as s-trans, all compounds gave evidence of a high energy s-cis conformers.

I.r. studies on diesters of fumaric acid have indicated[68] that the predominant conformer of each ester is s-trans, s-trans and a high energy form denoted s-trans, s-cis due to rotation of one ester group exists, whereas the diesters of maleic acid show no conformational activity, for steric reasons, existing only in the s-trans, s-cis conformer. The results of the fumarate diesters agree with a study of fumaroyl chloride[60], however, no evidence for internal rotation in fumarate and maleate monoesters[70] has been found, these compounds show significant intermolecular hydrogen bonding which may restrict rotation. Conformational activity internal to the ester group, COOR is due to s-cis $\rightleftharpoons$ s-trans isomersion of the CO-OR bond as in Diagram (1.5), and s-trans $\rightleftharpoons$ gauche isomersion of the COO-R bond, as in Diagram (1.4). Due to the complexity of the compounds involved any internal rotation present is masked by the more observable isomersion of the conjugated chain, It has therefore been assumed[3] that in line with unsaturated esters, these compounds normally exist s-cis about the CO-OR bond.

C. Calculation of the Thermodynamic Differences Between Conformers by Variable Temperature Vibrational Spectroscopy

In a system where high energy conformer B is in equilibrium with a low energy conformer A,

$$A \rightleftharpoons B$$

it is useful to be able to calculate ΔH^{θ} and ΔS^{θ} for the equilibrium. The value of ΔS^{θ} obtained is especially useful as it can be used to assign structures to A and B.

These calculations can be performed if the fundamental vibrational frequencies differ sufficiently to resolve in the spectrum to give a pair of discrete bands, and if the concentration of B is sufficiently high to allow accurate intensity measurement. The pair of bands due to the two conformers can be recorded over a range of temperatures and the i.r. absorbance or Raman intensity of each band calculated at each temperature.

For i.r. absorption, the Beer Lambert Law (1.2) holds,

$$A = \varepsilon c \ell \qquad \text{.....(1.2)}$$

where the absorbance of a sample length ℓ and concentration c is given using the molar extinction coefficient ε.

At any temperature, T, the equilibrium constant, K, can be expressed as equation (1.3), and related to thermodynamic parameters using the Van't Hoff equation (1.4)

$$K = \frac{C_B}{C_A} = \frac{A_B\ \varepsilon_A}{A_A\ \varepsilon_B} \qquad \text{.....(1.3)}$$

$$-RT\ell nK = \Delta H^{\theta} - T\Delta S^{\theta} \qquad \text{.....(1.4)}$$

$$\therefore\ \ell n\frac{A_B}{A_A} = \frac{\Delta H^{\theta}}{RT} + \frac{\Delta S^{\theta}}{R} - \ell n\frac{\varepsilon_A}{\varepsilon_B} \qquad \text{.....(1.5)}$$

Equation (1.5) can only be used if the ratio of extinction coefficients, ΔH^{θ} and ΔS^{θ} do not change over the range of temperatures used. This is normally assumed to be true and then a plot of $\ell n(A_B/A_A)$ against $1/T$ gives a slope of $-\Delta H^{\theta}/R$. However, ΔS^{θ} cannot be calculated from the intercept unless $\ell n(\varepsilon_A/\varepsilon_B)$ can be calculated.

A method for calculation of $\ell n(\varepsilon_A/\varepsilon_B)$ was given by Mizushima[71]. A pair of bands due to conformers is related to a band common to both conformers, but this method is complicated. A simpler method was proposed by Hartman et.al.[55]. In this method the total concentration c_T is calculated in equation (1.6).

$$c_A + c_B = c_T \qquad \text{.....(1.6)}$$

Substituting for c_A and c_B using equation (1.2) leads to equation (1.7).

$$\frac{A_A}{\varepsilon_A \ell} + \frac{A_B}{\varepsilon_B \ell} = c_T \qquad \text{.....(1.7)}$$

$$\therefore \quad A_A = -\frac{\varepsilon_A}{\varepsilon_B} A_B + \varepsilon_A c_T \qquad \text{.....(1.8)}$$

The absorbances are measured over a range of temperatures and if a plot of A_A against A_B gives a straight line of negative slope then the ratio $\varepsilon_A/\varepsilon_B$ is shown to be constant and can be evaluated. Using this value for $\varepsilon_A/\varepsilon_B$ in equation (1.5), ΔS^{θ} can be calculated.

For Raman spectra the relationship between a band intensity I and concentration is less simple. Because an emission spectrum is being collected and amplified it is not easy to calculate concentration, and it is easiest to use the relationship (1.9).

$$I = ExC \qquad \text{.....(1.9)}$$

Where E is an coefficient relating intensity and concentration and x accounts for the amplification of the signal. When two conformer bands are recorded together in the same scan at constant

temperature then x is the same for both bands and so equation (1.5) can be rewritten.

$$\ell n \frac{I_B}{I_A} = - \frac{\Delta H^\theta}{RT} + \frac{\Delta S^\theta}{R} - \ell n \frac{\varepsilon_A}{\varepsilon_B} \qquad .....(1.10)$$

However, when equation (1.8) is rewritten the unknown factor x appears,

$$I_A = - \frac{\varepsilon_A}{\varepsilon_B} . I_B + I_A x c_T \qquad .....(1.11)$$

and so a plot of I_A against I_B cannot be drawn, and ΔS^θ cannot be evaluated in this way. However, it is possible to calculate the equilibrium constant K, equation (1.3), using statistical mechanics (see chapter VIII) then ΔS^θ can be evaluated using equation (1.4)

The methods described above for calculating ΔH^θ and ΔS^θ do not lend themselves to simple calculation of the overall experimental error limits. Because of this, values of ΔH^θ are quoted with a standard deviation of the slope of the graph, and errors are not stated for ΔS^θ due to the long extrapolation involved to obtain the intercept.

D. The Interaction Between Vibrational and Rotational Energy

The Born-Oppenheimer separation indicates that a good approximation to the total energy of a molecule can be made by summing electronic, translational, rotational and vibrational energy. I.r. and Raman spectroscopy can observe rotational and vibrational energy levels only, or a combination of the two called Rotation-Vibration.

A diatomic molecule of reduced mass μ and atoms r apart is rotating in a plane with angular velocity ϕ about its centre of mass. This rotation has angular momentum P_ϕ and Kinetic energy T_ϕ, and the

moment of inertia of the molecule, I, is given by[72,73]

$$I = \mu r^2 \qquad \text{.....(1.12)}$$

$$T_\phi = \mu r^2 \phi^2/2$$

$$= I\phi^2/2 \qquad \text{.....(1.13)}$$

$$P_\phi = I\phi \qquad \text{.....(1.14)}$$

For a molecule rotating freely in space the kinetic energy is the same as the rotational energy E_r. Substituting for I into equation (1.13) gives:-

$$E_r = P_\phi^2/2I \qquad \text{.....(1.15)}$$

The momentum P_ϕ is quantised at the molecular level, and is given by equation (1.16), where m = 0,1,2,....

$$P_\phi = \pm mh \qquad \text{.....(1.16)}$$

The molecule can rotate in 3 dimensions and so the angular momentum must be resolved into its 3 components. For a general polyatomic molecule there are three Principal Moments of Inertia (see chapter VII for discussion) labelled according to convention $I_A < I_B < I_C$. The angular momentum P (and hence kinetic energy) are resolved around these three axes.

$$P = P_A + P_B + P_C \qquad \text{.....(1.17)}$$

$$\therefore \quad E_r = \frac{P_A^2}{2I_A} + \frac{P_B^2}{2I_B} + \frac{P_C^2}{2I_C} \qquad \text{.....(1.18)}$$

A diatomic molecule has $I_A = 0$ and $I_B = I_C$, hence $P_A = 0$.

$$\therefore \quad E_r = \frac{P_B^2 + P_C^2}{2I_B} = \frac{P^2}{2I_B} \qquad \text{.....(1.19)}$$

P is given by equation (1.20) where the rotational quantum number J is 0,1,2....

$$P = J(J + 1)h^2 \qquad .....(1.20)$$

$$E_r = \frac{h^2}{8\pi^2 c I_B} J(J + 1)\ cm^{-1} \qquad .....(1.21)$$

Each principal moment of inertia is related to the Rotational Constant in cm^{-1} by

$$B = h^2/8\pi^2 c I_B\ cm^{-1} \qquad .....(1.22)$$

Hence the rotational energy levels of a diatomic rotor are given by

$$E_r = BJ(J + 1)\ cm^{-1} \qquad .....(1.23)$$

The consequence of this is that the absorption spectrum due to pure rotation or vibration-rotation of a diatomic molecule such as HCl has a series of bands $2B\ cm^{-1}$ apart.

Most of the molecules studied in this thesis approximate to symmetric top rotors. A true symmetric top has two principal moments equal, the third is not equal to zero.

$I_A < I_B = I_C$ Prolate Rotor

$I_A = I_B < I_C$ Oblate Rotor

For such molecules a second quantum number, K, the angular momentum quantum number, is introduced, for a prolate symmetric top:-

$$p^2 = J(J + 1)h^2 \quad J = 0,1,2... \qquad .....(1.24)$$

$$P_A = \pm Kh \quad K = 0,1,2...J. \qquad .....(1.25)$$

Hence, substituting equations (1.24) and (1.25) into (1.18) gives the final expression for the energy levels of a prolate rotor (1.28)

$$E_r = \frac{K^2h^2}{2I_A} + \frac{P_B^2 + P_C^2}{2I_B} \qquad .....(1.26)$$

$$= \frac{h^2}{8\pi^2 c I_A} K^2 + \frac{p^2 - K^2h^2}{8\pi^2 c I_B} \qquad .....(1.27)$$

$$\doteq BJ(J + 1) + (A - B)K^2\ cm^{-1} \qquad .....(1.28)$$

Similarly for a prolate symmetric rotor $P_c = \pm Kh$ and so the rotational energy levels are

$$E_r = BJ(J + 1) - (B - C)K^2 \text{ cm}^{-1} \quad \text{.....(1.29)}$$

The selection rules for the rotational transitions are $\Delta J = 0, \pm 1$ and $\Delta K = \pm 1$. Transitions in K give a series of sub-bands, with raised frequency if ΔK is + 1 and lowered if ΔK is - 1. Due to centrifugal effects the rotational constants A,B and C have slightly different values in the lower vibrational energy level, denoted B" etc. to that in the higher vibrational energy level B'. For those transitions when $\Delta J = 0$, $\Delta K = +1$

$$E_r'' = (A'' - B'')K^2$$

$$E_r' = (A' - B')(K + 1)^2$$

$$\therefore \quad \Delta E_r = (A' - B') + 2(A' - B')K + \left[(A' - B') - (A'' - B'')\right]K^2 \quad \text{.....(1.30)}$$

Similarly when $\Delta J = 0$ and $\Delta K = -1$

$$\Delta E_r = (A' - B') - 2(A' - B')K + \left[(A' - B') - (A'' - B'')\right]K^2 \quad \text{.....(1.31)}$$

where K refers to the original quantum number, K'.

A similar expression can be written for an oblate rotor. The consequence of this is that a symmetric top shows a series of Q peaks $2(A'-B')$ or $2(B'-C')$ cm^{-1} apart. An accidental or near symmetric top also has $\Delta K = 0$ transitions on C contour bands giving the characteristic sharp central Q band. ΔJ transitions also give further splitting of $2B$ cm^{-1} for each sub-band but in most cases this is too small to be resolved.

However, the observed spacing between sub-bands will not be exactly $2(A'-B')$ due to the modification of the term in K^2, to cancel this effect which differs either side of the main Q branch a plot of

frequency of ${}^{R}Q_{K} - {}^{P}Q_{K}$ is drawn against K, this gives a slope of $4(A'-B')$. It is not always possible to assign K values to sub-bands above and below the main Q branch in which case the less accurate spacing on one side of the Q branch can be calculated.

The term in K^2 can be evaluated by plotting ${}^{R}Q_{K} + {}^{P}Q_{K}$ against K^2. This gives an intercept of $2\left[\nu_0 + (A' - B')\right]$ and slope of $2\left[(A' - B') + (A'' - B'')\right]$. This is only possible if sub-bands can be assigned on both P and R branches.

When discussing the symmetry of a rotor it is important to be able to define the degree of deviation of the rotor from a symmetric top. A useful measure of asymmetry is κ, given in equation (1.32).

$$\kappa = \frac{2B - A - C}{A - C} \qquad .....(1.32)$$

κ is a convenient parameter as it varies from + 1·0 for an oblate rotor to - 1·0 for a prolate rotor, and is 0·0 for a totally asymmetric molecule.

E. Effect of the Population of Torsional Energy Levels on Vibrational Frequencies.

A torsion is an oscillating partial rotation of one group around a single bond with reference to another group. Like all other molecular vibrations, torsional energy is quantised and a quantum leap from one torsional energy to a higher level gives rise to absorption of energy at a specific frequency, called a torsional frequency. Typical torsional frequencies are below 250 cm^{-1}.

Diagram (1.8a) shows the energy potential well of a torsion associated with a high energy barrier. Torsional quantum jumps are

indicated on the diagram and are denoted $0 \rightarrow 1$, $1 \rightarrow 2$ etc., and these give rise to torsional frequencies which will coincide only if the spacing between the levels is constant (due to an ideal parabolic function). On the diagram any splitting of the energy levels by sublevels is ignored for simplicity. In practice the torsional potential function deviates from the parabolic approximation and the energy levels do not have equal spacing, instead the spacing becomes progressively smaller as the torsional levels increase, and a series of absorptions are observed in the i.r. spectrum. The relative intensity of each torsional frequency is proportional to the concentration of molecules with the torsional energy before the transition occurs, i.e. the intensity of the $2 \rightarrow 3$ transition will depend on the concentration of molecules occupying the 2 level, as long as the extinction coefficient ε in equation (1.2) does not vary with the torsional level.

According to the Maxwell-Boltzmann distribution, equation (1.33), the number of molecules occupying an energy level ε_i is given by

$$n_i = A \exp(-\varepsilon_i/kT) \qquad .....(1.33)$$

where A is a constant and k is the Boltzmann constant. This expression can be altered to express molar concentration c_i,

$$c_i = A \exp(-\varepsilon_i/RT) \qquad .....(1.34)$$

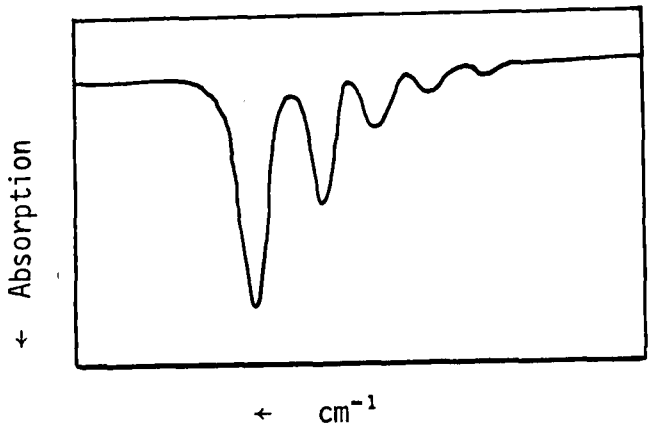

Diagram (1.9)
Typical I.r. Spectrum of a torsion associated with a high barrier to internal rotation.

Diagram (1.9) shows a typical i.r. spectrum of torsion with a high potential barrier. The strongest (0 → 1) transition is observed at the highest frequency and higher transitions are successively weaker in intensity and lower in frequency.

To a first approximation, the ratio of the number of molecules occupying energy levels ε_i and ε_j, where $j = i + 1$, is given by the ratio of the torsional bands $i \rightarrow j$ and $j \rightarrow j + 1$, assuming that the extinction coefficient of the molecules is the same in both energy levels. From equation (1.34) the ratio of the concentrations in energy levels ε_i and ε_j is given by

$$\frac{c_i}{c_j} = \frac{\exp(-\varepsilon_i/RT)}{\exp(-\varepsilon_j/RT)} \qquad .....(1.35)$$

$$\therefore \ln(c_i/c_j) = (\varepsilon_j - \varepsilon_i)/RT \qquad .....(1.36)$$

In equation (1.36) $\varepsilon_j - \varepsilon_i$ is the torsional frequency $\Delta\varepsilon_i$, and substituting concentration for absorbance using equation (1.2) gives the result,

$$\Delta\varepsilon_i = RT\ln(A_i/A_j) \qquad .....(1.37)$$

Bands other than the $0 \rightarrow 1$ transition are termed hot bands and are not only found for torsions but also for other vibrations. However, the hot bands will become progressively weaker as the frequency of the vibrations increases and so are only observable for low frequency bands. Table (1.1) shows the ratio of the absorbances of a fundamental (A_i) and first hot band (A_j), or any two adjacent members of a series of hot bands; using equation (1.37), for a range of vibrational frequencies $\Delta\varepsilon_i$, and temperatures. The effect of increasing temperature is to increase the relative intensity of the hot band, and in increasing vibrational frequency decreases this intensity. Normal i.r. measurements occur at about 300K, at this temperature no observable hot bands are

expected above about 600 cm^{-1}.

	A_i/A_j		
$\Delta\varepsilon_i (cm^{-1})$	T = 200	T = 300	T = 400
100	2·05	1·62	1·43
200	4·22	2·61	2·05
300	8·66	4·22	2·94
400	17·8	6·81	4·22
500	36·5	11·0	6·04
600	74·9	17·8	8·66
800	316	46·4	17·8
1000	1300	121	36·5

Table (1.1)

Values for the Ratio (A_i/A_j) Calculated for each Vibrational Frequency

During the work for this thesis high resolution gas spectra of several compounds showed similar splitting on out-of-plane vibrations to that shown in diagram (1.9). The vibrations involved had energies between 600 and 1200 cm^{-1} and so hot bands of the vibration would be so weak as to be unobservable.

These bands are considered to be caused by the vibration modifying the torsional potential. Diagram (1.8) shows the torsional potential function for a molecule in both ground and first excited quantum levels of vibration. The potential in the excited state is distorted from the ground vibrational state and hence deviates more from the ideal parabola. This results in the torsional energy levels 0', 1', 2' etc. in the excited vibrational state converging at a different rate from those in the ground vibrational state, and so the vibrational quantum jumps originating from the various torsional levels 0,1,2, etc. will have

slightly different energy. The spectrum observed is similar to the torsional spectrum diagram (1.9). There are several conclusions to be drawn from phenomena of this type.

1) The hot bands will be at progressively lower or higher frequencies than the fundamental and the intensity of each band will fall off according to equation (1.37).

2) Different vibrations will alter the torsional functions to a different amount so the splittings observed will not neccessarily be equal on different vibrations, vibrations will either have no splitting, an unresolved broadening to either higher or lower frequency or well resolved splitting.

3) A high energy conformer may well show a larger splitting than a low energy conformer on the same vibration because the high energy potential well deviates more from the ideal parabola.

4) The frequency of the torsional vibration can be calculated using the hot band intensities of a high frequency vibration.

In the compounds of interest to this work the interaction has only been observed for out-of-plane vibrations with the same symmetry as the high barrier torsion. However, a study of methyl isocyanide[74] has shown interaction between the methyl torsion and the C-N and NEC stretches, which are bands of different symmetry.

Examples of this interaction between torsion and vibrations are discussed later for the compounds which portray the effect.

Diagram (1.8) Alteration of the Torsional Potential Function by a Vibrational Transition

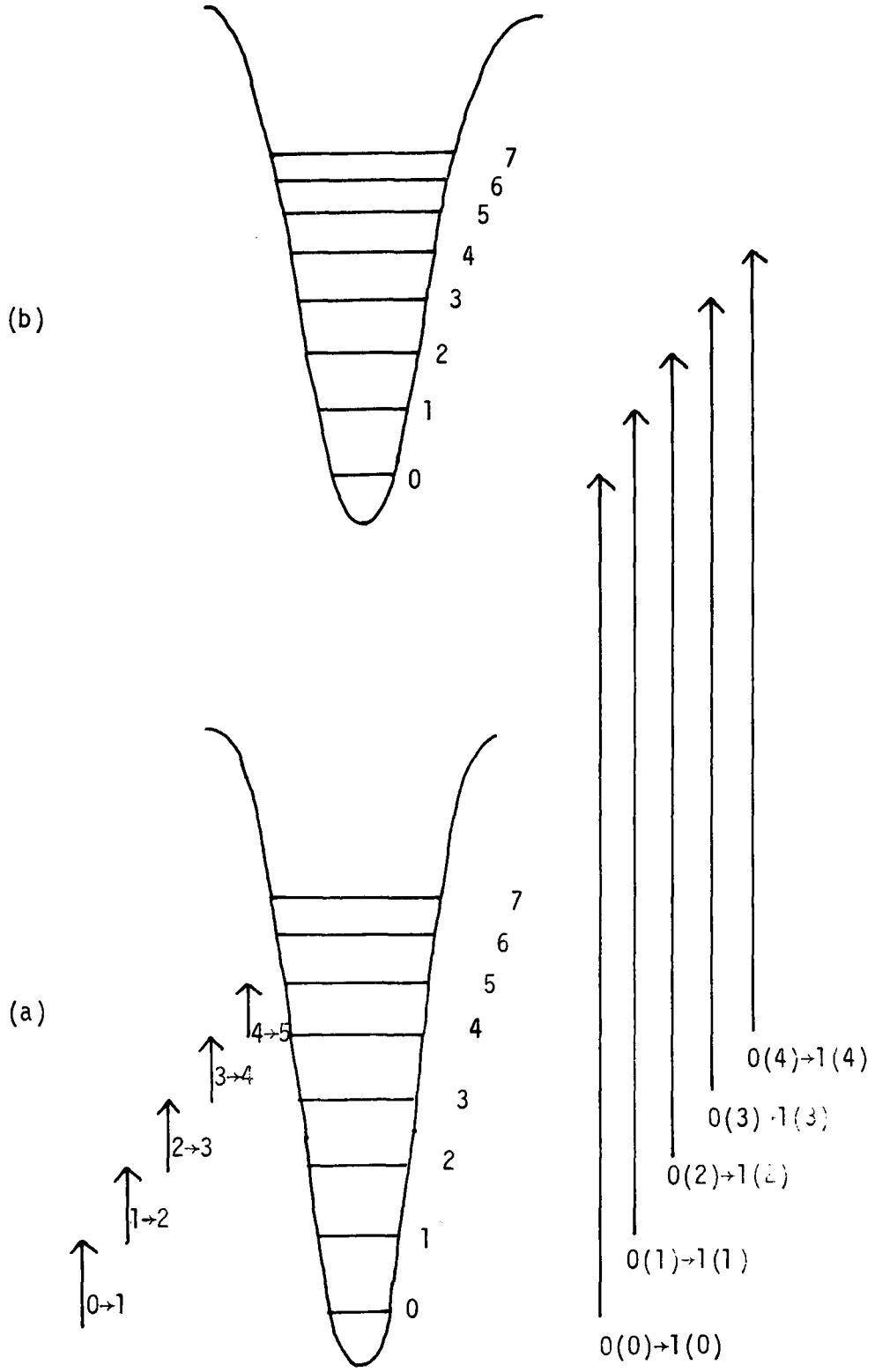

Torsional Quantum Jumps

Vibrational Quantum Jumps at Higher Frequency.

a) Torsional Potential in Vibrational Ground State

b) Torsional Potential in Excited Vibrational State.

CHAPTER II

Experimental Techniques

A Raman Spectra

B Mid-Infrared Spectra

C Far-Infrared Spectra

D Matrix Isolation Apparatus

E Operation of the Matrix Isolation Apparatus

F Purification of Samples

CHAPTER II

Experimental Techniques.

A. Raman Spectra

Raman Spectra were recorded on a JEOL JRS-S1 spectrophotometer using a Coherent Radiation 52G Argon Ion Laser. Laser lines at 514·5 nm. and 488·0 nm. giving up to 100 and 250 mw. power respectively were used to obtain Raman Spectra of samples held either in liquid cells or capillary tubes. The tubes were filled with sample on the vacuum line described later.

Spectra of liquid and solid samples were obtained over the temperature range from liquid nitrogen to +210°C, using a JEOL variable temperature accessory. The temperature calibration was checked by 3 freezing point measurements chosen over the extremes of this range and the temperature shown to be recorded 5° too high over the whole temperature range. Temperature stability was ±1° at any temperature.

A useful feature of the variable temperature equipment used is the visibility of the sample. This enables careful slow annealing of a sample as the solid/liquid interface moves slowly up the capillary tube during freezing and can be held at the height of the laser beam to allow the most stable crystalline state to be produced.

The frequency scale was calibrated using laser lines, and the digital wavenumber readout was found to be accurate. However, the chart pen drive was found to give frequency inaccuracy and so accurate readings were made on expanded scale with manual chart

calibration. The pen was stopped scanning and calibrated on the chart at known frequencies. This method of calibration was found to be accurate to ± 2 cm^{-1}.

Scans were made using a range of slit widths (1·5 to 14 cm^{-1}), and scan speeds selected at 250 cm^{-1} min^{-1} for a full scale scan or down to 10 cm^{-1} min^{-1} for measurement of intensity.

The Raman bands were found to be often highly symmetrical, which enabled an accurate estimate of peak area to be made by measuring peak intensity, and simplified curve resolution of overlapping bands. Polarisation measurements were made using a manual polariser.

B. Mid-Infrared Spectra

Mid-i.r. spectra were recorded variously on Perkin Elmer 457, 521 and 580 spectrophotometers. Frequency scales were calibrated using hydrogen chloride, ammonia or water vapour. The resolution available using the 457 was approximately 2 cm^{-1}, and using the 580, 0·5 cm^{-1}.

Gaseous samples were held in 10 or 20 cm cells with KBr or polyethylene windows, or a Wilks long path gas cell which has a path length variable from 0.75 m to 22.75 m and KBr windows. Liquid cells were equipped with CsI, KBr or polyethylene windows and frozen solids were examined using cells with AgCl or KRS5 windows held in a Beckmann-RIIC VLT-1 low temperature unit.

Solutions of samples were run in CCl_4 at varying concentrations and thickness.

C. Far-Infrared Spectra

Far-Infrared spectra were either run on the Perkin Elmer 580 or the RIIC FS 720 interferometer. The lower limit on the 580 was 180 cm^{-1} and the only gases or liquids could be examined in polyethylene cells.

The interferometer could scan between 40 and 400 cm^{-1}. This enabled low frequency torsions to be examined easily, but due to the weakness of these vibrations a 1 metre gas cell was fitted. Great difficulty was found in drying the samples and excluding all traces of water from the cell. The traces of water show up strongly in an interferometer which is a single beam instrument, as the rotational spectrum of water has many strong bands. To dry samples these were left overnight in contact with a suitable drying agent, and phosphorous pentoxide, molecular seive, calcium and magnesium sulphates were all used. The vapours were distilled off the drying agent and either distilled through a drying column or the cell was left open to drying agent, but even so water vapour was not entirely excluded from spectra of isoprene. Gas spectra were run at resolution of 1 cm^{-1}, and liquid and solid samples were examined using the Beckmann RIIC VLT 1 variable temperature unit in polyethylene cells at resolutions of 5 cm^{-1}.

The frequency scale of the interferometer was calibrated using hydrogen chloride gas and found to be accurate, the frequencies listed are accurate to $\pm$ 5 cm^{-1} for liquids and solids and $\pm$ 0·4 cm^{-1} for gases. Spectra were calculated from the FS 720 interferogram using off line computing. The theory of the method, computer program used and data handling required are detailed in the Appendix.

D. Matrix Isolation Apparatus

This is based on the Air Products AC2L cryogenic system which

requires liquid nitrogen to precool hydrogen on a two stage cascade system. The apparatus for matrix isolation work can be divided into three sections, the cryotip, a vacuum line for handling gaseous samples and service trolley designed to evacuate the cryotip shroud and deliver hydrogen coolant to the cryotip. The cryotip is mounted on the service trolley by a horizontally extendable arm on a vertically raisable platform so that the cryotip position can be altered to suit different spectrometers. The trolley and spectrometer used are both on wheels and can be moved independantly to bring the cryotip into the i.r. beam. The trolley is connected to a bank of 4 hydrogen cylinders and vacuum line by moderately flexible couplings.

The framework of the cryotip trolley is made of Dexion with a single $^{5}/_{16}$" Aluminium sheet floor, and all pumps and the pillar are bolted directly onto the floor. The cryotip position is adjustable both vertically and horizontally on a sliding bed.

Diagram (2.1) shows a schematic exploded view of all the equipment on the trolley except electrical components and the cryotip mounting. On the diagram hydrogen is delivered (from a bank of four cylinders fitted with a pressure regulator) to the cryotip assembly, P, via a hydrogen handling system shown to the left of the cryotip. The cryotip shroud is evacuated by an Edwards E02 Diffusion Pump and Edwards ES50 Rotary Pump shown to the right. The cryotip vacuum is measured with Pirani and Penning guages, and the normal room temperature vacuum achieved is 10^{-5} Torr, and 10^{-6} Torr on cooling.

As far as possible the apparatus controls have been sited on a console on the trolley, with the gauges and a Doric APD-T1 temperature readout, which monitors the temperature at the cold tip by thermocouple. The console is shown in diagram (2.2.) and the lettering for

Diagram (2.1) Schematic Diagram of Apparatus Mounted on the Service Trolley. The Cryotip Support and Electrical Equipment are not Shown

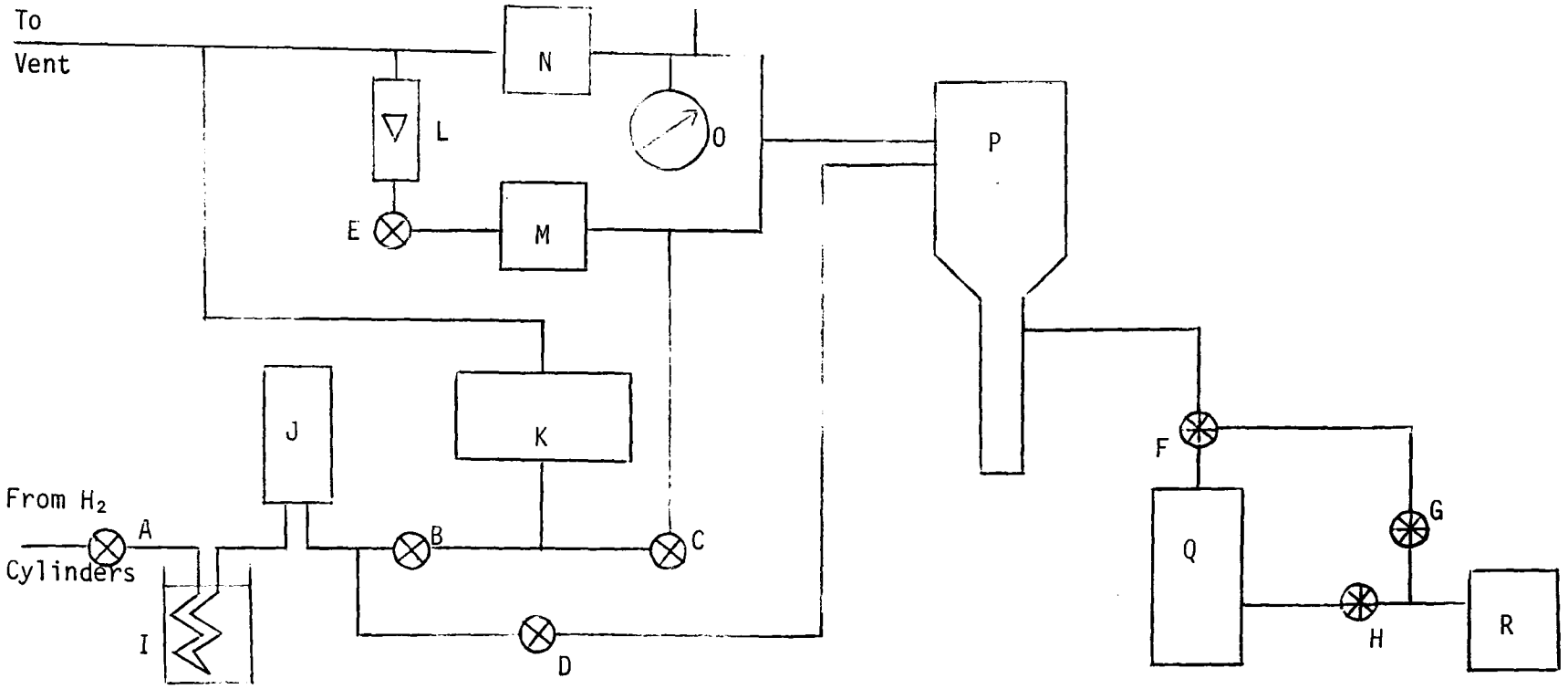

A - E	Hoke Valves	K	Backing Pump	O	Back Pressure Gauge
F - H	Metal Valves	L	Flowmeter	P	Cryotip Assembly
I	Liquid N_2 trap	M	Back Pressure Regulator	Q	Diffusion Pump
J	Warm Absorber	N	Safety Valve	R	Backing Pump

Diagram (2.2) Operating Console on the Matrix Isolation Service Trolley.

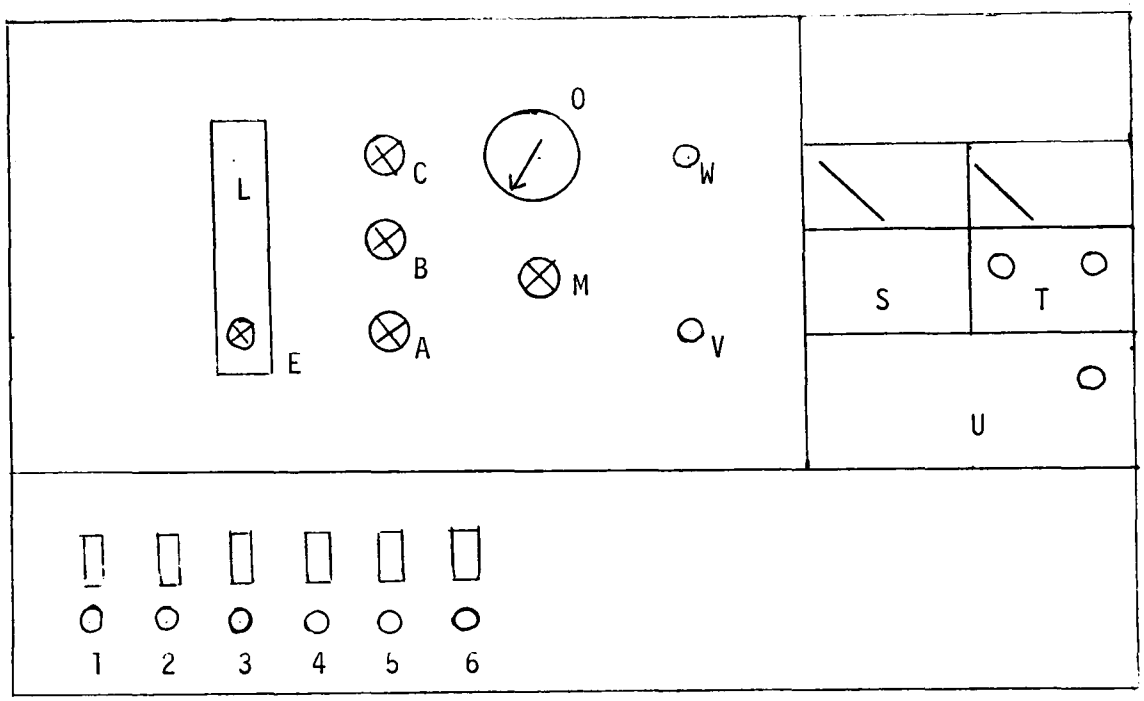

A High pressure shutoff
B High pressure evacuate
C Low pressure evacuate
E Flowmeter Valve
L Flowmeter
M Back pressure regulator
O " " gauge
S Pirani Gauge
T Penning Gauge
U Temperature readout
V H_2 out to cryotip
W H_2 in from cryotip

Switches
1 Backing Pump
2 Diffusion Pump
3. Hydrogen Line Pump
4 Diffusion Pump Fan
5 Pirani Gauge
6 Warm Absorber Heater

the components is the same as that used in diagram (2.1), to give easy comparison. Switches 1,2 and 4 are coupled so that the diffusion pump cannot be operated unless both the rotary pump and the diffusion pump fan are running.

The commercial grade hydrogen used as coolant must be purified before use to remove any gases which would freeze and block the cryotip nozzle. The purification is carried out in two stages. A liquid nitrogen trap removes water vapour and carbon dioxide, and a warm absorber then removes nitrogen and oxygen. Before and after use the hydrogen lines, the trap and absorber are pumped at room temperature to remove any free gas.

The Vacuum Line

The gas handling line was designed as a multi purpose system for filling i.r. gas cells, Raman capillary tubes, the interferometer gas cell and mixing the matrix isolation gas samples. Diagram (2.3) is a schematic representation of the line. Pumping was performed by an NGN PSR12 backing pump and an NGN diffusion pump. These pumps gave vacuums of 2×10^{-5} Torr with, and 10^{-2} Torr without the diffusion pump. Wherever possible greasless Teflon taps were installed on the line as the samples studied interfered with grease seals and thus caused leaks. The bulbs were 3,2 or 1 litre so that a range of volumes could be mixed for matrix isolation work. For very low concentrations of samples the line 'dead space' under the bulbs was used to hold a small amount of sample as the volume of this 'dead space' is about 220 cm^3. The matrix sample ratios quoted are approximate as accurate measurement of both volumes and pressures is not easy, especially at low pressure.

Argon gas was introduced onto the line from a cylinder, and so to ensure that excess pressures were not allowed to build up quickly in the line the gas was introduced via a pressure regulator and finally via a needle valve onto the line.

Diagram (2.3) Schematic Representation of the Vacuum Line for Handling Gaseous Samples.

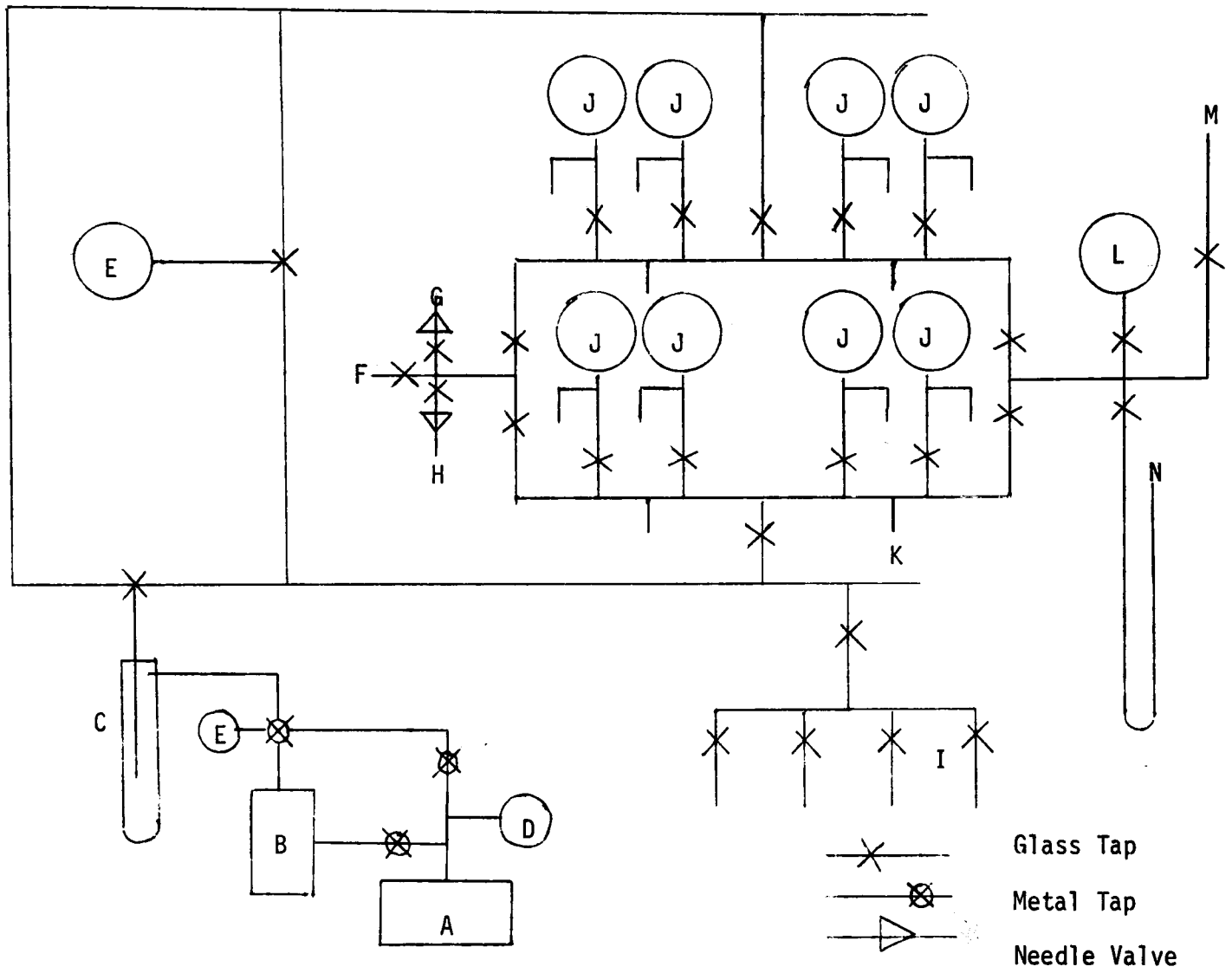

A Backing Pump
B Diffusion Pump
C Cold Trap
D Pirani Guage
E Penning Guage
F To 10 cm Gas Cell
G To Cryotip
H Argon Input
I Raman Sampling Points
J Gas Bulbs with Traps
K Sample Input Point
L Pressure Gauge
M To Interferometer or Wilks Long Path Cells.
N Barometer.

The sample/argon mixtures were sprayed onto the cryotip via a needle valve on the line which controlled the rate of flow of deposition. No quantitative estimate of rate of flow was made as during spray on the pressure drop in the line meant that constant alteration to the needle valve setting was necessary.

The Service Trolley.

The service trolley acts as a mobile mount for the matrix isolation cryotip and also carries all the necessary equipment for evacuating the cryotip shroud and delivering hydrogen coolant to the cryotip at a regulated pressure.

The absorber can be regenerated by pumping whilst heating for 24 hours. The maximum voltage used is 50 volts, and a Variac is fitted on the trolley to provide 50V. Regeneration of the heater is only neccessary after several months use.

The temperature of the sample is controlled by altering the rate of hydrogen flow through the cryotip once a low temperature has been achieved. This can be done either by altering the pressure of the incoming hydrogen using the pressure regulator on the cylinder bank, or by building up a back pressure on the exhaust hydrogen using the back pressure regulator. This enables annealing of a matrix to be carried out by raising the temperature of the matrix until it is just mobile (35K for argon), higher temperatures result in matrix degradation.

The Cryotip Assembly.

This is depicted in diagram (2.4). The cryotip is manufactured by Air Products Ltd., and is capable of cooling a sample to approximately 17K by a two stage cascade process. Purified hydrogen gas is input from the service trolley and passed through liquid nitrogen to cool the gas to 77K. The cold gas cools the cryotip to the same

Diagram (2.4) Schematic Representation of the Cryotip Assembly, Showing the Brass Inlet Tubes Angled Towards the Cold Window.

A. Glass Vacuum Shroud
B. Metal Outer Case
C. Cryotip Cooling Column
D. Heat Shield (with cutaway section)
E. Thermocouple Mounting
F. Turned Brassed Nozzle
G. Ground Glass Socket
H. Cryotip Assembly
I. Caesium Iodide Window
J. Gas Input Tube
K. Potassium Bromide Outer Window
L. Thermocouple Lead.

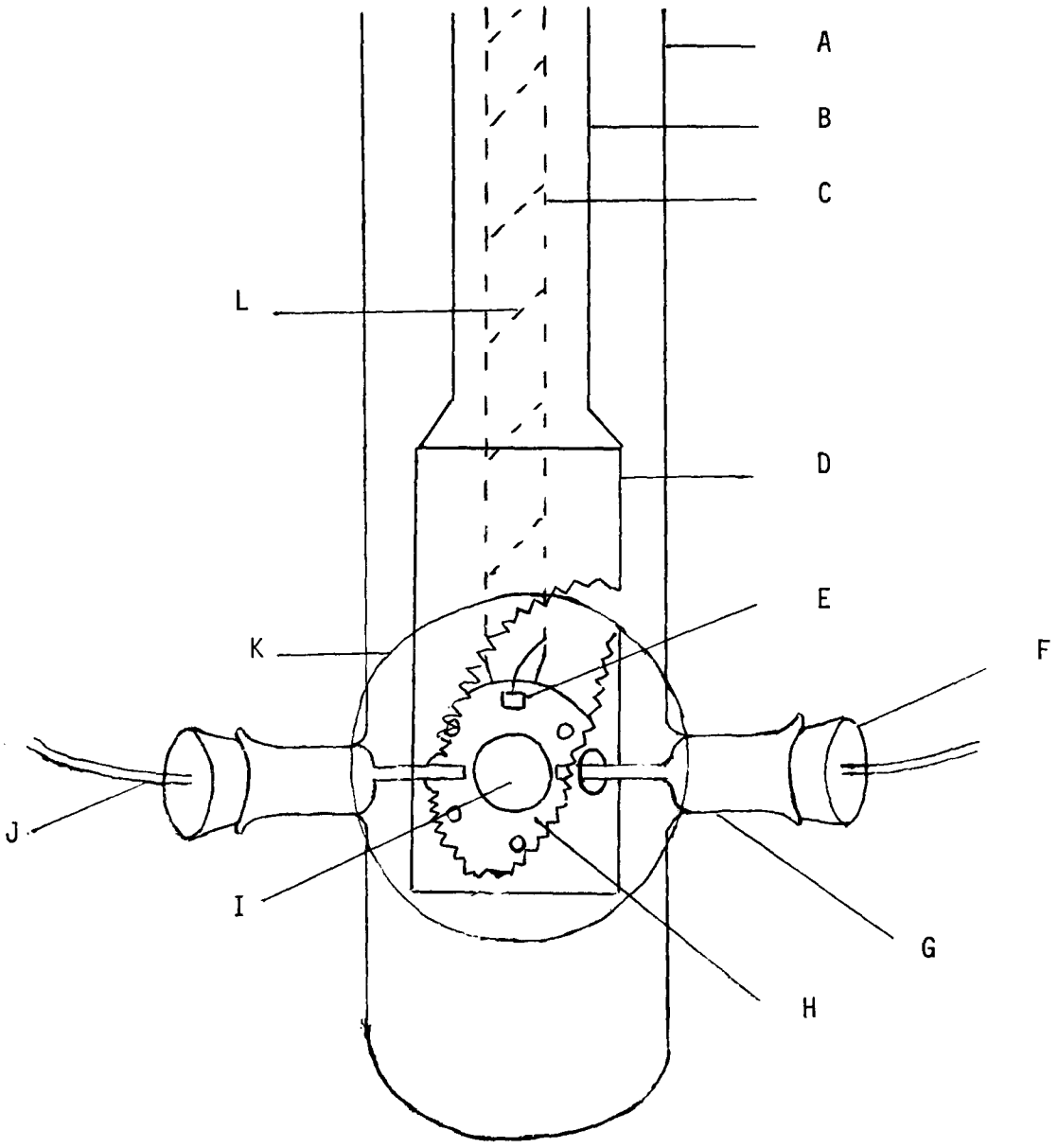

temperature, exhaust hydrogen cools the incoming hydrogen in a heat exchanger. Once below its inversion temperature, cooling can be accelerated by increasing pressure to 1000 psi. when Joule Thompson cooling occurs and a running temperature of about 23K is quickly reached. Pumping out the exhaust hydrogen gives the lowest temperature of approximately 17K, but this pumping is not carried on for more than a few minutes since pump damage may occur.

The cryotip temperature can only be maintained if thermal energy is stopped from reaching the tip. The three normal methods of transfer of heat are by convection, conduction and radiation. Convection and conduction by air is stopped by holding the cryotip in a vacuum of a least 10^{-5} Torr, a glass shroud with KBr windows and sample input ports encloses the cryotip. Conduction from the rest of the assembly is minimised by placing the tip on the end of the long column which also acts as a hydrogen heat exchanger. Radiation can be troublesome and so a radiation shield surrounds the tip, holes are cut in the tip for sample spray on and spectroscopic examination.

E. Operation of the Matrix Isolation Apparatus

The operation of valves etc. is laid out according to the notation as used in diagrams (2.1) and (2.2) Commence with all valves shut and back pressure regulator off.

(a) The hydrogen handling lines are pumped out before use by using backing pump K (switch 3), opening valves A,B,C and D. This removes any air which would not only clog the cold trap and absorber, but form a dangerous mixture. A Pirani gauge can be fitted above pump K to check the vacuum achieved. Of course hydrogen cannot be used if this line does not hold vacuum. Switch on the warm absorber J (switch 3) and set the Variac to 50 Volts.

(b) The cryotip shroud is evacuated, first using the backing pump R (switch 1), by passing the diffusion pump Q and then pumping with the diffusion pump (switch 2) on line once a pressure of 10^{-2} Torr is achieved. The final pressure should be less than 10^{-5} Torr at room temperature, otherwise a leak is present.

(c) After pumping out the hydrogen lines close valves A,B,C and D and switch off pump K. Fill the nitrogen trap I. Introduce hydrogen onto the line at about 250 psi. using the regulator on the cylinder bank. Open D and E consecutively, and the hydrogen flow rate will register on the flowmeter L, if not check that the back pressure regulator is off. Allow ten minutes for any air to be flushed out of the system before starting cooling.

(d) Check all piping and connections for hydrogen leaks using a brush and weak soap solution.

(e) Meanwhile connect a nitrogen gas supply to the small vertical pipe inside the cryotip liquid nitrogen dewar. This pipe must be kept clear whilst the liquid nitrogen is added as it is a siphon to allow nitrogen gas bubbles formed inside the cryotip to escape easily, but any water or carbon dioxide freezing in the pipe on addition of liquid nitrogen blocks it and hampers cool down. Pass a small flow of gas down the pipe whilst cautiously adding the liquid nitrogen through a small funnel. Once the reservoir is full and violent boiling has ceased the gas flow is removed.

(f) The cool down now commences. Once the inversion temperature of hydrogen has been reached (about 160K) the hydrogen pressure can be increased to 1000 psi. and the cooling rate increased. Once 23K has been achieved the pressure is reduced to 250 psi. which should be sufficient to hold the cryotip at this temperature. A lower temperature

can be achieved (19K)if the pump K is switched on, valve C opened and valve E closed, thus lowering the backpressure.

(g) Move the spectrometer so that the cold tip is in the beam and check that maximum possible transmission is available by fractionally moving the cryotip position adjustments on the pillar. The matrix is slowly sprayed on using the vacuum line needle valve, build up of the matrix is monitored by repeat scanning of the infrared spectrum. As the gas pressure on the line decreases the needle valve must be opened a little to keep a steady flow rate. If the overall transmission of the matrix starts to lower then the flow rate is too high. A typical spray on time is 15 minutes for a 100:1 matrix and more dilute matrices correspondingly longer.

(h) Record the i.r. spectrum. Typical run conditions using the P.E. 580 are mode 3 giving resolution down to $2cm^{-1}$. Selected portions can be recorded at higher resolution if so desired.

The sample is now annealed to ensure that the sample is in its most stable state. This is done by closing valve F, raising the matrix temperature until the matrix softens and molecules can slowly move, at about 35K for argon. Raising the temperature higher gives loss of matrix and molecular aggregation and so must be avoided unless it is desired to study aggregation.

The temperature is raised by controlling the hydrogen flow. This is done either by lowering the hydrogen pressure at the pressure regulator or by increasing the back pressure using the back pressure regulator M. The back pressure is monitored on gauge O and must not exceed 150 psi. Cooling is performed by reversing the operation used and valve F is opened to resume pumping, once a temperature of 23K is regained.

(g) Warm up is achieved by reducing the hydrogen flow to slightly positive (about 50 psi.) and alowing the liquid nitrogen reservoir in the cryotip to boil dry. The diffusion pump should be bypassed but do not stop pumping otherwise the argon vapour will probably become excessive in the shroud as the matrix vaporises. If desired, once the argon has been pumped off leaving the sample only on the window, the system can be closed down completely and left to warm up overnight.

Close down is performed by closing valves F,G and H, switching off pumps Q and R, stopping the hydrogen flow from the cylinder regulator, closing valve E and pumping out the hydrogen linesusing pump K and opening B and C. Whilst pumping switch off the warm absorber and allow the nitrogen trap to dry up so that any gases can be pumped off. After pumping close A,B,C and D to keep air out of the hydrogen line and absorber.

Premature warm up or difficulty in cooling can be due to several factors.

(1) Thermal contact between the cyrotip and the outside shroud. One common reason is that the radiation shield has slipped and touches the metal gas inlet ports. Another is air leaking in, this is apparent from the gauges.

(2) Blockage of the hydrogen lines can be found at several points and is recognised by slow flow rate. Highly impure hydrogen can cause a blockage in the cold trap I, or swamp the warm absorber J which then allows impurities to pass to the cyrotip and block the cyrotip jet. The run has to be abandoned and the warm absorber purged or a new hydrogen cylinder tried. Another form of blockage is by dust accumulating at the cryotip head inlet port which has a porous metal filter. This can often be cleared by loosening the gyrolock coupling, the escaping

hydrogen blasts the dust away. Provided adequate ventilation is provided and normal precautions taken this method is safe.

(3) Blocking of the thermal siphon will slow down the cooling rate, this should be avoided by blowing nitrogen gas down whilst initially adding liquid nitrogen. Once blocked the run may have to be abandoned.

Safety Precautions.

The following safety precautions must be observed when using the matrix isolation system.

1) Adequate ventilation must be allowed, and the hydrogen lines tested for leaks using dilute soap solution before use.

2) All hydrogen is vented to atmosphere at roof top level.

3) Ensure that all air is removed from the gas line before pressurising the system with hydrogen, otherwise explosive mixtures may be pressurised.

4) Wear safety glasses and observe all normal safety precautions when both using the vacuum line and handling liquid nitrogen.

5) Open valves slowly, and build up or reduce pressures slowly.

6) Do not exceed 1500 psi. on the high pressure line, or 200 psi. on the low pressure line.

F. Purification of Samples

The following compounds are available commercially and were either purchased or supplied by British Petroleum Trading Ltd.,:-

Butadiene, commercial grade gas from a cylinder was purified on the vacuum line by repeated trap to trap distillation and stored at liquid nitrogen temperature during use.

Isoprene and cis- and trans-pentadiene were obtained as spectroscopic grade samples in sealed ampoules. These were stored during use on the vacuum line over drying agent in darkened tubes to prevent polymerisation, and used without further purification.

Acryloyl chloride was obtained as 98% pure liquid and purified by distillation on the vacuum line. The i.r. spectrum of gaseous acryloyl chloride showed peaks due to hydrogen chloride gas, but no other impurities. Samples were stored on the vacuum line like isoprene.

Chloroprene was obtained from B.P. as a 98% pure liquid kept over 0.1% stabilizer. Before each use a fresh sample was prepared by distillation and the purity checked by g.l.c., as slow degradation of the sample occurred with time.

Dimethyl, diethyl and di-n-butyl esters of fumaric and maleic acids were purchased from commercial sources, and analysis by g.l.c. showed at least 99% purity so the samples were used without purification and stored in a refrigerator. Dimethyl fumarate is a solid at room temperature and the purity of the sample was checked by its melting point, measured at 103.5^{o}, which compares with the Chemical Rubber Company Handbook value of 101^{o}.

CHAPTER III

Variable Temperature Raman Studies and Vibrational Assignments of Dimethyl, Diethyl and Di-n-butyl Fumarate and Maleate Esters

A. Introduction

B. Experimental

C. Vibrational Assignments of Fumarate Esters

D. Vibrational Assignments of Maleate Esters

E. Conformational Equilibria

CHAPTER III

Variable Temperature Raman Studies and Vibrational Assignments of Dimethyl, Diethyl and Di-n-butyl Fumarate and Maleate Esters.

A. Introduction

A previous study[69] of dimethyl, diethyl and di-n-butyl esters of fumaric and maleic acids using variable temperature i.r. spectroscopy indicated that conformational activity was present in esters of fumaric acid only.

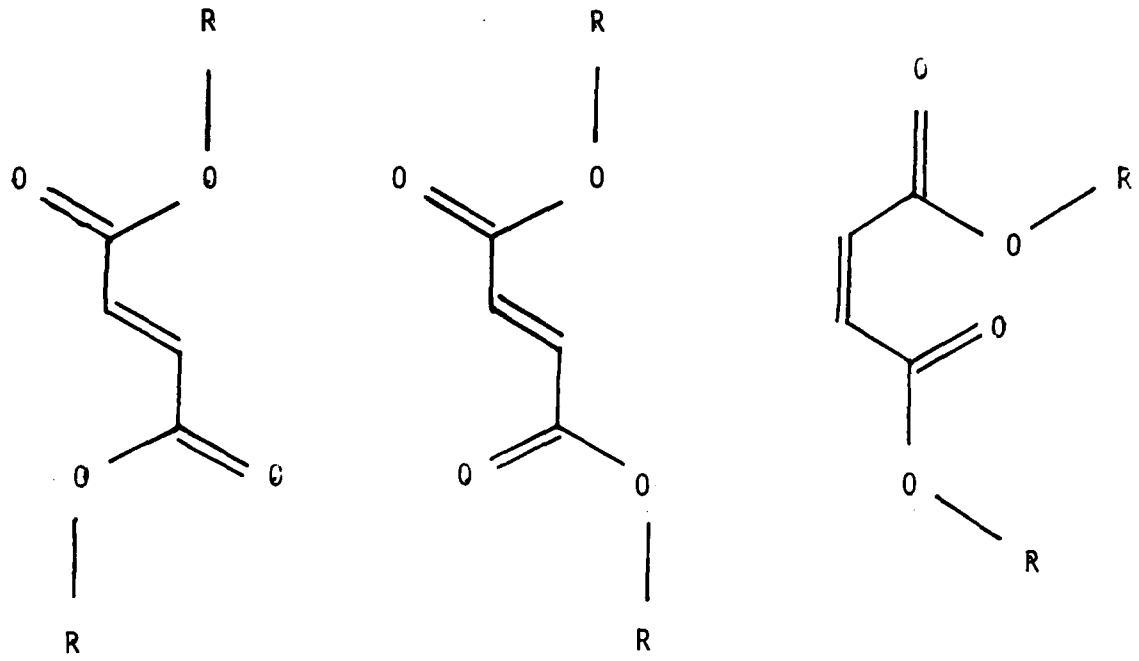

I
trans,trans

II
trans, cis

III
cis, trans

Diagram (3.1)
Probable Conformers[69] of the Fumarate Esters (I,II) and Maleate Esters (III)

The results obtained were analysed[69] on the basis of an equilibrium between

a predominant trans, trans conformer (I) and a high energy trans, cis conformer (II) for the fumarate esters, shown in diagram (3.1), as suggested by an earlier study[75].

No conformational changes were observed for the maleate esters and it was suggested that these compounds exist in the cis, trans conformer (III)[69], because of steric hindrance in the trans, trans conformer, although it was pointed out that the structure could be non-planar due to the high lone pair repulsions present in the molecule.

I.r. and n.m.r. studies[60,76] on fumaroyl chloride, fluoride and maleoyl fluoride show that these halides are a mixture of at least two planar conformers. The conformational activity present in maleoyl fluoride is not barred on steric grounds, as in maleate esters.

The energy difference, ΔH^{θ}, between the conformers (I)and (II) of di-n-butyl fumarate was calculated [69] to be 372 ± 20 cal mol^{-1} (1·56 ± 0·08 KJ mol^{-1}), but no estimate was given for ΔH^{θ} for the other fumarate esters.

The spectrum of each compound can be resolved into two parts if the alkyl groups are considered as single units (R), first the modes due to the molecular skeleton ROO:CHC:CHC:OOR, and secondly the modes internal to the alkyl group. The skeletal modes should be at approximately the same frequency in all three esters of each acid, whereas the alkyl modes are already well known and not discussed in detail. The skeletal modes of the fumarates depend on the conformations present and because of the different symmetries of these conformers, (the trans, trans conformer has C_{2h} symmetry whilst the trans, cis conformer has C_s symmetry), will show different i.r. and Raman activity.

The vibrational spectra of the fumarate and maleate esters are given in tables (3.1) and (3.2) respectively. I.r. data is taken from the previous study by George and Porter[69]. Table (3.3) compares the tentative assignments of the fundamental skeletal frequencies for the esters. In this table only the fundamentals of the trans,trans conformer (I) of the fumarate esters are listed. The assignments given follow those given to esters of acrylic and crotonic acids[77].

B. Experimental

The Raman spectra of the maleate and fumarate esters were recorded as liquids and solids as reported in chapter II. All the esters except dimethyl fumarate are liquids at room temperature and solid samples were obtained by freezing and annealing. Dimethyl fumarate is a solid at room temperature and the liquid spectrum was recorded at elevated temperatures. However, the compound was found to be sensitive to both blue and green laser lines, even after purification, at high temperatures and so liquid spectra were recorded using low laser power, 17 amps and wide slits set at 14 cm^{-1} on the green laser line. Even so the hotter spectra show high baseline drift, but on recording the sample no time dependant spectral changes had occurred.

The Raman spectra of the fumarate and maleate esters as room temperature liquids and low temperature solids (except dimethyl fumarate which is a solid at room temperature and melts at 103^{o}) are shown as spectra 1-6 in the appendix. The vibrational spectra are given in tables (3.1) and (3.2).

C. Vibrational Assignments of Fumarate Esters

The trans, trans conformers (I) of the fumarate esters have C_{2h} symmetry and if the alkyl groups are considered as single units the 30 fundamental modes divide into $11a_g$ (Raman,polarised) + $4b_g$ (Raman, depolarised) + $5a_u$ (i.r.) + $10b_u$ (i.r.). The trans, cis conformer (II) belongs to the C_s point group which has no centre of symmetry and so all modes are Raman and i.r. active. The modes divide into 21a' (polarised) and 9a" (depolarised).

The spectra of the fumarate esters are discussed by regions of the spectrum. Tentative assignments proposed are given in table (3.3). The complete vibrational spectra, including i.r. data[69], are given in table (3.1) where bands which increase on cooling are denoted (↑) and those which decrease on cooling are denoted (↓).

The a_g and b_u olefinic C-H stretches are assigned to bands near 3060 in Raman and i.r. peaks below 3000 cm^{-1} are assigned to the alkyl chains 2000 - 1500 cm^{-1}.

Two carbonyl stretches are expected, one i.r. active and one Raman active but as both i.r. and Raman bands in this region are strong and coincident it seems that the two vibrations occur at similar frequencies, indicating little interaction between the groups. The C=C stretch at about 1600 cm^{-1} is only observed in the Raman as a strong polarised a_g band, the absence of corresponding i.r. bands is good evidence for a centrosymmetric C_{2h} structure. Satellites about 15 cm^{-1} below these Raman bands do have i.r. counterparts, but these satellites are absent or very weak in the solid and so the bands have been assigned to C=C stretch of the asymmetric high energy conformer.

1500 - 1000 cm^{-1}.

The bands between 1480 and 1360 cm^{-1} have been assigned to CH_3 and CH_2 bending modes. As in the acrylic and trans-crotonic esters[77], and a number of pairs of conformer bands occur between 1300 and 1000 cm^{-1} for which an accurate assignment is not simple. Comparisons of wavenumber values and consideration of Raman and i.r. band intensities amongst various fumarates, acrylates and trans-crotonates suggest that the asymmetric C-O stretching mode is associated with a pair of bands near 1300 and 1260 cm^{-1} (low and high energy conformers respectively) whereas the corresponding C-O symmetric stretch is associated with a pair of bands near 1220 (high energy conformer, i.r. active only) and 1212 cm^{-1} (low energy conformer, Raman active only). A third pair of conformer bands occurs near 1170 and 1150 cm^{-1}. The higher wavenumber band is polarised in the Raman but is only observed as a shoulder in the i.r. and so is assigned to the a_g C-H bend. The lower frequency band is only observed in the i.r. as a high energy conformer band. It is likely to be the corresponding a' C-H bend.

A similarity of a pattern of five i.r. bands in a range of esters of fumaric acid and of temperature dependence in the dimethyl, diethyl and di-n-butyl compounds was noted previously [69]. The additional Raman data in the present study assists the assignments of these bands. Of the four C-O and C-H fundamentals in this region only the b_u C-H bend is not split into a pair of conformer bands, and is assigned to an i.r. shoulder at 1270 cm^{-1}.

A prominant pair of conformer bands are present in the Raman spectrum of dimethyl funarate at 1031 and 990 cm^{-1}, the latter peak being part of a doublet. The lower frequency band has a weak Raman counterpart in the diethyl and di-n-butyl fumarates, which is polarised

and so assigned to a_u O-R stretch. The higher band is coincident with medium intensity i.r. bands near 1030 cm^{-1} which are assigned to the b_u O-R stretch.

1000 - 500 cm^{-1}.

Assignment of the a_u out of plane C-H deformation is well established in trans disubstituted compounds at about 975 cm^{-1}, but that of the corresponding b_g out of plane C-H deformation is less certain. It is assigned to a medium or weak depolarised Raman band around 890 cm^{-1} in the fumarate esters. Both modes obey the mutual exclusion rule rigorously and the bands occur at somewhat higher frequency than the corresponding modes[77] in the trans crotonates. Other fundamentals expected in this region are the a_g and b_u C-C stretching modes. The former band is assigned to the medium intensity polarised Raman band near 850 in the di-n-butyl and diethyl esters, but the 850 cm^{-1} band in dimethyl fumarate appears to be a high energy conformer band and so the corresponding low energy band is considered to be superimposed on the b_g C-H deformation at 888 cm^{-1}. The medium intensity Raman bands at 850 cm^{-1} all have weak i.r. counterparts, suggesting that either there is no splitting between the a_g and b_u C-C stretching motions or that the mutual exclusion rule is not rigorously obeyed. In this case the b_u C-C stretching modes are assigned to weak i.r. bands near 770 cm^{-1} in all fumarates.

The in-plane and out-of-plane C=O bending modes of esters are normally assigned to the 600 - 700 cm^{-1} region. The weak i.r. band near 665 cm^{-1} may be assigned to both the a_u and b_u C=O bending modes. The weak Raman bands at about 740 are assigned to both the a_g and b_g C=O bending modes.

Assignment of the skeletal modes in the 600 - 100 cm^{-1} region is

only tentative. Bands near 650, 420 and 340 cm^{-1} are likely to be associated with the various skeletal modes but other bands in this region are dependent on the alkyl group and are therefore associated with the bending modes of these groups.

D. Vibrational Assignments of Maleate Esters

The cis, trans conformer (III) postulated by George and Porter[69] has C_s symmetry and so all fundamental modes are both i.r. and Raman active. The 30 modes (if the alkyl groups are considered single units) divide into 21 a' (polarised) and 9 a" (depolarised).

The spectra are discussed by regions of the spectrum, and tentative assignments given are shown in table (3.3) with those of the fumarate esters. The complete vibrational spectra are given in table (3.2).

Variable temperature Raman studies uphold earlier i.r. results as no high energy conformer bands disappeared on freezing the sample, hence only one conformer (or two equivalent structures) are present in these esters. The cis, trans conformer (III) is considered most likely from a consideration of molecular models. This leads to Raman and i.r. coincidence for all bands which holds except for the C-H bends, which are in the central pseudo-symmetrical portion of the molecule.

The tentative assignments for the maleate esters shown in table (3.3) follow those for the fumarate esters closely, a' species in the maleates correspond to the fumarate a_g and b_u bands and the a" maleate bands correspond to the a_u and b_g fumarate bands. The distinction between symmetric and antisymmetric modes is made by comparison with the fumarates

E. Conformational Equilibria.

Comparison of the Raman spectra of the fumarate esters as liquids and annealed solids reveal a number of pairs of conformer bands. High energy conformer bands are denoted as (↓) for bands which decrease in relative intensity on cooling and are absent in the solid state after annealing, and low energy conformer bands as (↑) for bands which increase in intensity on cooling. In many cases band overlap precludes accurate measurement.

The Raman spectra of di-n-butyl fumarate in the region 1350 - 1100 cm^{-1} as a liquid at + 119°, -8° and annealed frozen solid at -30°C are shown in diagram (3.2). In the solid state certain bands are split, intensified

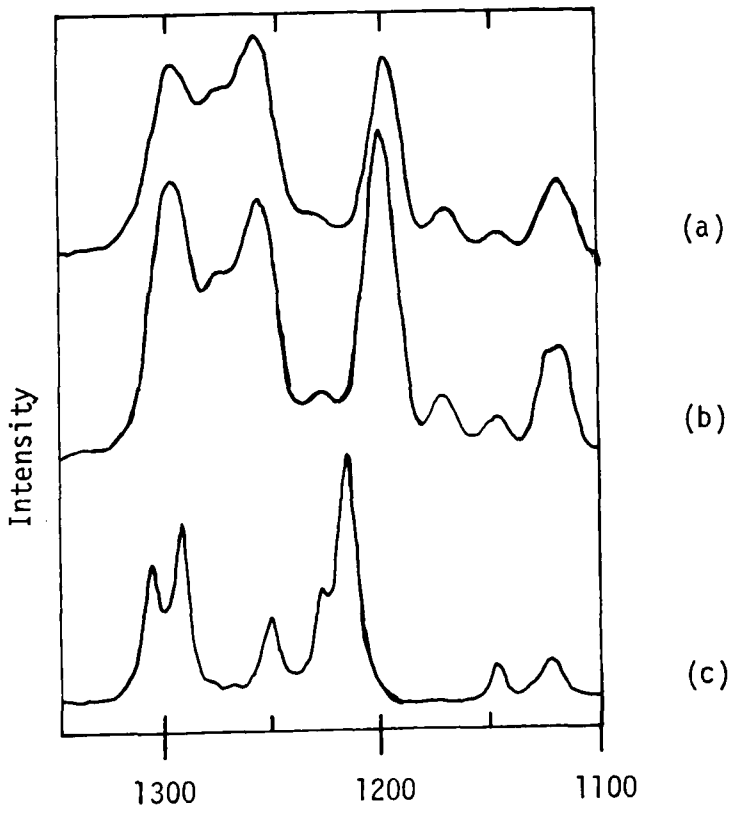

Diagram (3.2)
Raman Spectra of di-n-butyl Fumarate, 1350 - 1100 cm^{-1}. (a) + 119°C, (b) - 8°C and (c) annealed solid at -30°C.

or shifted to higher wavenumber value. The strongest band in this region at 1261 cm^{-1} is absent in the solid. In the liquid the intensity of this band was measured relative to that of the 1300 cm^{-1} band over a 200°C temperature range. Using equation (1.10) a plot of $\log(I_{1261} - \log I_{1300})$ against 1/T gave a value for the enthalpy difference between conformers, $\Delta H^{\theta} \pm \sigma$, of 1·66 ± 0·18 KJ mol^{-1}. This pair of bands corresponds to the conformer pair used for i.r. studies[69] to obtain a value for ΔH^{θ} of 1·56 ± 0·08 KJ mol^{-1}. The close agreement between the ΔH^{θ} values obtained by Raman and i.r. spectroscopy is encouraging because the two techniques can be considered independant in terms of experimental errors; also it provides good support for the existence of an equilibrium with this enthalpy difference.

The Raman spectra of diethyl fumarate are shown under similar conditions over the range 1325 - 825 cm^{-1} as solid at - 21°C and liquid at - 3°C and + 126°C.

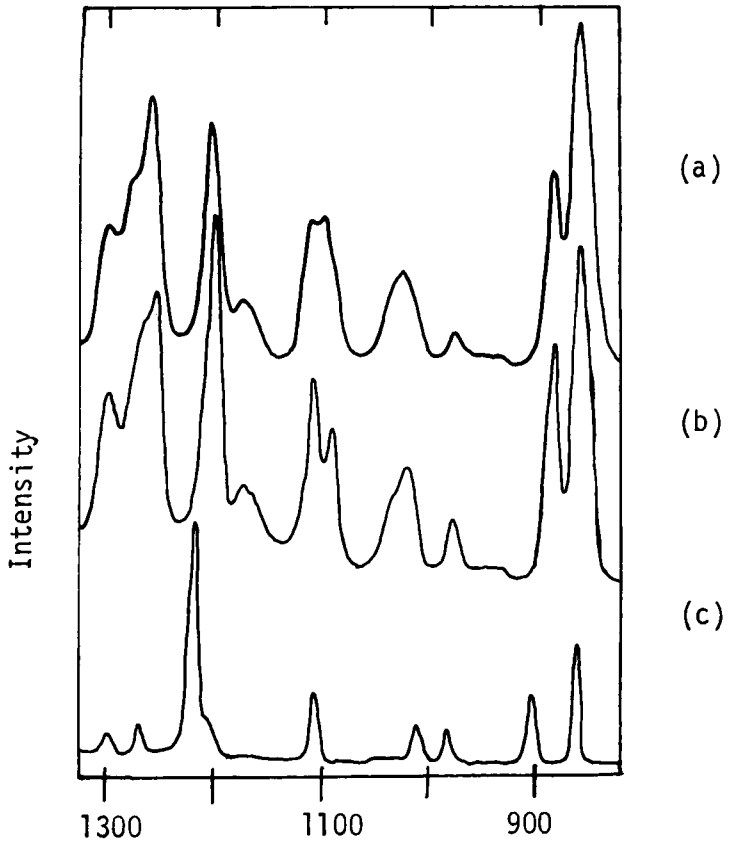

Diagram (3.3)
Raman Spectra of Diethyl Fumarate between 1325 and 825 cm^{-1}. (a) + 126°C, (b) - 3°C, (c) annealed solid at - 21°C.

Bands in the liquid spectrum at 1259, 1092, 1032 and 1025 weaken on cooling and are absent in the solid. Intensity measurements of bands at 1300 and 1259 cm^{-1} over the temperature range -14^{o} to $152^{o}C$ led to a value for ΔH^{θ} of 916 ± 117 J mol^{-1}, using equation (1.10).

Dimethyl fumarate is a solid at room temperature and so diagram (3.4) shows a comparison between Raman spectra of

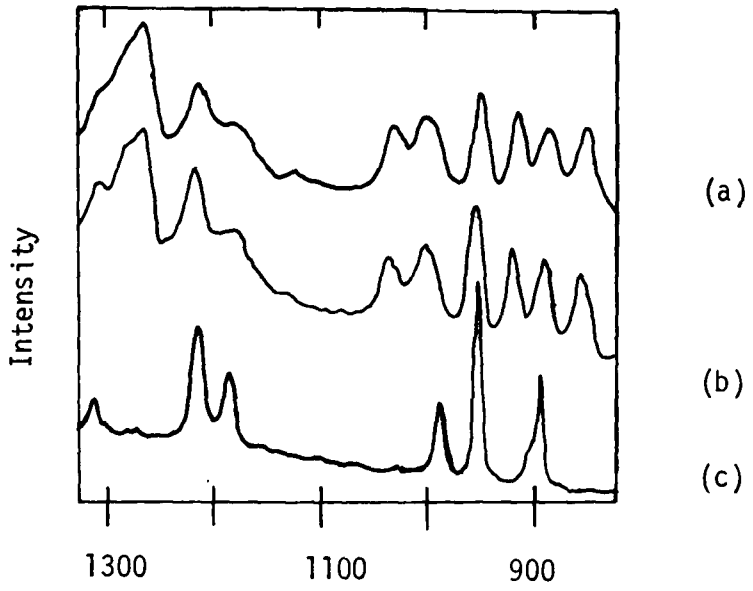

Diagram (3.4)
Raman Spectra of Dimethyl Fumarate between 1325 and 825 cm^{-1} (a) $202^{o}C$, (b) $118^{o}C$ and (c) annealed solid at $20^{o}C$.

melts at 202^{o} and $118^{o}C$ with the spectrum of the annealed solid at room temperature. Due to the low laser power used to record the spectra the bands are poorly resolved above 1100 cm^{-1} in the liquid spectra. However, a number of bands absent in the solid appear in the liquid spectra, at 1261, 1021, 1000, 912 and 851 cm^{-1}. Various pairs of bands were studied in an endeavour to relate intensity changes with temperature to conformational equilibria, and the most favourable pair was found to be at 950 and 915 cm^{-1}. Intensities of this pair between

+ 112° and 202°C provided a value for ΔH^{θ} of 3·24 ± 0·77 J mol^{-1}. This value is significantly larger than that found for the other esters and may be associated with the same stabalising features which cause this ester to exist as a solid at room temperature, although the detailed relationship between the (I) $\rightleftharpoons$(II) and solid$\rightleftharpoons$liquid equilibria is not understood.

Comparison of the Raman spectra of maleate esters, spectra (4 - 6) run as liquids and annealed solids does not show any pattern of bands absent in the solid due to conformational activity as in the case of the fumarate esters, agreeing with the previous i.r. study[69]. Both di-n-butyl and diethyl maleate show no differences apart from those expected on freezing a sample, such as solid state splitting and sharper bands.

On freezing dimethyl maleate two different solid state spectra can be obtained, shown in spectrum (4), by annealing the sample. It is assumed that the upper solid spectrum is due to a similar structure to that found in the liquid whereas the lower solid spectrum is due to a different solid state where the molecule is distorted from its normal liquid structure. One very weak liquid band at 1295 cm^{-1} is absent from both solid spectra but because no pattern of conformer bandd is observed as for dimethyl fumarate and no differences are reported in the i.r. spectra we have concluded the disappearance is due to a phase sensitive intensity change.

Table (3.1)

Vibrational Spectra of Fumarates (ν/cm^{-1})

Methyl Fumarate			Ethyl Fumarate			n-Butyl Fumarate		
I.r.	Raman	P	I.r.	Raman	P	I.r.	Raman	P
	204w	dp		172w	dp			
	275vw,sh	dp		250w	sp		225m	sp
	330vw	sp		348vw	sp		340w	sp
390vw	389vw	sp		384vw	sp		420w	sp
			520w	525vw			510w	mp
				555vvw			545vw	sp
			650w	650vw	dp		650vw	mp
661w			665w			667w		
	745w	sp		730vw	sp	734w	735vw	mp
770w	780w	dp	771w	782vw		771w	760vw	
							808w	mp
850sh	851m↓	sp	856w	864m↓	sp	835w	840m↓	sp
	888m↑	dp		890w	dp		890	dp
	902w,sh							
915w	912m↓	sp						
	950m↑	sp		935vw			949w	sp
976m			975m			975m		
1015sh	995w↑	mp		980w↑	sp		985w↑	mp
	1000m↓	dp		1025w↓	dp		1010vw	dp
1028m	1031w↓	mp	1033m	1032sh↓	dp	1021m	1025w↓	mp
			1090w↓	1092sh↓	sp	1058m	1061w	dp
			1100sh	1110w	sp	1125w	1122w	sp
1154s↓			1151s↓			1151s↓		
1170sh	1177w	mp	1174sh	1175w	sp	1171m,sh	1150w	sp

Table (3.1) Contd.

Methyl Fumarate			Ethyl Fumarate			n-Butyl Fumarate		
I.r.	Raman	P	I.r.	Raman	P	I.r.	Raman	P
1190sh	1182w	mp					1175w	sp
	1215m↑	sp		1203m↑	sp		1200m↑	sp
1225w↓			1221w↓			1220w↓		
1260m↓	1261m↓	sp	1256s↓	1259m↓	sp	1255s↓	1261m↓	sp
1270sh	1275m↓	sp		1275m	mp	1265sh	1277w↓	
1302s↑	1302w↑	dp	1292s↑	1300m,sh↑	dp	1291s↑	1300m↑	dp
			1364m	1363w	sp		1365w	sp
			1388sh	1390w	mp	1380w	1380w	sp
1438m	1435w	sp	1443w	1450m	dp		1450	dp
	1456w	dp						
			1642w	1460w	dp	1460m	1462m	
			1472sh	1477w	dp	1470m	1470m	
1640w↓	1640s↓	sp	1641w↓	1644m,sh↓	sp	1640w↓	1645sh↓	sp
	1655s↑	sp		1663s↑	sp		1662s↑	sp
1731s	1730s	sp	1720s	1726s	sp	1721s	1730s	sp
			2865w					
2840w	2851w	sp	2880w	2873w,sh	sp	2870w	2871s	sp
2900sh			2895sh			2890sh		
			2920w	2910w,sh	sp		2910s	mp
2950m	2959m	sp	2930sh	2936s	sp	2930sh	2932s	mp
2990w			2975m	2975s	sp	2955m	2957s,sh	mp
3055w,sh	3061m	sp	3060w	3060m	sp	3100w	3057m	sp
3440w			3430w			3430w		

Table (3.2)

Vibrational Spectra of Maleates (v/cm^{-1})

Methyl Maleate			Ethyl Maleate			n-Butyl Maleate		
I.r.	Raman	P	I.r.	Raman	P	I.r.	Raman	P
	180vw,sh			178w	mp		178vw,sh	
	245w	mp		244w	mp		244w	
				283w	dp		272vw	mp
	333w	mp		320w	sp		320w	sp
	350w	mp		385w	sp		380w	sp
	460w	mp		465w	mp		465vw	mp
				500vw			500vw	dp
	490w	sp		525w	sp		528vw	sp
600w	600w	sp	590w	600w	sp		588w	sp
720w	725vw	dp	715w	730w	dp	732vw	730vw	dp
			790sh	785w	sp			
812w	815w	mp	802w	800w	sp	809w	805w,sh	sp
			834w	833w	sp			sp
860w	862vs	sp	860w	861s	sp	840w	836s	sp
880w	885vvw			880w,sh	sp		875w,sh	sp
			910w	908w,sh	sp		904m	sp
935w	938vw	mp				945w	942sh	mp
990w	987w	mp	970w	975w	mp	960w	964w	mp
						980w		
						1002sh		
1004w	1002w	mp	1025m	1025w	dp	1020w	1016w	dp
			1090w	1096m,sh	sp	1060w	1056w	dp
			1108sh	1109m,	sp		1116w	sp
1160s	1160m	mp	1156s	1160w	mp	1161s	1160m	mp
	1182w,sh	mp						

Table (3.2) contd.

Methyl Maleate			Ethyl Maleate			n-Butyl Maleate		
I.r.	Raman	P	I.r.	Raman	P	I.r.	Raman	P
1215s	1215vvw		1208s	1209w	mp	1207s	1204w,sh	
							1224w,sh	dp
1246m			1244m			1243m		
				1270w	mp		1260w,sh	mp
1296m	1298vw	sp	1294m	1296w	mp	1290m	1298m	mp
			1364w	1363w,sh	mp	1375sh	1370w,sh	sp
1387m	1387w	mp	1380m	1380w,sh	mp	1375sh	1370w,sh	sp
			1400m	1400m	mp	1402m	1400w	mp
1435m	1438w,sh	mp	1441w				1430m,sh	dp
	1450w,	dp		1450m	mp		1445m	dp
			1470sh			1462w		
1642w	1645vs	sp	1640w	1645s	sp	1640w	1645s	sp
				1660m,sh	sp			
1730s	1730vs	sp	1725s	1725vs	sp	1728s	1725s	sp
2840w	2848w	sp	2870sh	2868w,sh	sp	2870sh	2868s	sp
2895sh	2900vw	sp	2895sh	2898w,sh	sp	2890sh	2909s	sp
2950w	2952s	sp	2930sh	2932s	sp	2930sh	2924s	sp
2995w	3004uw	mp	2975m	2968m	mp	2960m	2955m,sh	sp
3055w	3056m	sp	3055w	3052m	sp	3055w	3050w	sp
3440w			3435w			3440w		

* sp= strongly polarised; mp= medium polarised; dp= depolarised

Table (3.3)

Fundamental Frequencies of Fumarate and Maleate

(trans- and cis- ROO:CHC:CHC:OOR) Esters (cm^{-1})

Methyl	Ethyl	Butyl		VIBRATION		Methyl	Ethyl	Butyl
330	348	340	a_g	C-O-R sym bend	a'	333	320	320
389	384	420		C=C-C sym bend		460	465	465
	650	650		C-C-O sym bend		600	588	588
745	730	735		C=O sym bend		490	525	528
851	864	840		C-C sym Str.		862	861	836
995	980	985		O-R sym str.		1002	1025	1016
1177	1175	1150		C-H sym bend		1160	1160	1160
1215	1203	1200		C-O sym str.		1215	1209	1204
1655	1663	1662		C=C sym str.		1645	1645	1645
1730	1726	1730		C=O sym str		1730	1725	1725
3061	3060	3057		C-H sym str.		3056	3052	3050
			b_u	C-O-R asym bend				
				C=C-C asym bend				
	650			C-C-O asym bend		600	590	

Table (3.3) contd.

Methyl	Ethyl	Butyl		VIBRATION		Methyl	Ethyl	Butyl
661	665	667		C=O asym bend				
770	771	771		C-C asym str		812	802	809
1028	1033	1021		O-R asym str		1160	1156	1161
1270		1265		C-H asym bend		1246	1244	1243
1302	1292	1291		C-O asym str		1296	1294	1290
1731	1720	1721		C=O asym str		1730	1725	1728
3055	3060	3100		C-H asym str		3056	3052	3050
204	172		b_g	C-O-R sym torsion	a"		178	178
				C-C sym torsion				
745	730	734		C=O sym def				
888	890	890		C-H sym def		720	715	732
			a_u	C-O-R asym torsion				
				C-C asym torsion				
				C-O-C asym def				
661	665	667		C=O asym def				
976	975	975		C-H asym def				

CHAPTER IV

Variable Temperature Studies and Complete Vibrational Assignments of Butadiene and Isoprene

A Introduction

B Experimental

C Variable Temperature Studies

D Torsional Frequencies

E Vibrational Assignments

F High Resolution Gas Phase Studies

CHAPTER IV

Variable Temperature Vibrational Studies and Complete Vibrational Assignments of Butadiene and Isoprene

A. Introduction

Both butadiene[15-25] and isoprene [16,40,41] have been shown to exist predominantly in the s-trans conformation, but controversy exists over the structure of the high energy conformer, which may be s-cis or gauche. Some n.m.r. studies[31,32] have been interpreted to mean that the high energy conformer of both compounds is out-of-plane (gauche) whilst other n.m.r. work[30] indicates the butadiene high energy conformer to be planar. Theoretical studies by ab.initio Molecular Orbital techniques disagree on the structure of the high energy conformer. P.N. Skancke and J.E. Boggs[27] obtained results indicating a gauche form, whereas L. Radom and J.A. Pople[26] calculated that the s-cis form is more stable. Recently L.A. Carriera[21] has assigned low frequency gas phase Raman bands to overtones of the s-cis torsion and calculated the complete potential function for butadiene, and Kuznetsov assigned bands present in the gas phase Raman spectrum of isoprene to the s-cis conformer[16].

The variable temperature study described in this chapter does not support many of the previous conclusions, and enables revised thermodynamic functions to be calculated. (See chapter VIII).

Molecular models show that the rotation of the methyl group in s-trans isoprene is hindered by proximity to a vinyl hydrogen whereas s-cis isoprene shows no such steric hindrance. Hence we would expect

the methyl torsion to have a higher barrier in the s-trans conformer. Steric factors also suggest that the enthalpy difference between conformers, ΔH^{θ}, will be lower for isoprene than butadiene, as the steric hindrance will destabalise the s-trans conformer, but not the s-cis conformer.

B. Experimental

Raman spectra were recorded of liquid and solid samples as described in Chapter II. The Raman spectra of isoprene as a liquid at 20°C and solid at - 162°C are shown as Spectrum (7) in the Appendix.

Mid i.r. spectra were run on P.E. 457 and 521 instruments as gas, liquid solutions in CCl_4, solid and matrix isolated samples.

Far i.r. spectra were run for both compounds as gases, at 1 metre path length, and solutions in cyclohexane at 1mm path length. Spectra of liquid and solid isoprene were recorded in 0·1 mm polythene cells; but liquid and solid butadiene were not recorded due to difficulty in filling the cells, as butadiene is a gas at room temperature. Difficulty was found in drying the gases, as explained in Chapter II.

The complete vibrational spectrum of isoprene is given in table (4.2), but the spectrum of butadiene has not been tabulated as no significant new data was found.

C. Variable Temperature Studies

High temperature i.r. gas studies have been performed on butadiene[28] and isoprene[49], and bands have been assigned to the high energy conformers of both compounds on the basis of their temperature dependance. In this work the high temperature studies were repeated

and the studies extended to low temperatures to obtain sharper spectra and avoid possibilities of chemical changes.

Reznikova et.al. examined the i.r. spectrum of butadiene up to 130°C and assigned bands at 462m 565, 1125 and 1140 cm^{-1} to the s-cis conformer[28], and a value for ΔH^{θ} of 7·1 KJ mol^{-1} was calculated. Very little correspondence between the published data and the spectrum measured was found, and so the assignments and value of ΔH^{θ} cannot be supported. Low temperature i.r. and Raman spectra showed no temperature dependant bands which could be attributed to the high energy conformer.

Dzesshati et.al.[49] report marked increase in the high temperature i.r. spectrum of isoprene in the regions 500-575, 1210-1290 and 1490-1570 cm^{-1}, and obtain a value of ΔH^{θ} of 6·3 KJ mol^{-1}. In the present work the i.r. spectrum of isoprene was measured up to 480 K (at which point polymerisation was noted) and a marked increase in intensity was observed in the 1250-1290 cm^{-1} region only, a series of weak shoulders increased with a weak band at 1300 cm^{-1}. However, on freezing liquid samples these peaks do not disappear and so cannot be assigned to a high energy conformer. The 1300 cm^{-1} band is strong in the Raman in which no temperature dependance is apparent.

A liquid sample of isoprene at 0·5 mm path length was carefully examined over a range of low temperatures in the i.r. A very weak shoulder at 525 cm^{-1} increased on cooling and another very weak shoulder at 555 cm^{-1} disappeared. In the Raman a medium intensity band at 526 cm^{-1} has a weak shoulder at approximately 555 cm^{-1} which disappears on freezing, and so this was assigned as a pair of conformer bands

A series of 11 intensity measurements were made over the temperature range 136·5 - 306 K and using the equation (1.10) a value

for $\Delta H^{\theta} \pm \sigma$ of 4·59 ± 0·16 KJ mol^{-1} was obtained. Diagram (4.1) shows the plot of the experimental results, log (I_{555}/I_{526}) against 1/T.

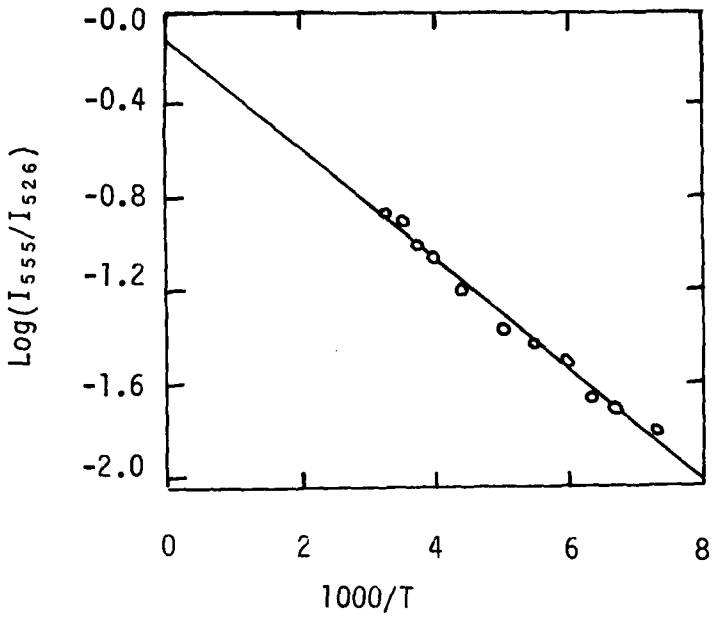

Diagram (4.1)
Plot of Log (I_{555}/I_{526}) Versus 1/T for Liquid Isoprene to Determine ΔH^{θ} using Equation (1.10).

D. Torsional Frequencies

The torsional frequencies of both gaseous butadiene and isoprene were first observed by W.E. Fateley et.al.[78] at low resolution, and barrier heights calculated. A.R.H. Cole et.al.[20] examined the torsion of butadiene at high resolution and assigned only the s-trans torsion with hot bands at lower frequency. L.A. Carriera located overtones of the s-cis torsion and hot bands in the Raman spectrum, leading to a value of approximately 137 cm^{-1} for the fundamental[21]. Carriera was

able to calculated the complete torsional function using this data and calculated ΔH^{θ} and the s-trans → s-cis barrier to be 10·4 and 30·0 KJ mol^{-1} respectively.

Examination of the far i.r. spectrum of butadiene gave results which agreed with those of Cole et.al[20].

The far i.r. spectrum of gaseous isoprene was found to be complex below 200 cm^{-1}. Only one asymmetric C-C torsion was located at 152·7 cm^{-1} with hot bands observed at approximately 150·7 and 149·6 cm^{-1}, this was assigned to the s-trans conformer.

Two close bands just below 200 cm^{-1} were assigned as 0 → 1 torsions of the methyl group. The stronger band at 199·3 cm^{-1} was assigned s-trans and the s-cis band assigned at 196·7 cm^{-1}. Diagram (4.2) shows these torsional fundamentals and the first hot bands of each torsion.

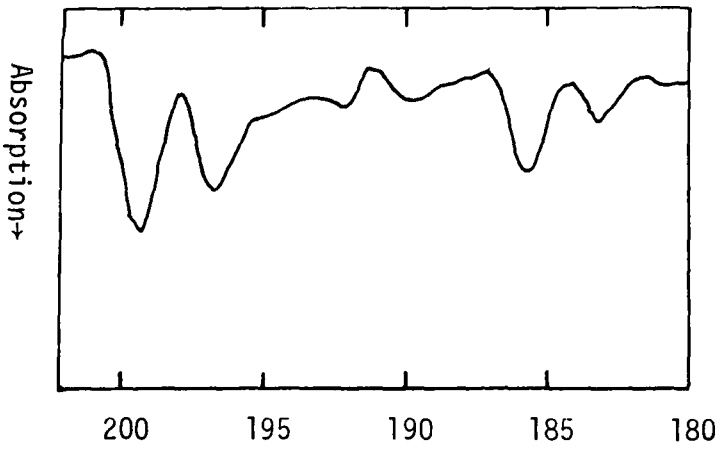

Diagram (4.2)
Far i.r. spectrum of gaseoue isoprene from 202 to 180 cm^{-1} showing the first two torsional frequencies of both conformers.

Using the frequencies of these 0 → 1 torsions frequencies of higher torsions were predicted for each conformer, using the Mathieu equation (7.16)[79,80]. Where possible the weak higher torsions were tentatively assigned, but this process was hindered by the presence of traces of water which we were unable to exclude. Table (4.1) compares

calculated and observed frequencies and the first two torsions of each conformer are shown in diagram (4.2).

Torsion	$\nu_{calc.}$	ν_{found}	ν_{calc}	ν_{found}
$0_A \longrightarrow 1_A$		199·3		196·7
$0_E \longrightarrow 1_E$				
$1_E \longrightarrow 2_E$	185·4	185·7	182·3	183·1
$1_A \longrightarrow 2_A$	185·3		182·2	
$2_A \longrightarrow 3_A$	169·9	170·5	166·4	165·3
$2_E \longrightarrow 3_E$	168·9	168·7	166·8	164·7
$3_E \longrightarrow 4_E$	151·6	a	147·5	146·5
$3_A \longrightarrow 4_A$	143·2	144·7	135·2	136·1
$4_A \longrightarrow 5_A$	154·1	155·5	158·2	b
$4_A \longrightarrow 6_A$	195·0	b	189·8	189·7

Table (4.1)
Methyl Torsions of Gaseoues Isoprene
a = Absorption by C-C torsion. b = Absorption by water vapour

To confirm the assignments the $0 \rightarrow 1$ assignments were reversed and an attempt to predict the higher torsions was again made. However, this test proved sensitive, and even the $1 \rightarrow 2$ torsions inaccurately predicted by 2·7 and 1·3 cm^{-1}, and these differences increased greatly to higher torsional levels.

The calculated barrier heights (see chapter VII) were 11·33 to 10·80 KJ mol^{-1} for s-trans and s-cis isoprene respectively.

An attempt to verify equation (1.37) relating hot band intensity and torsional frequency was made. The intensities of the asymmetric torsion of isoprene at 152·7 cm^{-1} and two hot bands were measured (in absorbance) to have relative values of 108, 62 and 24·5 mm. However,

the first hot band at 150·7 cm^{-1} is very close to a water vapour band at 150·5 cm^{-1} and so only the fundamental and second hot band intensities can be used. These give an average value for the torsional frequency of 155 ±20 cm^{-1}, agreeing well with the observed value of 152·7 cm^{-1}.

Intensity measurements on the methyl torsion hot bands did not give such good results. Intensities of the fundamental and first hot band of each conformer gave values for the s-trans and s-cis methyl torsion of 155 and 219 cm^{-1} respectively. It is noted that the higher torsions are much stronger than expected from the normal exponential fall off in intensity, and it is concluded that the extinction coefficients of the methyl torsions of molecules in different energy levels are not the same, and so equation (1.37) does not hold.

The same condition seems to hold for the C-C torsion of butadiene. Intensity measurements of the fundamental and first three hot bands give relative values of 39,31, 18 and 8·5mm. These lead to estimations of the torsional frequency of 48, 113 and 156 cm^{-1}. This indicates that the intensities are perturbed because the equation (1.37) does not hold due to variation in extinction coefficients.

E. Vibrational Assignments.

Butadiene belongs to the C_{2h} point group and so has a centre of symmetry as well as a plane of symmetry. This results in splitting the vibrational spectrum into Raman or i.r. active bands, like the fumarate esters, due to the rule of mutual exclusion. The 24 fundamentals fall into the following groups:-

$9A_g$ (in-plane, Raman, Polarised), $4A_u$ (out-of-plane, i.r.), $3B_g$ (out-of-plane, Raman, depolarised), $8B_u$ (in-plane, i.r.).

Careful examination of the Raman and i.r. spectra of butadiene from 40 - 4000 cm^{-1}, giving special regard to depolarisation and band contour data, supports existing assignments given by Yu.N. Panchenko[81,82]. The assignments and fundamental frequencies used in calculation of thermodynamic functions are presented in table (4.3). The frequencies have been slightly altered, especially in the C-H stretch region and several other values have been taken from work by A.R.H. Cole et.al.[19,20] who examined several bands at high resolution.

The isoprene molecule differs from butadiene by replacement of one of the hydrogens by a methyl group. This results in loss of the centre of symmetry found in butadiene and breakdown of the rule of mutual exclusion. Isoprene is a member of the C_s point group due to its plane of symmetry, as the methyl group has its orientation of lowest energy symmetric to the general molecular plane. The 33 fundamentals fall into the groups:- 22 A' (in-plane, polarised) and 11 A'' (out-of-plane, depolarised). All these bands should be active in both i.r. and Raman. However, it has been observed that the rule of exclusion is not lost altogether for molecules like isoprene[83] and chloroprene[84] where substitution is near the centre of symmetry; in practice bands are found to be weak in one mode and strong in the other. A good example of this observation is the strength of the 2 C=C stretching vibrations. One is strong in the i.r. and the other is strong in the Raman and so can be assigned as asymmetric and symmetric respectively. This effect has been used as evidence to show that isoprene is predominantly s-trans, as the s-cis conformer has no approximate centre of symmetry. The basic butadiene spectrum is altered by substitution of a methyl group to the isoprene spectrum in the following way:-

a) Loss of 1C-H stretch, 1 C-H bend, 1 cis wag and 1 trans wag.

b) Gain of two methyl rocks (1 o.p.), 1 o.p. methyl torsion, 3 methyl C-H stretches (1 o.p.), 3 methyl deformations (1 o.p.), 1 C-methyl stretch and 3 other skeletal modes (2 o.p.).

A''. The C-methyl and C-C torsions have already been discussed. The two out-of-plane skeletal modes are assigned at 412 and 401 cm^{-1} on the basis of their respective strong polarised Raman and strong C contour i.r. bands. The hydrogen wagging vibrations are easily located as strong i.r. bands with C contours at almost the same frequencies as the corresponding vibrations in butadiene. Methyl deformations and methyl rocks tend to vary in frequency, but many compounds with methyl compounds have been studied elsewhere and typical frequencies listed[85]. Vibrations with C band contours at 1071 and 1442 cm^{-1} have been assigned to the out-of-plane methyl rock and methyl deformation respectively. Methyl C-H stretching vibrations are found between about 2900 and 2970 cm^{-1}, in this region there are found two polarised and one polarised band.

A'. Most of the in-plane vibrations can be assigned close to their corresponding frequencies in butadiene. Difficulty was found in assigning the two $=CH_2$ rocking motions. The frequencies observed for butadiene are 892 and 985 cm^{-1} for the Raman (symmetric) and i.r. (asymmetric) rocks respectively. The polarised Raman band at 780 cm^{-1} in the spectrum of isoprene was assigned to the symmetric rock as the bands near 900 cm^{-1} were depolarised, corresponding to the out-of-plane $=CH_2$ wags.

Examination of a spectrum of a sample dispersed in an argon

matrix at 20K showed two bands at 982 and 990 cm^{-1} which are close at room temperature. The former band is the stronger characteristic trans wag and the latter is assigned to the asymmetric $=CH_2$ rock, close to the frequency in butadiene. In the Raman spectrum of the liquid only one medium polarised band is observed in this region due to the coincident polarised and depolarised vibrations.

Stretching frequencies of C-C bonds vary according to the environment. In butadiene the C-C stretch is a Raman active at 1203 cm^{-1}. Isoprene has two C-C stretches and these appear to be coupled as the central C-C stretch has been raised in frequency to 1291 cm^{-1}, and the C-methyl stretch has been assigned to a medium band at 950 cm^{-1}, strongly polarised in the Raman.

The in-plane methyl deformations, rock and C-H stretches have been assigned to polarised bands near to the corresponding out-of-plane frequencies.

The complete vibrational spectrum of isoprene is listed in table (4.2). The tentative assignments are listed alongside those of butadiene in table (4.3). No attempt has been made to assign the low frequency bending modes to specific vibrations.

Where isoprene fundamentals were observed as strong Raman bands, gaseous frequencies were taken from work by Kuznetsov et.al.[48].

F. High Resolution Gas Phase Studies

The torsional frequencies of both isoprene and butadiene have already been discussed in section D of this Chapter.

High resolution studies of butadiene have already been carried out on out-of-plane modes of butadiene. The very strong $=CH_2$ wag at

907·8 was studied by D.J. Marais et.al.[17] and more recently by A.R.H. Cole et.al.[19] at high resolution. Rotational fine structure was observed arising from both a fundamental and several hot bands due to higher torsional levels. J.F. Ogilvie and K.C. Cole[86] examined bands at 1013·3, 907·8, 524·5 and 1296·2 cm^{-1} at high resolution and observed Coriolis Coupling between the $=CH_2$ rock at 985 cm^{-1} with the $=CH_2$ wag at 907·8 cm^{-1} and the trans wag at 1013·2 cm^{-1}.

The i.r. spectrum of gaseous isoprene has not previously been examined at high resolution. A spectrum run at approximately 0·7 cm^{-1} resolution showed unresolved broadening to lower frequency on the Q bands of the vibrations at 891, 903, 990 and 1603 cm^{-1} which was concluded to be due to torsional hot bands.

The out-of-plane methyl rock at 1071 cm^{-1} is shown in diagram (4.3). This shows shoulders to high frequency at approximately 1071 and 1072 cm^{-1}, and a well resolved sharp band at 1069cm^{-1}. Relative intensities of these bands, in absorbance, are 65,25,10 and 20 mm respectively. From these intensities it is concluded that the bands at 1071 and 1072 are hot bands due to the methyl torsion at 199 cm^{-1} because use of equation (1.37) gives an average value for the torsional frequency of 195 ± 30 cm^{-1}. It is considered likely that the methyl torsion will affect the potential function of the out-of-plane methyl rock. The band at 1069 cm^{-1} appears too strong to be due to a hot band (giving a value for the torsional frequency of 246 ± 30 cm^{-1}) and so is assigned as a fundamental of the s-cis conformer.

The various out-of-plane modes of isoprene show no rotational fine structure. For the s-trans conformer the rotational constants A,B and C have respective values of 0·29, 0·14 and 0·09 cm^{-1} which gives κ a value of - 0·54. This indicates that the conformer is a poor approximation to a prolate rotor with a splitting of approximately 0·3 cm^{-1}.

Similarly s-cis isoprene is also a poor approximation to a prolate rotor with κ having a value of -0·69, and rotational spacing of 0·4 cm^{-1} is predicted. The predicted splittings of both conformers are therefore not resolvable on the spectrometer used.

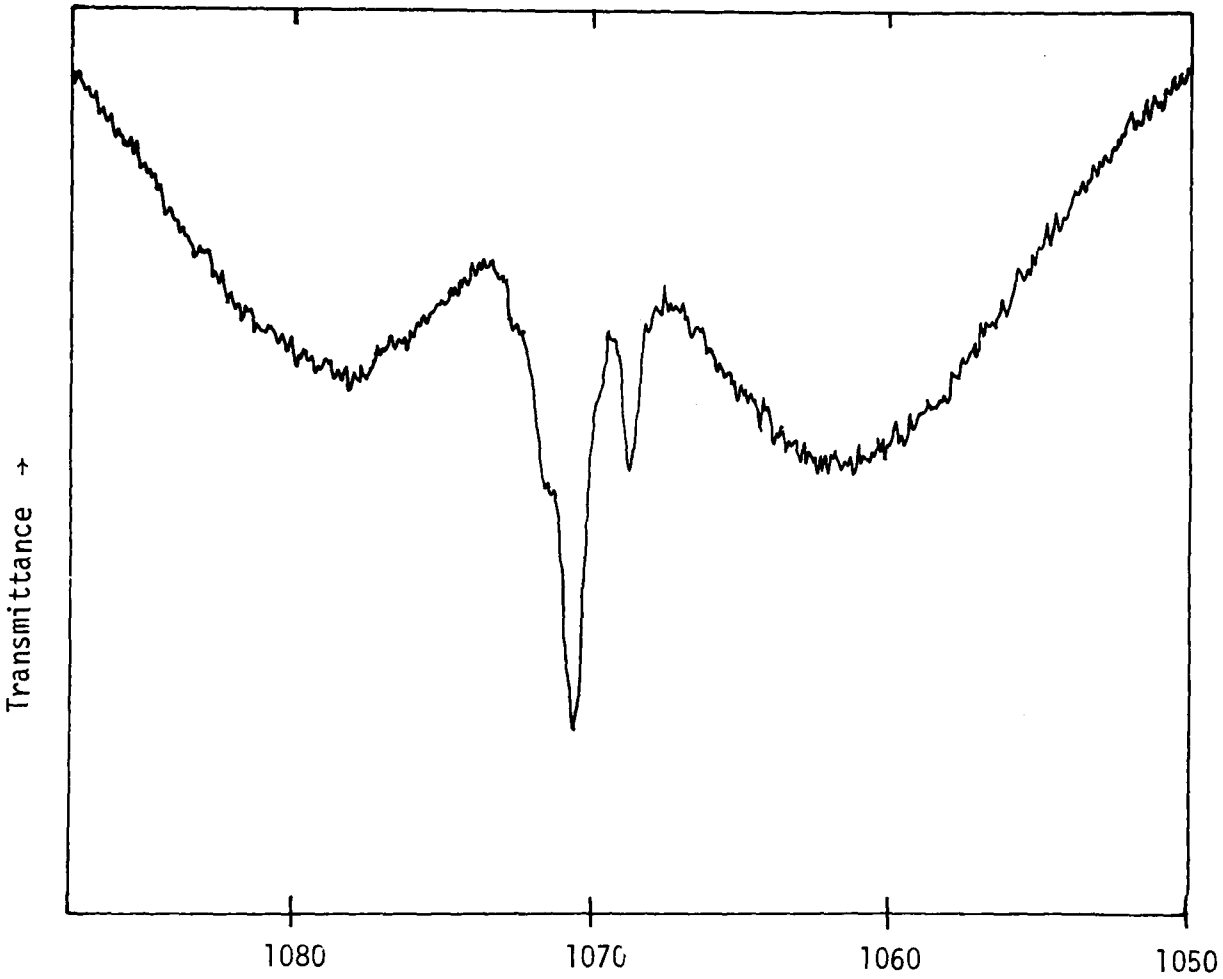

Diagram (4.3)
Spectrum of Gaseous Isoprene Between 1087 and 1050 cm^{-1} Showing the Out-of-Plane Methyl Rock

Table (4.2)

The Vibrational Spectrum of Isoprene

	Raman					Infrared							
	Liquid		Solid			Gas		Liquid		Solid		Con-tour
T	160	wsh	176	w	dp	153	vw	165	vw	181	vw	C
C						196.7	vw					C
T			210?	vw	-	199.3	vw	194	vw	209	vw	C
T	280	w	288	w	dp	288	w	287	w	287	w	B
C	311	wsh	-			311	vw	303	vw	-		
T	403	w	406	w	dp	401	m	403	s	400	m	
C	419	vw	-		dp			420?	wsh			
T	423	w	423	m	dp			425	vw	428	w	
C	435	wsh	-		sp			450?	vw			
	495	vw			sp			498	w	498	w	
T	526	m	527	s	sp			523	vw	530	w	
C	555	wsh	-		sp			555?	vw			
T	622	w	635	w	sp	622	w	630	w	625	w	
C	635	wsh	-		mp							
	700	vw	695	vw	p			690	vw	693	w	
T	756	wsh	761	vw	p	755	m	765	w	767	m	C
T	776	m	780	m	sp			783	vw	783	w	
	802	wsh	810	vw	sp			803	vw	809	w	
	820	wsh	830	vw	sp			830	vw	829	w	
T	892	m	900	m	dp	893	vs	887	vs	897	s	C
T	902					906	vs	904	s	912	s	C
T	950	m	949	m	sp			950	w	953	w	
T+T	991	w	991	w	sp	991·6	s	988	s	996	s	C
	1030	vw	1038	vw	sp	1040	w			1039	w	
C						1069	w					

Table (4.2) Continued.

	Raman			Infrared			
	Liquid	Solid		Gas	Liquid	Solid	Con-tour
T	1066 m	1063 m	mp	1071 m	1063 m	1063 m	C
T	1159 vw	1160? vw		1145 w	1158 w	1148 w	
	1210 vw	1210? vw		1205 vw	1210 vw	1215 vw	
		-		1245 vw	1246 vw	1246 w	
T	1288 s	1290 s	sp		1290 vw	1290 w	C
T	1295 wsh	1300 vw	mp	1303 w	1301 w	1301 m	
				1312 wsh	1306wsh	1306 w	
	1375 vw	1369 vw	dp	1375 w	1374wsh	1369 w	
T	1388 w	1390 vw	sp	1388 m	1379 m	1384 m	
		1400 vw		1405 w		1400 w	
T	1411 vw	1406 vw	p	1414 w	1412 w	1412 w	
T	1421 m	1420 m	sp	1425 w	1420 vw	1421 w	
T	1445 vw	1439 vw		1442 m	1440 m	1438 m	C
	1455 vw	1460 vw		1454 w	1453 vw	1462 w	
T	1467 vw	1464 vw		1466 w	1462 m	1465 m	C
	1475 vw	1475? vw		1475 w	1470 vw	1470 w	
	1549 vw	1559 vw	sp	1520 w		1520 w	
	1581 vw	1582 vw	sp			1585 w	
T	1599 vw	1596 w	sp	1603 s	1600 vs	1599 s	
T	1637 vs	1632 vs	sp	1645 w	1642 m	1638 m	
	1674 vw	1670 vw	sp	1660 w	1670 vw	1670 w	
				1790 w	1788 w	1800 w	
				1818 m	1826 w	1830 m	
	2731 w	2730 vw	sp			2730 w	
	2840 vw		sp			2838 w	

Table (4.2) Continued.

	Raman				Infrared			
	Liquid	Solid		Gas	Liquid	Solid	Con-tour
	2861 w	2861 vw	sp	2860 w	2860 w	2858 w	
T	2909 m	2905 m	sp	2910 w	2910 w	2916 w	
T	2933 m	2930 w	sp	2928 w	2925 w	2925 w	
T	2950 vw	2948 w	dp	2956 m	2954 m	2946 m	C?
T	2978 vw	2976 vw	mp	2978 m	2978 m	2979 m	
T	2986 w	2982 w	sp	2988wsh		2985wsh	
T	3009 s	3008 s	sp	3024 w	3007 m	3015 m	
T	3090 w	3087 w	mp	3092 s	3093 m	3096 m	
T	3095 m	3095 m	dp	3100? w	3100wsh		

NB. dp = depolarised, mp = medium polarised, sp = strongly polarised

Table (4.3)

The Fundamental Vibrations of Butadiene and Isoprene

Butadiene				Isoprene		
S-trans	S-trans	S-cis	Vibration	S-trans	S-cis	S-trans
A_u	163.7	137.4	C-C torsion	152.7	-	A''
			Me torsion	199.3	196.7	A''
B_u	299.7		i/p skel. mode	288	311	A'
			o/p skel. mode	401	419	A''
			o/p skel. mode	412*	435	A''
A_g	512		i/p skel. mode	523*	555	A'
A_u	524.5		o/p cis wag			
			i/p skel. mode	622	635	A'
B_g	753		o/p cis wag	755		A''
A_g	892		i/p $=CH_2$ rock	780*		A'
A_u	907.8		o/p $=CH_2$ wag	893		A''
B_g	910		o/p $=CH_2$ wag	906		A''
			C-C str	953*		A'
B_g	966		o/p trans wag			
B_u	985		i/p $=CH_2$ rock	991.6		A'
A_u	1013.2		o/p trans wag	991.6		A''
			o/p Me rock	1071	1069	A''
			i/p Me rock	1145		A'
A_g	1203		C-C str	1291*		A'
A_g	1278		C-H bend			
B_u	1296.2		C-H bend	1303		A'
B_u	1384		asym $=CH_2$ scissor	1388		A'

Table (4.3) Contd.

Butadiene			Isoprene	
S-trans	S-trans S-cis	Vibration	S-trans S-cis	S-trans
		i/p sym Me def	1414	A'
A_g	1438	sym $=CH_2$ scissor	1425	A'
		o/p asym Me def	1442	A''
		i/p asym Me def	1466	A'
B_u	1598	asym C=C str	1603	A'
A_g	1638	sym C=C str	1638	A'
		i/p sym Me str	2910	A'
		i/p asym Me str	2928	A'
		o/p asym Me str	2956	A''
B_u	2982	sym $=CH_2$ str	2978	A'
A_g	3008	sym $=CH_2$ str	2988	A'
A_g	3028	sym =CR-H str	3020*	A'
B_u	3056	asym =CR-H str		
B_u	3095	asym $=CH_2$ str	3092	A'
A_g	3102	asym $=CH_2$ str	3097*	A'

* Gas values from Ref. 48.

CHAPTER V

Variable Temperature Studies and Complete Vibrational Assignments of Cis-Pentadiene and Trans-Pentadiene

A. Introduction

B. Experimental

C. Variable Temperature and Matrix Isolation Studies

D. Vibrational Assignments

E. High Resolution Gas Phase Studies

CHAPTER V

Variable Temperature Studies and Complete Vibrational Assignments of Cis-Pentadiene and Trans-Pentadiene

A. Introduction

A microwave study of both compounds[42] has shown that in each case the predominant conformer is s-trans. The spectrum was searched for evidence of high energy conformers but none was found, and the methyl barrier heights were calculated to be 3·10 and 7·55 KJ mol^{-1} for cis- and trans-pentadiene respectively.

N.m.r. studies[31,87,88] on the pentadienes have been hampered by the complicated nature of the splitting of the spectrum. However, a variable temperature n.m.r. study[31] on butadiene, isoprene and both pentadienes reported a temperature dependence of certain coupling constants for all compounds studied, except cis-pentadiene. These results were explained using an equilibrium between a planar s-trans and 90^{o} out-of-plane structure. Thermodynamic calculations on butadiene in chapter (VIII) suggest that the high energy conformer is planar s-cis.

A kinetic study on the Diels Alder reaction of the pentadienes and other dienes with maleic anhydride indicated that trans-pentadiene can easily convert from s-trans to the s-cis conformer required for the reaction, but cis-pentadiene only reacts under forcing conditions because the s-cis conformer suffers steric hindrance. This also explains why no temperature dependence[31] of n.m.r. coupling constants of cis-pentadiene was observed.

The i.r. spectrum of the gaseous pentadienes was first observed by R.S. Rasmussen and R.R. Brattain[89]. N.V. Tarasova and L.M. Sverdlov[90] attempted to fit this data[89] and Raman data from previous works[91,92] to calculate values of the vibrational frequencies. The spectral data is incomplete, one Raman study was carried out on a mixture of the pentadienes[92] and so band overlap hindered assignment, also no estimates were made for the frequencies of the methyl torsions in the theoretical study[90].

In this work the compounds were examined separately, and the Raman frequencies given differ from those previously reported. Complete vibrational spectra of cis- and trans-pentadiene over a range of temperatures and phases are given in tables (5.1) and (5.2), and the selected assignments are shown in table (5.3).

B. Experimental

Samples of 99% purity were obtained from Fluka Chemicals, Switzerland, in sealed ampoules and used without further purification.

Raman spectra of liquid and solid samples were recorded as described in chapter (II).

I.r. spectra were recorded on the P.E. 580 between 180 and 4000 cm^{-1}. Gas samples were held in a 20 cm cell between either KBr or polyethylene windows, liquid samples in CsI Polyethylene cells and solid samples in a KRS5 cell of various thicknesses. A high temperature gas cell of 10 cm path length was used to record the spectrum at temperatures up to 200^{o}C.

C. Variable Temperature and Matrix Isolation Studies

The Raman and i.r. spectra of both compounds were recorded over a range of liquid temperatures from the melting point to above room temperature. The liquids were frozen and solid spectra recorded at liquid nitrogen temperature after careful annealing. High temperature gas i.r. spectra were recorded up to 200°C.

No peaks present in liquid spectra of either compound were absent in the solid spectra in Raman or i.r. and no weak peaks in the liquid or gas spectra intensified on heating. These results lead to the conclusion that neither compound exists as a measurable mixture of conformers.

I.r. spectra of samples deposited in an inert Argon matrix at 20K were recorded over a range of concentrations 100:1 (Matrix:sample) to 1000:1. The mixtures were sprayed slowly on to the cold window and spectra run at medium (2 cm^{-1}) resolution. Then the window temperature was raised slowly with repeat recording. No spectral changes were observed until new peaks appeared (at approx. 35K) which were assumed to be due to aggregation of the sample molecules as the matrix degraded.

No marked differences either in band frequencies or intensities were noticed by altering the matrix sample ratio, except that higher ratios enabled sharper peaks, and better resolution. The frequencies given in tables (5.1) and (5.2) refer to the highest matrix:sample ratio where the peak was observable.

D. Assignments

Assignment of the fundamental vibrations of both compounds is simplified by the planar nature of the molecules which causes the 33

fundamentals to be all i.r. and Raman active and fall into two species. There are 22 A' in-plane polarised vibrations and 11 A" out-of-plane depolarised vibrations, the latter are expected to give C type gas band contours. The assignments follow the assignments of butadiene and isoprene in Chapter (IV).

A" The central C-C torsion was assigned to the weak depolarised Raman band present at 150 and 140 cm^{-1} in the liquid spectrum of trans- and cis pentadiene respectively, which compares with the values obtained for butadiene and isoprene of 160 and 165 cm^{-1} in the liquid state. Methyl torsions are usually weak in the i.r. spectrum, and the corresponding Raman peaks are usually weaker still. The torsion in liquid s-trans isoprene was observed at 194 cm^{-1} only in the i.r., but the solid showed weak bands at about 209 cm^{-1} in both i.r. and Raman which were assigned to the methyl torsion. Diagrams (5.1) and (5.2) show the low frequency Raman and i.r. spectra of the pentadienes. In cis-pentadiene the liquid shows a broad peak in the i.r. at 228 cm^{-1}, and the Raman shows a depolarised band at 214 cm^{-1}. The i.r. active band has been assigned as the torsion, the other mode is another A" skeletal frequency. Similarly trans-pentadiene shows two liquid bands, one i.r. band at 205 cm^{-1} assigned as the torsion and the Raman band at 202 cm^{-1} assigned as a skeletal mode. In both compounds the Raman liquid band assigned as a skeletal frequency sharpens and strengthens considerably on cooling, unlike a torsional frequency.

The remaining A" fundamentals were located by their sharp C contours in the gas phase and depolarised nature in the Raman. Most of these vibrations had frequencies very close to those observed in isoprene, the only exceptions being the cis wags. These vibrations tend to shift frequencies in similar molecules and are often difficult to locate. Strong i.r. gas bands at 621 and 777 cm^{-1} were assigned

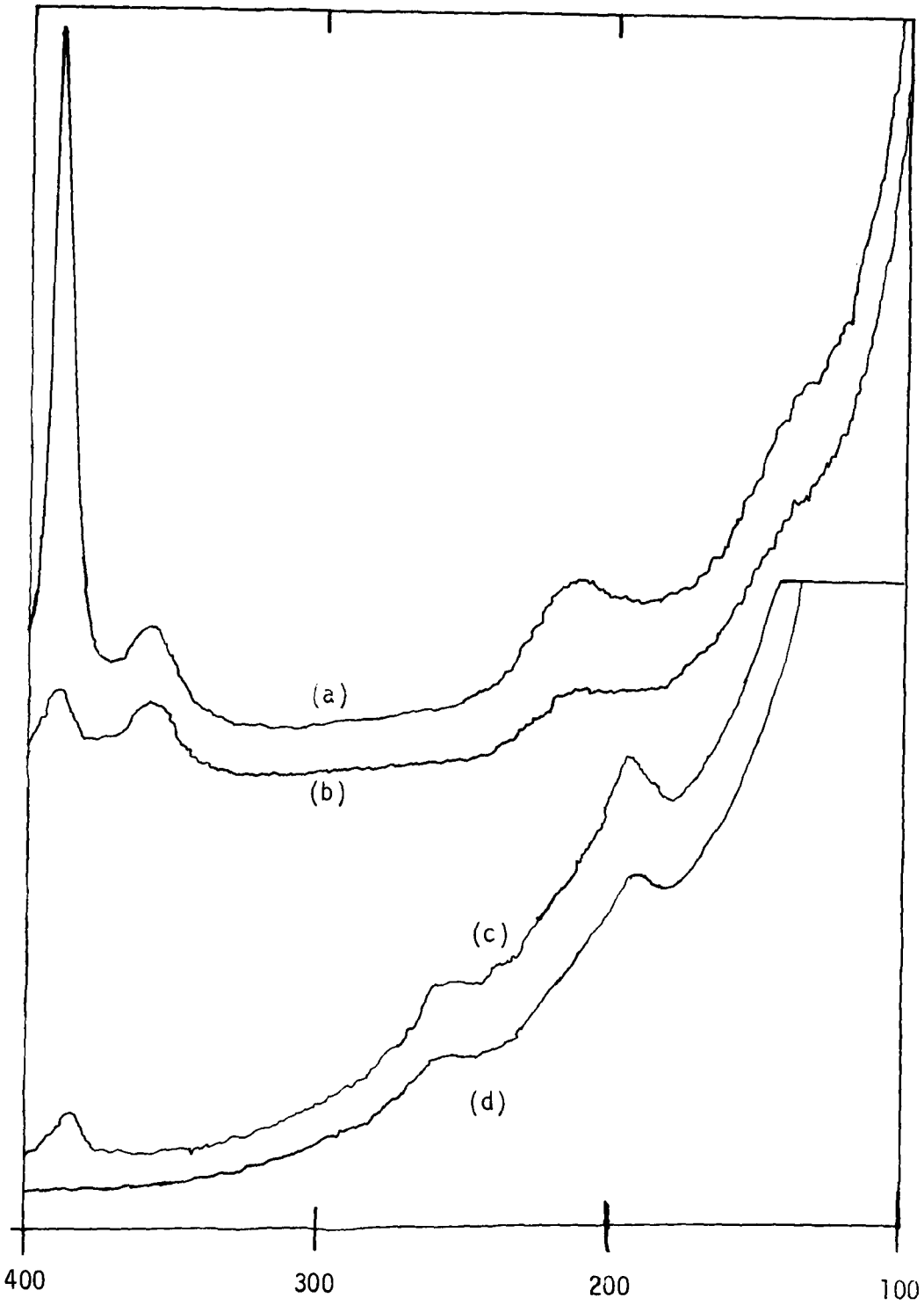

Diagram (5.1)
Polarised Raman Spectra of Cis-Pentadiene (a) 0^{o} (b) 90^{o} and Trans-Pentadiene (c) 0^{o} (d) 90^{o}.

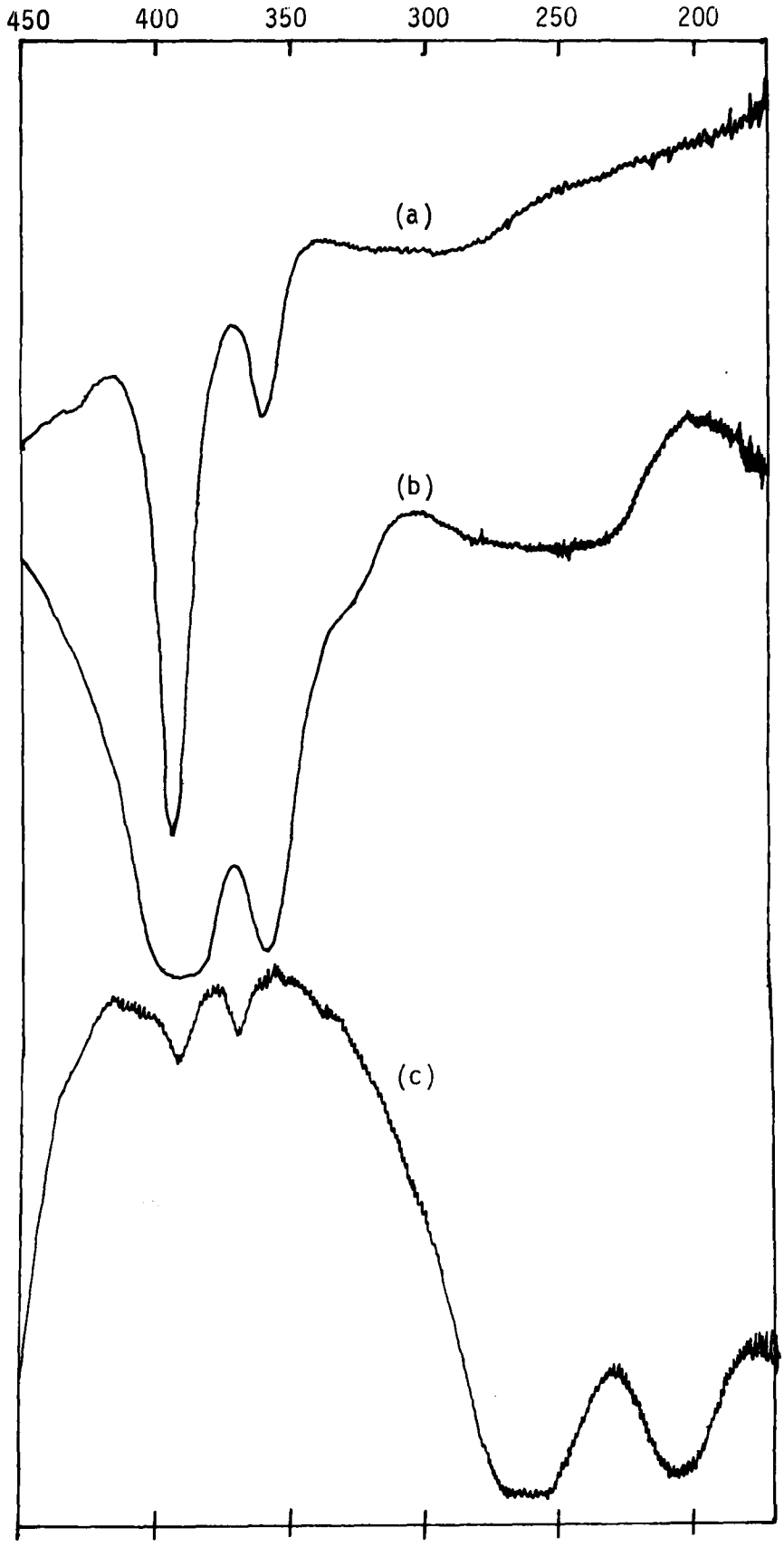

Diagram (5.2)
I.r. Spectra in Transmittance between 450 and 170 cm^{-1}.
(a) Empty Polyethylene Cell, (b) 1mm Liquid Sample of Cis-Pentadiene and (c) Trans-Pentadiene Under the Same Conditions.

to these wags in the cis-pentadiene, (755 cm^{-1} was assigned to the sole isoprene cis wag). Two weak C contour gas bands are observed in the spectrum of trans-pentadiene at 698 and 818 cm^{-1}. The former was assigned as the cis wag, the 818 cm^{-1} band is slightly stronger but the frequency is rather high. This band could be a combination of two A' modes 383 + 454 = 837 cm^{-1}.

A' No attempt to characterise the low frequency skeletal modes has been made. Butadiene has two $=CH_2$ rocking modes at 892 and 985 cm^{-1}, and a medium band in the Raman spectrum of isoprene at 780 cm^{-1} was assigned to the $=CH_2$ rock. Weak i.r. bands at 873 and 977 have been tentatively assigned to these rocks in cis- and trans-pentadiene as these frequencies are similar to those in butadiene. These rocking frequencies are dependant on environment and their frequencies often differ in similar compounds.

The two C-C stretches in each molecule are difficult to assign. In isoprene coupling of these modes was noted which raised thestretch of the =C-C= bond from the butadiene value of 1203 to 1298 cm^{-1} in isoprene, still keeping the character of a Raman active band. In the pentadienes medium Raman bands are found at 1180 and 1166 which are weak in the i.r. and so are assigned to these stretches. Similarly the C- Me stretch at 953 in isoprene was found to be stronger in the Raman than i.r., but this condition appears to have been lost in the pentadienes as the methyl group is no longer in the centre of the molecule. Tentative assignments have been made to weak bands at 954 and 1,082 cm^{-1} for cis-pentadiene and trans-pentadiene.

The remaining in-plane vibrations have frequencies close to those assigned in isoprene.

A comparison of the assignments of trans- and cis-pentadiene is given in table (5.3).

E. High Resolution Gas Phase Studies

Both Compounds were studied at high resolution in the gas phase in order to find any rotational fine structure, or hot bands due to the torsional energy levels, on bands with sharp Q bands as discussed in chapter I. Resolution of up to 0·6 cm^{-1} was available using the P.E. 580 in scan mode 9B.

Both trans-pentadiene and cis-pentadiene approximate well to prolate symmetric rotors with values of κ of -0·99 for trans- and -0·95 for cis-pentadiene respectively, using the rotational constants A,B, and C calculated by microwave spectroscopy[42]. The spacing between rotational sub-bands is predicted to be 2(A - B) for a prolate rotor, giving a value of 1·74 cm^{-1} for trans-pentadiene, and 0·86 cm^{-1} for cis-pentadiene.

Trans-pentadiene shows rotational fine structure on all the bands with strong Q branches. Diagram (5.3) shows the rotational structure present on the trans wag at 1003 and $=CH_2$ wag at 899 cm^{-1}. A plot of 9 peaks between 1005 and 1020 cm^{-1} gave a good straight line of slope 1·73 cm^{-1}. Rotational satellite bands on other vibrational bands gave slopes of 1·77 (5 peaks on the trans wag at 949 cm^{-1}) and 1·62 (18 peaks on the non fundamental peak at 818 cm^{-1}). These results confirm that the predominant structure of trans-pentadiene is the s-trans conformer, as the experimental results agree with the theoretically predicted spacing. The s-cis conformer is also a reasonable approximation to a prolate rotor with κ = -0·96 but has a value for the rotational spacing of 1 cm^{-1}, which is lower than the spacing observed.

Cis-pentadiene shows no rotational sub-bands on any of the Q bands at the resolution available. The reason for the absence of any rotat-

ional spacing is not clear. One possibility is that the steric hindrance postulated for the methyl group puts a strain on the molecule which flexes continually and is not a rigid rotor. The Q bands on all the out-of-plane vibrations are broader than those of trans-pentadiene, which is probably due to the same cause as the lack of rotational spacing.

Hot bands due to torsional levels were observed for both compounds on the strong Q bands of some vibrations, but not all. The spectrum of trans-pentadiene showed no hot bands on the sharp Q bands at 948 and 899 cm^{-1}, but evidence of hot bands at lower frequency than the fundamental is present on the bands at 1003, shown in figure (5.3), 818 and 698 cm^{-1}. The very sharp, weak cis wag at 697·3 cm^{-1} shows hot bands at 696·5 and 695 cm^{-1} which are progressively weaker. The band was recorded four times on scan mode 10B, giving resolution of about 0·6 cm^{-1} in this region, and the average intensities of the 3 bands measured as 184, 55 and 15 mm respectively, whilst the noise level was approximately 10 mm. Using the method described in Chapter I these intensities were used to calculate values for the vibrational frequency of 252 and 271 cm^{-1}, the first value is more precise due to the relatively lower noise level. This indicates that the cis wag is affected by the population levels of the out-of-plane skeletal mode at 250 cm^{-1}.

The weak band at 818·0 cm^{-1} is broader than that at 697 cm^{-1}. The intensities of these bands gave values for the torsional frequency of 44, 70 and 96 cm^{-1} which indicates that the intensities are either enhanced or that a different effect is observed. However this band is probably a combination of the in-plane fundamentals at 383 + 454 = 837 cm^{-1}, which may not couple with out-of-plane frequencies.

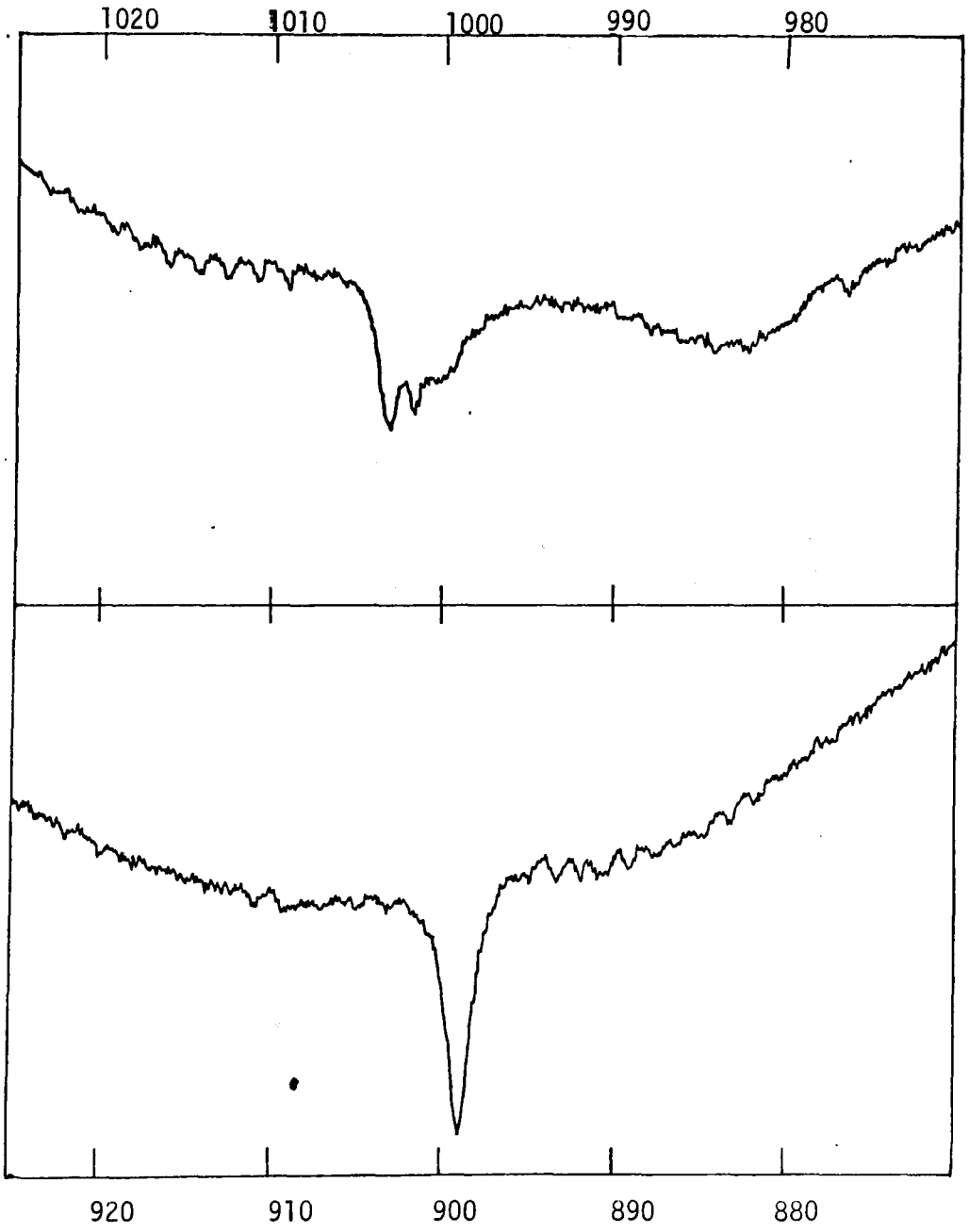

Diagram (5.3)

High Resolution I.r. Spectrum of Gaseous Trans-Pentadiene
(a) Trans wag at 1003 cm^{-1} (b) $=CH_2$ wag at 899 cm^{-1}.

The very strong trans wag at 1003.3 shown in figure (5.3) shows a relatively broad unresolved Q band with what is either a resolved hot band or a rotational sub-band at 1002·3 cm^{-1}.

The spectrum of cis-pentadiene shows no hot bands on the strong $=CH_2$ wag at 905 cm^{-1}, but other out-of-plane vibrations at 997, 777 and 621 cm^{-1} bands are not resolvable but the 777·0 cm^{-1} band has a strong well resolved hot band at 775·9 cm^{-1}, and a very weak hot band at 774·5 cm^{-1}. However these bands are close to the in-plane fundamental at approximately 772 cm^{-1} and accurate intensity measurement is not possible, especially as the first hot band appears to be stronger than expected.

Table (5.1)

The Vibrational Spectrum of Cis Pentadiene

Raman			Infrared					
Liquid	Solid	P	Contour	Gas	Liquid	Solid	M/I	
140 vw Br	158	dp						A"
214 vw	230	dp						A"
				212 vw	228 Br vw			A"
	310 vvw							
359 vw	361 m	dp	C	353 vw	358 vw			A"
390 m	394 s	sp	B	385 m	391 m	388 m	390 w	A'
482 vvw	480 vvw	sp		484 vvw	490 vvw			A'
612 w	610 w	sp		605 wsh	610 wsh	610 msh	610 m	A'
622 w	630 w	dp	C	621 s	623 s	631 s	633 s	A"
765 w Br	765 vw	sp		772 wsh		765 wsh		A'
776 w	780 w	dp	C	777 s	774 s	775 s	782 m	A"
					850 vw			
886 m	885 w	sp		893 w	886 wsh	882 wsh	881 w	A'
905 w	907 w	dp	C	905 vs	905 vs	902 vs	905 s	A"
				954 w)				
955	960 w	mp		958 w)	955 m	953 m	951 m	A'
	1000 vw		C	997 s	996 s	997 s	1004 s	A"
1035 w	1032 w	dp		1035 w	1030 w	1030 w	1031 w	A"
1043 w	1043 w	p		1055 br	1045 vw	1045 vw	1043 vw	
			B	1127	1129 w	1133 vw		A'
1166 m	1165 m	p		1166 w	1163 w	1163 w	1164 w	A'
1252 s	1251	p		1251 w	1250 w	1250 w	1250 w	A'
1297 s	1295 m	sp		1297 w	1295 w	1294 w	1294 w	A'

Table (5.1) contd.

Raman			Infrared					
Liquid	Solid	P	Con-tour	Gas	Liquid	Solid	M/I	
1361 w	1359 w	p		1358 w	1358 w	1357 m	1356 m	A'
1385 m	1384 m	sp		1390 m	1384 m	1381 m	1380 m	A'
1439 w	1440	mp	A	1437 m	1433 s	1432 s	1433 s	A'
1453 m	1451 vw	dp		1452 w	1449 w	1450 w	1450 m	A"
	1540 vw			1530 w	1530 w	1530 w		
	1578 vw			1575 w	1577 w	1580 w		
1594 m	1594 m	sp	A	1603	1595 s	1596 s	1592 s	A'
1645 vs	1643 vs	sp	A	1655	1645 m	1646 m	1642 m	A'
1745 vvw	1745 vvw	p		1736 w	1730 w	1730 w		
1769 w	1768 w	sp		1775 w	1776 w	1776 w		
				1819 m	1810 m	1812 m	1820 w	
1907 w	1906 w	sp	A	1987 w	1988	1990 w	1992 w	
2861	2863	sp		2874 m	2864 m	2862 m	2858 w	
2893	2888	p		2899 vw	2894 w	2892 w	2893 w	
2918 m	2910 m	sp		2928 m	2922 m	2920 m	2918 m	A'
2940 vw	2938 vw	dp	C?	2949 w	2940 wsh	2940 w	2937 m	A"
2969 w	2964 w	p		2970 vw	2970 w	2972 w	2965 w	A'
							2982 w	
2992 w	2998 w	sp		2990 wsh	2994 w	2997 w	2991 w	A'
3010 s	3005 s	sp		3012 wsh			3010 w	A'
3020 wsh			B	3033 s	3024 s	3022 s	3021 m	A'
3052 vw	3050 vw	p		3068 w	3054 w	3058 w	3057 w	A'
3087	3082 m	mp	B	3097 m	3089 m	3090 m	3082 m	A'

Table (5.2)

The Vibrational Spectrum of Trans Pentadiene

Raman			Infrared					
Liquid	Solid	P	Con-tour	Gas	Liquid	Solid	M/I	
	112 w	-						
150 vw	156 vw	dp						A"
202 vw	203 w	dp		196 vw				A"
	210 vwsh	dp		205 vw	205 vw			A"
265 w	268 w	dp	C	250 m	262 m			A"
392 vw		sp		383 vw	390 vw			A'
450 vw	449 vw	mp	B?	454 w	453 w	450 w	452 vw	A'
479 s	483 s	sp		483 vw	489 vw			A'
522 w	516 w	sp		530 vw				
					600 wsh		600 vw	
				630 w	631 m	632 w	630 w	A'
			C	698 w	700 wsh	700 w	700 w	A"
742 vw		sp			739 vvw	737 w		
818 w	820 w	dp	C	818 w	817 m	817 m	818 m	
898 w	892 w	dp	C	899.0s	896 s	892 s	896 vs	A"
944 vvw		mp	C	948.5m	948 m	948 m	948 m	A"
978 vw	975 vw	mp		977 w	976 wsh	973 m	974 w	A'
			C	1003.3vs	1000 s	1000 s	1004 vs	A"
1037	1034 w	dp	C	1048 vw	1040 vwsh	1035 wsh	1037 w	A"
1082 w	1078 vw	sp			1070 vwsh			A'
1170 wsh	1174 wsh	mp			1160 wsh	1175 wsh	1176 w	A'
1180 m	1184 m	sp			1183 w	1185 w	1188 w	A'

Table (5.2) contd.

Raman			Infrared					
Liquid	Solid	P	Con-tour	Gas	Liquid	Solid	M/I	
1262 wsh	1272 wsh	p			1269 w	1269 w	1269 w	
1279 s	1292 s	sp		1280	1280 wsh	1292 wsh	1290 w	A'
1323 vwsh		p			1306 m	1306 m	1307 m	A'
					1350 vwsh			
1378 w					1376 m	1374 m	1379 m	A'
1415 w		p	A/B	1420	1413 m	1411 m	1412 m	A'
1432 vwsh		dp			1435 wsh	1433 m	1436 m	A"
1452 w		p			1449 m	1448 m	1449 m	A'
					1526 w	1528 w		
1599 w		sp		1608 m	1602 m	1604 s	1606 m	A'
1653 vs		sp	B	1660 m	1653 m	1657 m	1653 m	A'
					1700 w			
					1723 w			
				1770 w	1762 w	1768 w		
			B	1802 m	1796 m	1800 m	1793 m	
				1850 w	1850 w	1856 w	1854 w	
2734 w	2730 w	sp	B	2742 w	2735 w	2733 w	2735 w	
2855 w	2855 w	sp	B	2867 w	2855 m	2852 m	2856 m	
2887 w	2887 w	sp	B	2899 w	2885 m	2885 m	2888 m	
2918 s	2916 s	sp	B?	2931 m	2917 m	2918 m	2922 m	A'
2937 wsh	2935 w	dp	C?	2946 w	2935 m	2937 m	2942 m	A"
2967 vw	2970 w		B	2973 m	2964 m	2963 m	2973 m	A'
					2980 wsh	2980 wsh	2980 wsh	A'
2997 s	3000 s	sp						
3012 vwsh	3015 vwsh	p	B	3018 s	3013 s	3014 s	3016 s	A'
	3035 vw			3050 wsh	3035 m	3039 m	3041 m	A'
3092 w	3088 m	sp	A/B	3098 m	3090 m	3090 m	3092 m	A'

Table (5.3)

Fundamental Frequencies of Trans- and Cis-Pentadiene (cm^{-1}).

Trans-Pentadiene	V I B R A T I O N	Cis-Pentadiene
	A" out-of-plane vibrations	
150 (L)	= C - C = torsion	140 (L)
196	skeletal mode	214 (L)
205	methyl torsion	212
250	skeletal mode	353
698	cis CH = CH wag	621
-	cis CH = CH wag	777
899.0	= CH_2 wag	905
948·5	trans CH = CH wag	997
1003·3	trans CH = CH wag	-
1048	methyl rock	1035
1435 (L)	methyl deformation	1452
2946	methyl C-H stretch	2949
	A' in-plane vibrations	
383	skeletal mode	385
454	skeletal mode	484
483	skeletal mode	612 (L)
630	skeletal mode	772
977	= CH_2rock	893
1082 (L)	C - CH_3 stretch	954

Table (5.3) Contd.

Trans-Pentadiene	V I B R A T I O N	Cis-Pentadiene
	A' in plane vibrations	
1170 (L)	methyl rock	1127
1180	= C - C = stretch	1166
1280	- CH = bend	1251
1306 (L)	- CH = bend	1297
1376 (L)	methyl sym deformation	1358
1420	= CH_2 scissor	1390
1449 (L)	methyl asym deformation	1437
1608	C = C asym stretch	1603
1660	C = C sym stretch	1655
2931	sym methyl C-H stretch	2928
2973	asym methyl C-H stretch	2970
2980 (L)	sym =C-H stretch	2990
2997 (L)	sym =C-H stretch	3010 (L)
3018	sym -CH= stretch	3033
3050	asym - CH= stretch	3068
3098	asym = C-H stretch	3097

CHAPTER VI

Infrared Spectra and Complete Vibrational Assignments of Chloroprene and Acryloyl Chloride

A. Introduction

B. Experimental

C. Gas Phase and Matrix Isolation Spectra of Chloroprene

D. Gas Phase Spectra of Acryloyl Chloride

E. Assignments

F. Conclusions

CHAPTER VI

Infrared Spectra and Vibrational Assignments of Chloroprene and Acryloyl Chloride

A. Introduction

The predominant structure of chloroprene was assigned as s-trans by i.r. spectroscopy[45,84]. The spectrum of chloroprene has bands which are strong in the Raman or i.r., but not in both, indicating that its structure is similar to butadiene and 2,3-dichlorobutadiene which are both s-trans. This has been taken as evidence that both isoprene[83] and chloroprene[84] are predominantly s-trans. The spectra of both liquid and solid chloroprene were studied by G.J. Szasz and N. Sheppard[45]. One very weak liquid band at 1127 cm^{-1} was absent in the solid spectrum, and another at 1632 cm^{-1} diminished in intensity. These results were taken as evidence of a high energy conformer, but a value for ΔH^{θ} could not be calculated although a minimum value of about 2 Kcal mol^{-1} was postulated.

The structure of the predominant conformer was verified by an electron diffraction study[93], although the results indicated that the structure might be skewed off s-trans. No attempt to interpret the results on the basis of an equilibrium between conformers was considered.

The low frequency vibrations of gaseous chloroprene were studied[44] below 800 cm^{-1} and 8 fundamental vibrations assigned in this region. The barrier height, V*, for the C-C torsion was calculated[78] as 31.7 Kcal mol^{-1}.

The vibrational frequencies of chloroprene have been calculated from force constants in two studies[94,95], and there is little difference in the calculated values. Using these calculated frequencies, a

complete assignment was made by R.A. Munos and Y.N. Panchenko[94], except for the cis wag which was assumed to be hidden under the strong C-Cl stretch.

A p.m.r. study[96] gave no evidence of a high energy conformer but noted that the s-trans conformer may be stabilised relative to butadiene by an attractive interaction between the chlorine atom and the nearest hydrogen on carbon 4. This would explain the high barrier to rotation in chloroprene relative to butadiene[78].

The predominant conformer of acryloyl chloride was found to be s-trans by microwave spectroscopy[59], lines possibly due to a second conformer were observed but not assigned.

The vibrational spectra of acryloyl chloride contain bands assigned to a high energy conformer[60,61]. A value for ΔH^{θ} of 600 cal mol^{-1} for the difference in energy between conformers was obtained for the gaseous state[60]. A matrix isolation i.r. study[61] gave a complete assignment for the s-trans conformer and listed different frequencies for most of the high energy conformer fundamentals, which was assumed to be s-cis as was the high energy form of acryloyl fluoride.[57]

The strong i.r. bands of the out-of-plane C-H bending modes of a range of α,β - unsaturated carbonyl compounds have been examined in order to correlate changes in bending frequency with substituent group[97]. The frequencies selected for acryloyl chloride differ slightly from those in the matrix isolation study[61].

B. Experimental

The mid i.r. spectra of samples of both compounds were examined on the PE. 580. Samples of chloroprene were examined as solids, liquids, gases and solutions in CS_2 and CCl_4. Gaseous samples only of acryloyl

chloride were studied. Gas spectra were recorded on scan mode 9B giving up to 0.6 cm^{-1} resolution, using a 10 cm KBr cell, or in a 10 cm polythene cell down to 170 cm^{-1}. Spectra of chloroprene samples isolated in a low temperature Argon matrix were recorded as described in Chapter II using matrix:sample ratios from 100:1 to 2000:1.

C. Gas Phase and Matrix Isolation Spectra of Chloroprene

A low temperature i.r. study on chloroprene by G.J. Szasz and N. Sheppard[45] reported that a very weak liquid band at 1127 cm^{-1} was absent in the solid spectrum. This observation was confirmed in the present work, also another weak liquid band at about 690 cm^{-1} disappeared in the solid state. This is taken as evidence of the existence of a high energy conformer, but it is not possible to assign either peak unambiguously to a specific vibration and so it is not possible to measure ΔH^{θ}.

In the liquid spectrum the C-Cl stretch at 630 cm^{-1} is intense and broad but on freezing this band sharpens to reveal a weak band at 660 cm^{-1} which is probably the cis wag expected in this region[94,95].

Spectra of chloroprene in CCl_4 solution show a weak band at 895 cm^{-1} which is hidden under a strong band at about 870 cm^{-1} in the liquid phase. Butadiene also has a weak band at 892 cm^{-1} which is assigned to the $=CH_2$ rocking mode, and so the chloroprene band at 895 cm^{-1} is likely to be due to the same mode.

Gas Phase Spectra. High resolution spectra of gaseous chloroprene were recorded above 400 cm^{-1}. A number of fundamental vibrations showed sharp Q bands allowing accurate frequency measurements to be made. Also there are a number of weak additional peaks in the spectrum, which have not been reported previously. Most of these weak peaks appeared

close to (within 5 cm^{-1}) of fundamental vibrations, the only exception being a weak band at 897 cm^{-1} which is assigned as a fundamental vibration, and so these vibrations are discussed together with the nearest strong band.

Side bands are observed on the Q bands at 522, 736, 877, 922.5, 975 and 1025 cm^{-1}. These side bands are part of the main sharp Q band.

Other additional bands are observed near the Q bands which have frequencies of 409, 522, 555.5, 877, 922.5 and 975.1 cm^{-1}.

The region of the spectrum 1050 - 850 cm^{-1} is shown in diagram (6.1a) at high resolution.

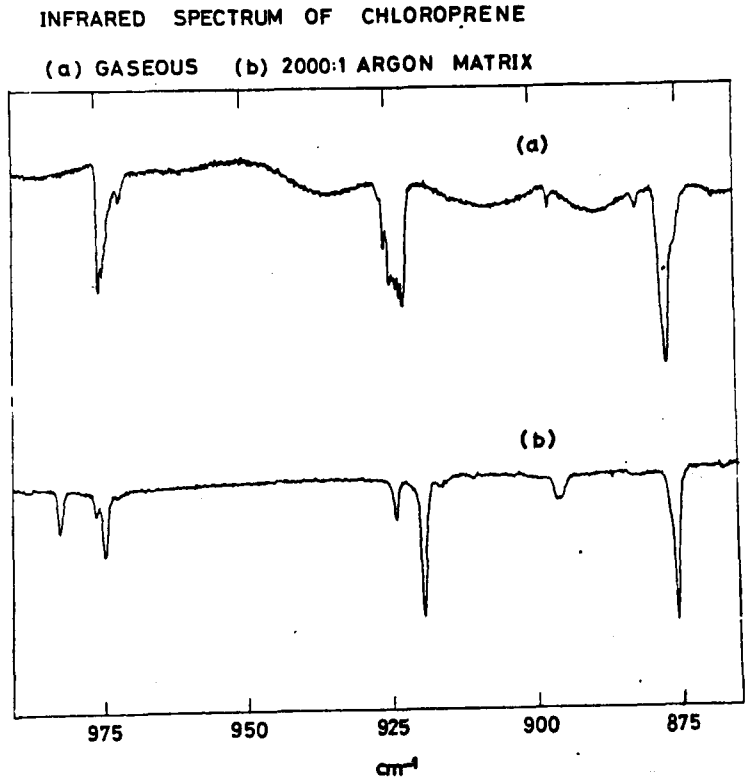

Diagram (6.1)
I.r. Spectrum of Chloroprene in Transmittance between 990 and 870 cm^{-1} (a) Gaseous Phase at 0.7 cm^{-1} Resolution. (b) 2000:1 Argon Matrix at 1.3 cm^{-1} Resolution 20K.

This region covers the strong out-of-plane C-H modes and demonstrates the different types of weak band observed. Those termed side bands are shoulders on strong Q branches, and those termed additional bands are

separate from, but close to, the Q branch.

These weak bands are considered to be due to one or more of the following effects:- (a) High energy conformer (b) Isotopic Effect (c) Aggregation (d) Molecular Rotation and (e) Hot bands due to torsional energy levels.

Bands in the liquid spectrum have already been attributed to a high energy conformer and so there is a possibility that weak bands in the gas close to a fundamental are due to this high energy form. A useful test for this would be to examine the gas at higher temperatures, in which the bands would increase in intensity if due to a high conformer.

The isotope effect should not affect all vibrations in the same way. Those vibrations with a large chlorine contribution should show a wider splitting than vibrations with a small contribution. The weaker band should have an intensity of approximately one third that of the stronger, and the intensity ratio and splitting should be independant of temperature, pressure and phase. The weak gas bands are not likely to be isotope bands as they are very weak compared with the nearest fundamental, and often more than one weak band is observable. However, to examine this possibility, a matrix isolation study was undertaken and is reported later.

Aggregation in the gas phase would give rise to extra bands near fundamentals. The best method of examining this possibility is to alter the pressure of the gas. An attempt to study chloroprene at different pressures was made using a 10 cm gas cell, and no relative intensity changes were noted, but the small pressure range used does not rule out the possibility of aggregation. A study using a longer path length cell would be useful.

Molecular Rotation could also cause side bands, as noted for trans-pentadiene, diagram (5.3). This effect normally gives a number of side bands to a Q band at regular spacing, both at higher and lower frequencies

than the Q band and comparison of diagrams (6.1) and (5.3) will show no similarities of the extra bands. The high moments of inertia of chloroprene give values of κ of 0.015 for the s-trans conformer and -0.813 for the cis conformer. This means that the s-trans conformer is asymmetric and hence no prediction of rotational spacing can be made. The s-cis conformer is a poor approximation to a prolate rotor and the rotational spacing is therefore 2(A-B), 0.4 cm^{-1}.

Two series of bands near 750 cm^{-1} in the gaseous spectrum of acryloyl chloride, diagram (6.4) are attributed later to the s-trans and s-cis cis wag fundamentals and hot bands of both vibrations. A feature of such hot bands is sequential fall in intensity to higher or lower frequency, and fairly regular spacing.

Because of this observation the i.r. bands of gaseous chloroprene termed side bands earlier are tentatively attributed as hot bands of the nearest fundamental. The side bands on the fundamentals at 1025 cm^{-1} (1024.4 and 1023.5), 975.1 cm^{-1} (poorly resolved hot bands to lower frequency) 922.5 cm^{-1} (a series of five side bands about 0.5 cm^{-1} apart to higher frequency) and 735.7 cm^{-1} (734.3, 732.8, 731.5 and 730.0) do not enable accurate calculations of the torsional frequency using equation (1.37) however. In most cases it appears that the hot band intensities are perturbed from the expected exponential function, and give either a low value for the torsional frequency or a range of values within the same series of bands. For instance the well resolved set of bands on the 735.7 cm^{-1} fundamental would be expected to give consistent results for the torsional frequency as this band is assigned to the cis wag like the 756 cm^{-1} band of acryloyl chloride, shown in diagram (6.4), which gives good results. However, the five bands near 736 cm^{-1} were recorded four times and averaged, but gave ΔE values of 74, 131, 164 and 112 cm^{-1} taking two adjacent bands for each calculation.

The weak band at 522 cm^{-1} shows hot bands at 520 and 518 cm^{-1}, and calculations on the intensities of these bands gave a value for the torsional frequency of 138 ± 20 cm^{-1}, using equation (1.37). This is in good agreement with the observed value[44] of 144 cm^{-1}.

Matrix Isolation Studies. In order to further investigate whether the additional bands present in gaseous spectra near fundamentals are due to isotope splitting, high energy conformer, rotation or aggregation, a matrix isolation study of chloroprene was undertaken.

Mixtures of argon and chloroprene between 400:1 and 2000:1 were slowly sprayed onto the cold cryotip held below 26K, and the i.r. spectrum recorded. It was noticed that the appearance of the strong bands between 1000 and 600 cm^{-1} was dependant on the concentration of this mixture. Diagram (6.2) shows the spectra of 500:1, 1000:1 and 2000:1 mixtures over the region 1050 - 850 cm^{-1}. It can be seen that the bands are broad at 500:1, resolving into doublets at 1000:1 and are completely resolved at 2000:1. An expanded spectrum of the 2000:1 matrix in this region is shown in spectrum (6.1b). Each fundamental vibration below 1000 cm^{-1} resolved into a doublet consisting of one strong major peak and one weaker band. The frequencies of the peaks are listed in table (6.3) at the highest matrix:sample ratio observable.

After recording the complete spectrum of each matrix, the cryotip temperature was raised to about 35K, held there for 10 minutes and re-cooled to 20K in an attempt to anneal the matrix. No spectral changes were observed for the 400:1 and 500:1 matrices. The weak peaks at about 1127 and 690 cm^{-1}, already assigned as s-cis peaks remained after annealing.

When the 1000:1 and 2000:1 matrices were annealed the weaker component of the doublet noted above increased in intensity whilst the stronger peak diminished. At the same time the overall transmission

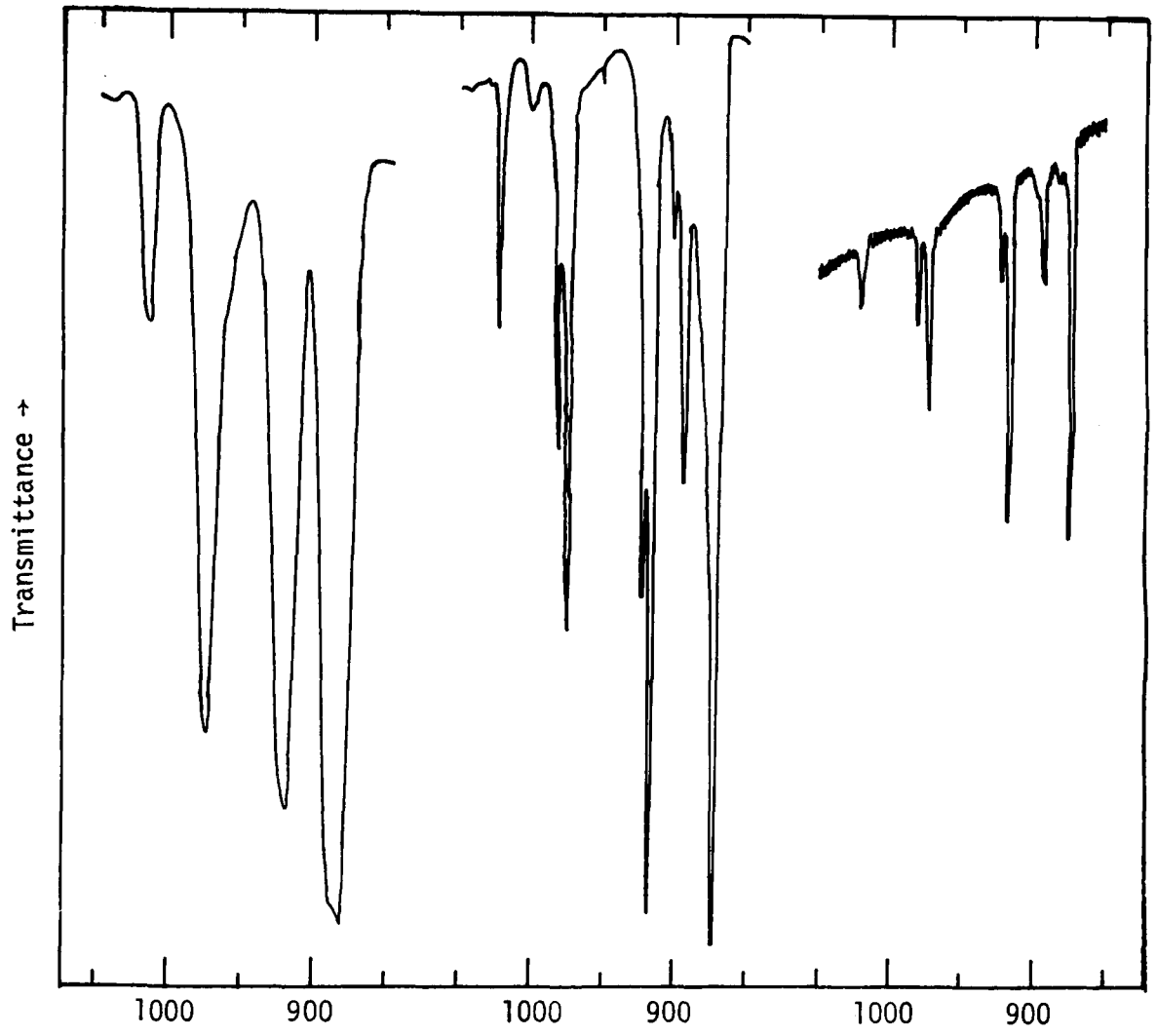

Diagram (6.2)
I.r. Spectra in Transmittance of Chloroprene in Matrices Between 1050 - 850 cm^{-1}. (a) 500 : 1 in Argon. (b) 1000 : 1. (c) 2000 : 1.

of the matrix and quality of the spectrum decreased.

The weaker bands present in the higher matrices could be due to several effects; a high energy conformer, aggregated molecules, multiple site trapping, rotation in the matrix or isotope effect.

Rotation in the matrix is unlikely for such a large molecule. A study of the smaller molecule, chloromethane, by M.L. Evans and H.E. Hallam[98] found no evidence for molecular rotation in a range of host matrices.

The isotope effect is also unlikely to cause the weaker bands because the relative intensities of the weaker bands were not constant, a third of the major peak, and the splittings between weaker and major peak were too large (up to 8 cm^{-1}).

The possibility of the weaker bands being due to high energy conformer is discounted for the following reasons. One would expect bands due to a high energy conformer to be absent at such a low temperature, but it is possible to trap the high energy form in the matrix at its room temperature concentration. The presence of bands at about 1127 and 690 cm^{-1}, which have already been assigned as s-cis bands, suggests that some high energy conformer is present. These peaks at 1127 and 690 cm^{-1} behave like the weak bands noted above and increase on annealing, and therefore are to be assigned differently.

The barrier height faced by the high energy conformer, V', governs the rate of conversion to the low energy conformer, according to the Arrhenius equation (6.1). In diagram (6.3) the rate of conversion k

$$k = A \exp(-V'/RT) \qquad .....(6.1)$$

is shown to be dependent on both V' and T.

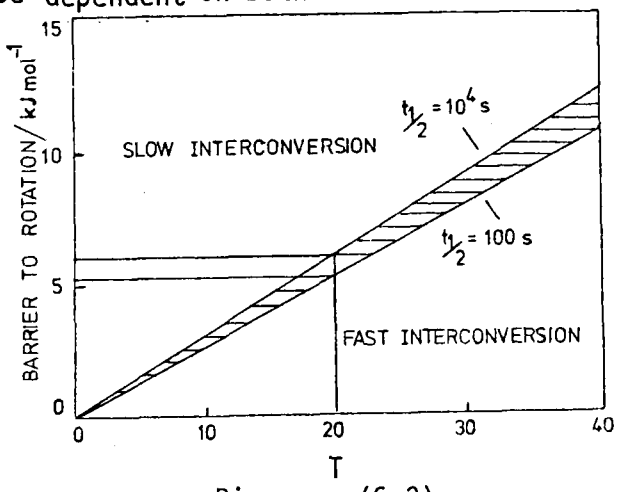

Diagram (6.3)
Interconversion of Conformers at Low Temperatures[99]. A in equation (6.1) is given a value of 10^{12} mol sec $^{-1}$.

Assuming that the relative energies of the conformers are approximately the same at low temperatures as at room temperature, bands due

to high energy conformers should react in three ways on altering the matrix temperature, according to barrier height.

1) A system with a low barrier will show an equilibrium between conformers in the matrix, and altering the temperature of the matrix will alter the relative concentration of the conformers. An example of this is shown by alcohols[9,9] which exist as an equilibrium in the matrix as the rotation barrier is about 5KJ mol^{-1}.

2) A system with a medium barrier (between 6 and 12 KJ mol^{-1}) will not show an equilibrium in the matrix at low temperatures. On raising the temperature and annealing, the high energy conformer will be able to cross the barrier, and bands due to this conformer will decrease and probably disappear.

3) A system with a high barrier (greater than 12 KJ mol^{-1}) will not show an equilibrium, even on annealing, as the high energy conformer will not have enough thermal energy to cross the barrier at an observable rate.

The barrier V' to the s-cis conformer will be approximately the same as that for s-cis butadiene which has been calculated[21] as about 20 KJ mol^{-1}. Hence this is a high barrier and no interconversion is expected at matrix temperatures, although interconversion should occur at the much higher liquid temperatures.

Aggregation of the molecules is possible at such a low temperature because the energy required to move through the matrix is small. The observed growth of the weaker bands on annealing could be due to molecules aggregating and not being able to dissociate, as the energy required for dissociation is probably much higher.

Spectra of chloromethane in a range of host matrices showed bands attributed to aggregation[98]. At 1000:1 monomer peaks predominated and at lower concentrations the intensity of peaks due to dimer and multimer increased.

In the same work[98], multiple site trapping of chloromethane was noted in carbon monoxide and nitrogen matrices, but not in argon or krypton. However, annealing the matrix containing chloromethane gave no spectral changes apart from a slight shifting and sharpening of fundamental frequencies. This effect could be the reason for weaker bands in the chloroprene spectra, although it is difficult to explain the growth of the weak bands on annealing. Also chloromethane did not show features attributed to multiple site trapping in inert gas matrices, which infers that the weak bands in the argon matrix of chloroprene are not due to multiple site trapping.

It appears therefore, that the weak bands in the matrix are most likely due to aggregated molecules. The work on chloromethane[98] indicates that the aggregates are likely to be dimers, and there are two dimeric systems possible, shown in diagram (6.4).

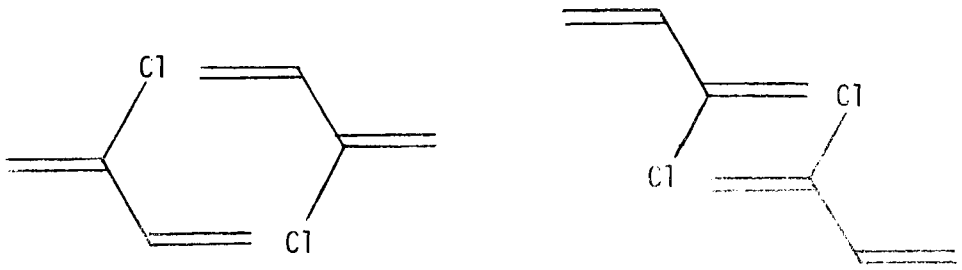

Diagram (6.4)
Possible Dimers of Chloroprene

However, the presence of aggregates in the matrix does not neccessarily mean that aggregation is present in the gas phase, as the aggregation

may occur at spray on. The matrix isolation study has shown, however, that the gas phase additional bands are unlikely to be due to the isotope effect as the observed splittings are not the same in gaseous and matrix phase, are larger than the normal splitting expected, and the intensity ratio of weak:strong bands is not approximately 1:3.

D. Gas Phase Infrared Spectrum of Acryloyl Chloride.

In an attempt to understand the spectra of gaseous and matrix isolated chloroprene, a high resolution study of the i.r. spectrum of gaseous acryloyl chloride was undertaken, because this compound is isolectronic to chloroprene.

R.L. Redington and J.R. Kennedy[61] studied the spectrum in argon and nitrogen matrices at 400:1. Bands in both gas and matrix phases were assigned to the s-cis high energy conformer, and several bands in the matrix showed shoulders stronger in the nitrogen matrix than the argon matrix[61]. The presence of these shoulders and behaviour on annealing was not discussed, but an estimate of 25% s-cis at room temperature was given, and complete assignments were given for both conformers.

In the present work, high resolution gas spectra showed weaker peaks near the s-trans fundamentals, but most of these can be assigned as s-cis fundamentals, as a previous study[60] calculated a relatively low value for ΔH^{θ}, 600 cal mol^{-1}. The frequencies of these fundamentals are given in table (6.3).

Peaks at 495, 607, 701, 743, 756, 980 cm^{-1} show additional weak peaks. The additional peaks on the s-trans and s-cis C-C stretch bands at 607 and 701 cm^{-1} are not properly resolved. These may be due to isotope splitting or another effect, but it is not possible to decide.

All the other additional weak peaks observed are very close to Q

bands and so are assigned as hot bands of the torsion.

The band at 495 cm^{-1} shows two side peaks at 494 and 493 cm^{-1}. Because these peaks show a regular splitting and fall off in intensity they are assigned as hot bands.

The sharp Q peaks at 756 and 743 cm^{-1} both show side bands to lower frequency. The strongest peaks are assigned in this work to the s-trans and s-cis conformer cis wags at variance with previous works[60,61] and the weaker bands as torsional hot bands. The hot bands of the 743 cm^{-1} fundamental are especially clear and are shown in diagram (6.5). These bands are listed in table (6.1) with the assignments according to diagram (1.8) and calculated values for the torsional frequencies, ΔE, from equation (1.37).

Frequency (cm^{-1})	Assignment	Intensity(mm)	ΔE (cm^{-1})
	S-trans Conformer		
755.7	0(0) → 1(0)	145 ± 6	
754.4	0(1) → 1(1)	62	99
753.5	0(2) → 1(2)	56	
	S-cis Conformer		
742.7	0(0) → 1(0)	60	
741.5	0(1) → 1(1)	46	83.3
739.6	0(2) → 1(2)	27	
738.1	0(3) → 1(3)	18	84.5
736.7	0(4) → 1(4)	12	84.5

Table (6.1)
Intensities of Hot Bands Shown in Diagram (6.5) and Torsional Frequencies of Both Conformers of Acryloyl Chloride

In both series of hot bands the 0(1) → 1(1) intensity is clearly perturbed and so the average value of ΔE over the fundamental and first two hot bands is calculated. The overall calculated values for the

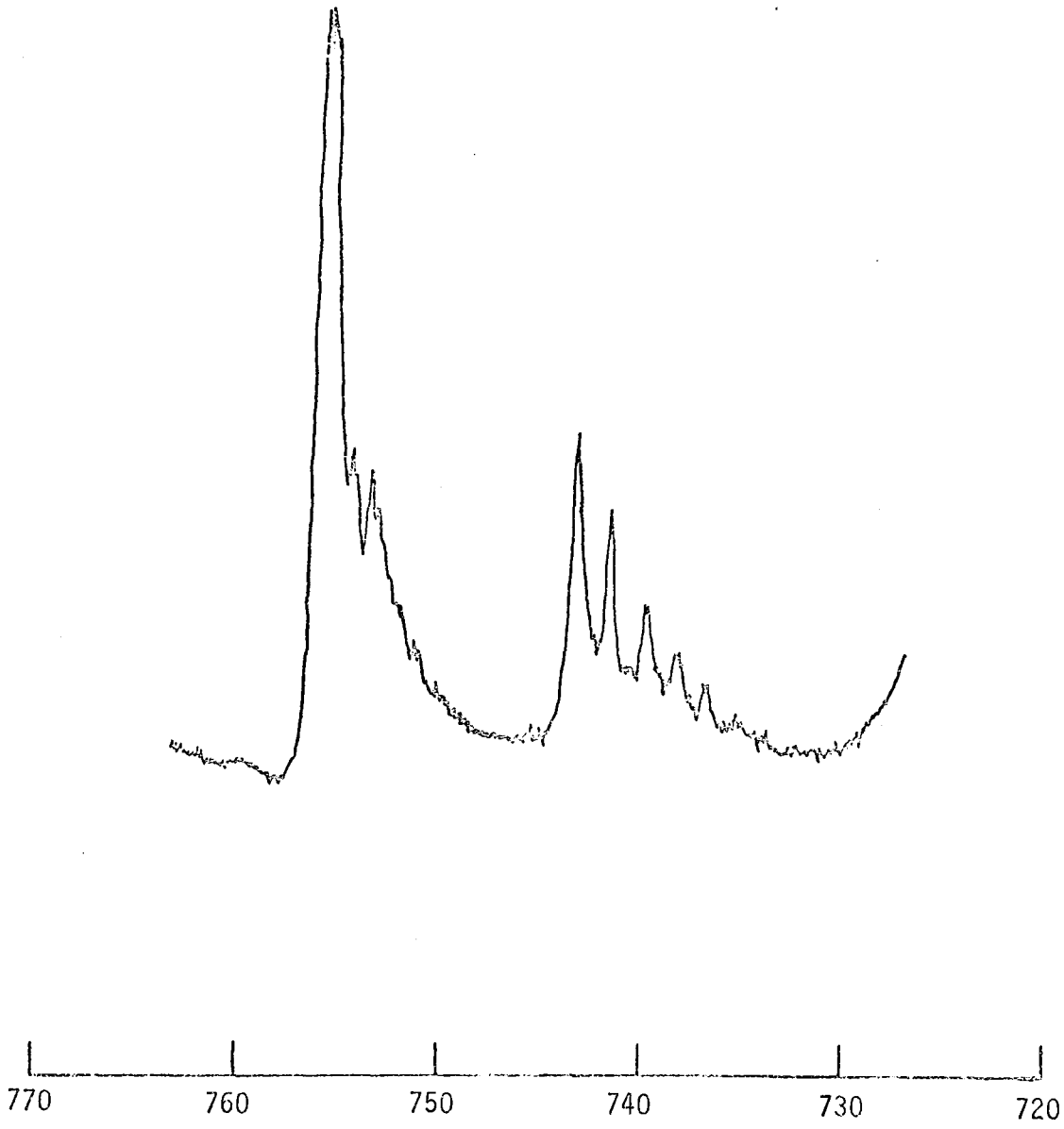

Diagram (6.5)

I.r. Spectrum of Gaseous Acryloyl Chloride between 770 and 720 cm-1.

s-trans and s-cis torsional frequencies are 99 and 84 cm^{-1} respectively, to a probable error limit of ± 10 cm^{-1}. The s-trans torsion has been assigned at 106 cm^{-1}, which shows good agreement.

A complex absorption occurs between 990 and 970 cm^{-1}. From a study of a range of α,β - unsaturated carbonyl compounds J.R. Cowles et.al. assigned two fundamental out-of-plane vibrations to this region[97], although only one absorption was observed with the resolution available. Diagram (6.6) shows this region at high resolution and shows at least 8 sharp bands.

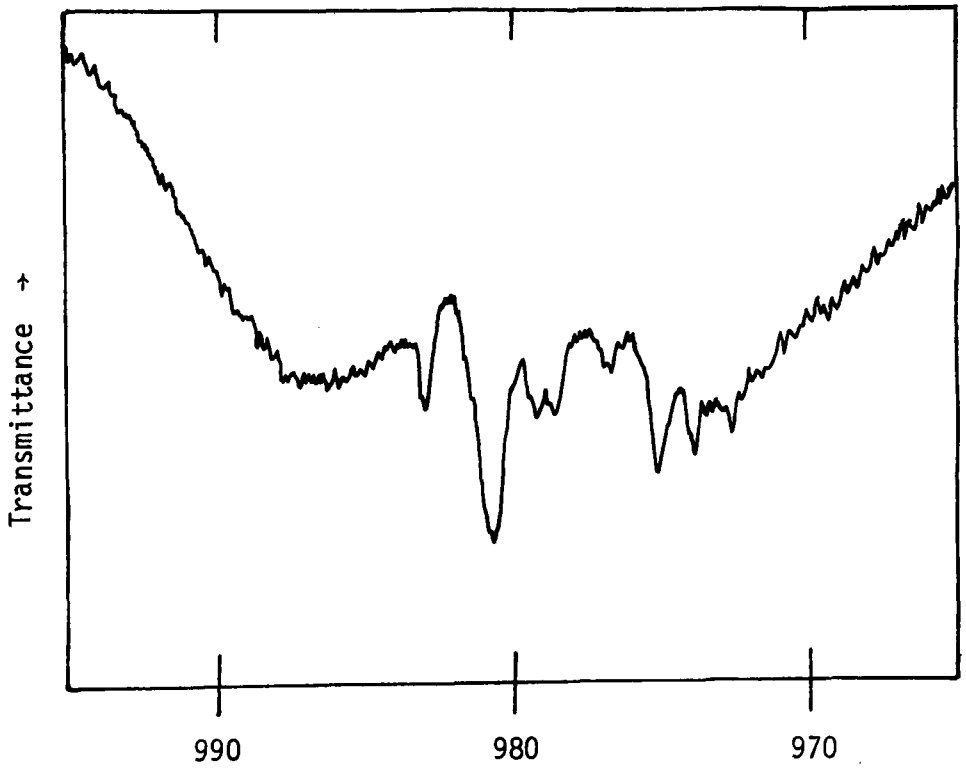

Diagram (6.6)
I.r. Spectrum of Gaseous Acryloyl Chloride Between 995 and 965 cm^{-1}

Peaks at 980.6 and 975 cm^{-1} have been considered s-trans fundamentals, with peaks at 983 and 977 cm^{-1} as the respective s-cis bands, although these assignments are ambiguous. No calculations on hot band intensities can be made.

The vibration at 1396.1 cm^{-1} shows a single satellite Q band at 1397 cm^{-1}. As only one side band is observed this is assigned as due to the s-cis conformer.

E. Vibrational Assignments.

The assignments of both compounds have been considered together because of the similarity of their structures and are listed together in table (6.3). Both compounds are members of the C_s point group and their vibrations hence are both Raman and i.r. active. Chloroprene has a 17 A' in-plane and 7 A'' out-of-plane depolarised vibrations, whilst acryloyl chloride has 13 A' and 5 A'' vibrations. Gaseous frequencies are listed where possible in table (6.3).

Chloroprene. The previous assignments[94,95] are similar to each other, and these assignments agree with the present results above 1000 cm^{-1}, although they differ slightly in frequency. The C-C stretch at 1225 cm^{-1} is strong for a vibration that is normally weak in the i.r., but the only other possible assignment is to the C-H bend, assigned at 1279 cm^{-1} However, these assignments agree with those of equivalent vibrations of butadiene, isoprene, the pentadienes and crotonaldehyde .

Spectra of chloroprene as a solution, isolated in a matrix and as a solid showed two bands at about 897 and 660 cm^{-1} normally hidden by the strong bands at 877 and 638 cm^{-1}. The band at 897 is assigned to the symmetric $=CH_2$ rock which is found at 892 cm^{-1} in butadiene, this mode was assigned to a weak Raman band at 931[94], although a previous work assigned it 890 cm^{-1}. The band at 660 cm^{-1} is assigned as a $=CH_2$ twist as this mode has been predicted[94,95] in this range, variously at 697 and 630 cm^{-1}.

The other low frequency modes have been assigned the same as previously reported. Frequencies below 400 cm^{-1} are taken from work by R.K. Harris and R.E. Witkowski[44].

Acryloyl Chloride. The assignments given for acryloyl chloride in table (6.3) agree with a previous assignment[61] above 1200 cm^{-1}. The strong band at 1149 cm^{-1} and weak band at 938 cm^{-1} were assigned[61] to the $=CH_2$ rock and C-C stretch respectively. These assignments have been reversed to agree with acrolein[18,34], which shows a strong band at 1158 cm^{-1} due to the C-C stretch and another strong band at 914 cm^{-1} which was assigned to the $=CH_2$ rock. Assignment of the C-C stretch to a strong mode at 1149 cm^{-1} supports the assignment of the corresponding vibration in chloroprene to a strong band at 1225 cm^{-1}.

The assignments of the out-of-plane vinyl modes are altered from those of R.L. Redington and J.R. Kennedy[61], who assigned the bands at 649 and 756 cm^{-1} to the cis wag and and $=CH_2$ wag of the s-trans conformer. The $=CH_2$ wag has been assigned to bands at 975 and 977 cm^{-1} shown in diagram (6.6) for the s-trans and s-cis conformers, in agreement with J.R. Cowles et.al[97]. The cis wag is assigned to the complex bands, shown in diagram (6.5), with fundamentals at 756 and 743 cm^{-1} for s-trans and s-cis conformers.

The other fundamentals are assigned to the same vibrations as previously[61]. The s-cis frequencies detected using matrix isolation techniques[61] are used in table (6.3), unless gas phase values are available.

F. Conclusions.

The spectra of both gaseous and matrix isolated chloroprene are complex, and the spectra of acryloyl chloride were examined because its isoelectronic structure may aid interpolation.

Acryloyl chloride shows a significant concentration of high energy conformer and all gas phase bands can be assigned to fundamentals of

either the s-trans or s-cis conformer or hot bands due to torsional levels. In matrix isolation spectra some satellite peaks are observed as very weak shoulders in argon matrices and weak shoulders in nitrogen matrices. Due to their higher intensity in the nitrogen matrix these peaks are probably due to multiple site trapping but they may also be due to aggregated species.

In chloroprene weak additional peaks are observable in both gaseous and matrix isolation spectra.

Some weak bands have been assigned to a small amount of s-cis chloroprene, but most of the additional peaks observed in matrix isolated spectra behave differently on annealing and hence are not assigned as s-cis peaks. These peaks could be due to multiple site trapping, but their presence in gaseous spectra and behaviour in the annealed matrix suggests that aggregation is occuring, although aggregation of gaseous chloroprene molecules would be caused by a weak attraction and so is unlikely at the relatively low pressures studied. Any aggregates formed are likely to be dimers.

In order to test these conclusions, various tests could be made on gaseous and matrix isolated chloroprene.

Tests on gaseous samples which would help to clarify the situation include varying the temperature and pressure of the gas independently. If weak bands decrease with pressure then they are likely to be due to aggregated species. A limited pressure study showed no intensity variation, but a study of the gas over a wider range of pressures and path lengths would be more definitive.

If the weak bands are observed to increase in relative intensity at higher temperatures then they can be tentatively assigned as high energy conformer bands.

Tests on matrix isolated samples which would clarify the situation are summarised in table (6.2). However, these tests may give ambiguous results and caution is necessary in drawing conclusions from them. In the present study equipment was not available to carry out these tests.

	Conformational Change	Aggregation	Multiple Site Trapping
Alter Concentration of Sample in Matrix		✓	✓
Annealing Studies	✓	✓	✓
Change Matrix		✓	✓
Alter Temperature of input gas	✓	✓	
Change from slow spray to pulse	✓	✓	✓
Photolysis of sample in matrix	✓		

Table (6.2)
Summary of Tests Which May be Used to Distinguish Between Different Effects in Low Temperature. Matrices.

Table (6.3)

Fundamental Vibrations of Chloroprene and Acryloyl Chloride

Chloroprene		VIBRATION	Acryloyl Chloride	
Matrix Frequency*	S-trans		S-trans	S-cis
A'' out-of-plane Vibrations				
	144	=C-C= torsion	106	84
410↓ 418↑	408.5	C-Cl wag	495	432
660	660(s)	$=CH_2$ twist	-	-
737	735.7	cis wag	756	743
876↓ 883↑	877.1	$=CH_2$ wag	-	-
919↓ 924↑	922.5	$=CH_2$ wag	975.0	977
974↓ 982↑	975.2	trans wag	980.5	983
A' in-plane Vibrations				
	244	skeletal bend	260	260
388	386	C-Cl bend	384	361
525↑ 517↓	521.5	skeletal bend	451	439
634↓ 630↑	638[c]	C-Cl stretch	607	701
896	897	$=CH_2$ rock	939	933
1022	1024.8	$=CH_2$ rock	-	-
1220	1224.8	C-C stretch	1149	1149
1260	1279	C-H bend	1285	1285
1363	1361.9	asym $=CH_2$ scissor	-	-
1398	1396	sym $=CH_2$ scissor	1396.1	1397.2
1589	1589	asym C=C stretch	1619	1626
1634	1628	sym C=C stretch	-	-
-	-	C=O stretch	1785	1770
3019	3017	sym $=CH_2$ stretch	-	-

Table (6.3) contd.

Chloroprene		VIBRATION	Acryloyl Chloride	
Matrix Frequency*	S-trans		S-trans	S-cis
A' in-plane Vibrations				
3030	3031	sym $=CH_2$ stretch	-	-
3060	3070	=CR-H stretch	2989	2989
3104	3115	asym = CH_2 stretch	-	-
3118	3124	asym $=CH_2$ stretch	3123	3123

s Solid phase frequency.

* Frequency taken from most dilute matrix where vibration is observable.

↑ and ↓ are intensity change on annealing the matrix

c s-cis frequency taken as 700 cm^{-1}.

CHAPTER VII

Calculation of the Barrier Heights to Internal Rotation From Torsional Frequencies

A. Barrier Heights.

B. Method of Calculation.

C. Calculation of the Barrier Heights of Crotonaldehyde.

D. Results.

CHAPTER VII

Calculation of the Barrier Heights to Internal Rotation from Torsional Frequencies

A. Barrier Heights

In the early part of this century it was believed that rotation about a C-C single bond was unrestricted and hence a group rotated freely about the C-C bond with respect to the other group. However, in 1936 it was shown that calculations of thermodynamic functions of ethane by statistical methods based on spectroscopic data gave lower values than those based on calorimetric work[1]. These results were interpreted by proposing a barrier to internal rotation of about 13 KJ mol^{-1}, and this barrier effectively stored energy in the molecule. To accurately predict thermodynamic functions for a molecule with internal rotation it is important to first calculate the barrier height, and the method of calculation is given in this chapter.

There are two types of barrier, as briefly explained in the introduction, symmetric and asymmetric. A methyl group is a good example of a symmetric top and because it has three equivalent spatial positions it is said to have a threefold barrier denoted V_3. A typical asymmetric top is an aldehyde group which has two prefered spatial orientations due to its planar structure and so has a twofold barrier. This barrier is denoted by V_2, but in practice a particular function of V_2 known as V* may be calculated as reported.

A torsion is an oscillating partial rotation of one group around a single bond with reference to another group. Like all other vibrations,

torsional energy is quantised and a quantum leap from one torsional energy level to a higher level gives rise to absorption of energy at a specific frequency, called a torsional frequency. Typical torsional frequencies are below 250 cm^{-1}, and so significant population of levels above the ground state often occurs, and if the levels near the top of the rotation barrier are populated then the likelihood of rotation occuring is increased.

The rate of conversion across a barrier of height V can be considered in terms of equation(7.1) where A is a constant. Because of this the barrier heights can be considered in three categories based

$$K = A \exp(-V/RT) \qquad .....(7.1)$$

on the rates of interconversion.

1) When the barrier height is large relative to RT the interconversion will be relatively slow, and the molecule can be considered to exist in well defined conformers. In this case the torsion is approximately harmonic and can be treated normally, but calculation of thermodynamic functions must take into account both the torsional vibration and mixing of conformers. A method of calculating the functions for a mixture of conformers is given later. Restricted rotation between conjugated double bonds is an example, and results in different conformers due to the asymmetric potential.

2) If a barrier height of equivalent value to RT is present then some of the torsions will occupy energy levels below the barrier giving separate conformers, but those with higher energy levels will be rotating, giving an overall situation of rapid interconversion of conformers called hindered rotation. An example of such a barrier is the methyl barrier height, and the calculation of V_3 in this chapter is complex.

3) If the barrier height is small compared to RT then unrestricted

rotation occurs, and the barrier can be ignored in calculations. Such systems are not common but one example is found in dimethyl acetylene.

The work on barriers to internal rotation for this thesis encountered two main types of barrier, the symmetric methyl group undergoing a hindered rotation and asymmetric tops with high twofold barriers undergoing restricted rotation between conformers. The method of calculation of the respective barrier heights is explained below and a sample calculation performed for crotonaldehyde which has both methyl and aldehyde tops. In the calculation any interaction between the tops is ignored.

B. Method of Calculation

Principal Moments of Inertia

To calculate barrier heights it is necessary to know the molecular principal moments of inertia and the angles these make with a frame of reference. First the coordinates of the atoms (x_i, y_i, z_i) in the molecule are calculated and the coordinates of the centre of mass (x_0, y_0, z_0) found by

$$x_0 = \Sigma_i m_i x_i / \Sigma_i m_i \qquad \text{.....(7.2)}$$

Moments of inertia can be calculated on this frame of reference by the method of Hirschfelder[100] such that

$$\begin{vmatrix} I_{xx} & I_{xy} & I_{xz} \\ I_{yx} & I_{yy} & I_{yz} \\ I_{zx} & I_{zy} & I_{zz} \end{vmatrix} = I' \qquad \text{.....(7.3)}$$

By rotating the frame of axis it is possible to reduce all the cross terms (I_{xy} etc.) to zero when I_{xx} becomes I_A etc. and

$$I' = I_A I_B I_C \qquad \text{.....(7.4)}$$

In practice the principal moments of inertia I_A, I_B and I_C are calculated using the determinent[100]

$$\begin{vmatrix} (A-I) & -D & -E \\ -D & (B-I) & -F \\ -E & -F & (C-I) \end{vmatrix} = 0 \qquad \text{.....(7.5)}$$

$$\begin{aligned} A &= \Sigma m_i (x^2 + z^2) - 1/M (\Sigma m_i y^2) - 1/M (\Sigma m_i z^2) \\ B &= \Sigma m_i (x^2 + z^2) - 1/M (\Sigma m_i x^2) - 1/M (\Sigma m_i z^2) \\ C &= \Sigma m_i (x^2 + y^2) - 1/M (\Sigma m_i x^2) - 1/M (\Sigma m_i y^2) \\ D &= \Sigma m_i \; xy \; - 1/M (\Sigma m_i x) (\Sigma m_i y) \\ E &= \Sigma m_i \; xz \; - 1/M (\Sigma m_i x) (\Sigma m_i z) \\ F &= \Sigma m_i \; yz \; - 1/M (\Sigma m_i y) (\Sigma m_i z) \end{aligned} \qquad \text{.....(7.6)}$$

where $M = \Sigma m_i$

For a planar molecule because $z = 0$ the solution of the determinent reduces to $I^2 - I(A+B) + AB - D^2 = 0$ .....(7.7)

Solving these equations for the roots of the equation I gives the principal moment of inertia. It is now possible to calculate the directional cosines of the angles between the principal axes and the frame of reference using the following matrix relationship,

$$\begin{vmatrix} (A-I) & -D & -E \\ -D & (B-I) & -F \\ -E & -F & (C-I) \end{vmatrix} \times \begin{vmatrix} \alpha \\ \beta \\ \gamma \end{vmatrix} = 0 \qquad \text{.....(7.8)}$$

where α, β and γ are the directional cosines, and $\gamma = 0$

thus $(A - I)\alpha - D\beta = 0$ .....(7.9)

and $- D\alpha + (B - I)\beta = 0$ .....(7.10)

The ratio of $\alpha : \beta$ can be calculated for each value of I and then because $\alpha^2 + \beta^2 = 1$ the direction cosines can be calculated.

For this work well tested computer programs were used to calculate the principal moments of inertia and directional cosines.

Threefold Barrier Height

The potential energy opposing the internal rotation of a symmetric methyl top is a periodic function of α, the angle of rotation, because the methyl top axis is also a threefold symmetry axis. Such a potential can be expressed as a Fourier expansion:-

$$V_\alpha = a_3 \cos 3\alpha + a_6 \cos 6\alpha + a_9 \cos 9\alpha + \ldots \qquad \ldots\ldots(7.11)$$

It may be shown that to a good approximation only the first term is significant [10 1]. If the frame of reference (α=0) is chosen to coincide with that in diagram (7.1) the potential can be rewritten in terms of V the potential barrier.

$$V_\alpha = V_3(1 - \cos 3\alpha)/2 \qquad \ldots\ldots(7.12)$$

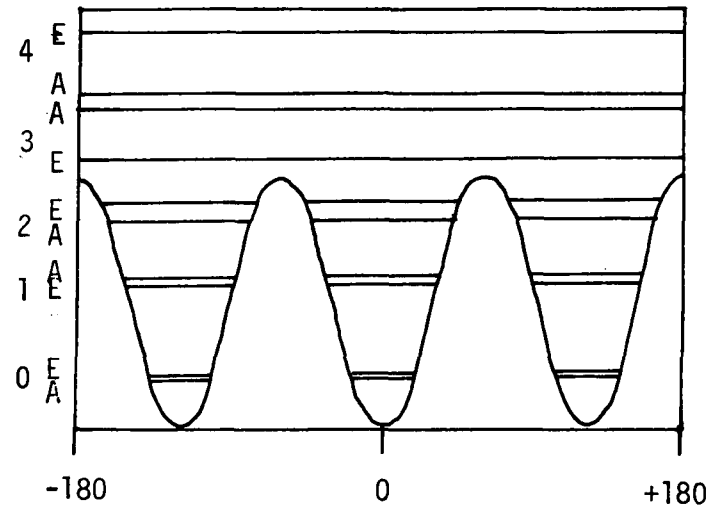

Diagram (7.1)

Potential Function and Energy Levels for the Hindered Rotation of a Threefold Symmetric Top, where α is the Torsional Angle.

If this general expression is used in the Schrodinger wave equation for one dimension (α)[72].

$$F \frac{d^2\psi(\alpha)}{d\alpha^2} + \left[E - \frac{V_3}{2}(1 - \cos 3\alpha) \right]\psi(\alpha) = 0 \quad .....(7.13)$$

Where F is the effective internal rotational constant given by

$$F = h^2/8\pi^2 c I_r \quad .....(7.14)$$

and

$$I_r = I_\alpha(1 - I_\alpha \Sigma_i \lambda_i^2/I_i) \quad .....(7.15)$$

I_r is the reduced moment of inertia of the top, I_α is the moment of inertia of the top about its own axis, I_i is the ith principal moment of inertia of the whole molecule at an angle with cosine λ_i with the top axis.

The expression (7.13) is similar in form to the general Mathieu Equation[73, 102], and substitution gives the following expression

$$\frac{d^2\psi}{dx^2} + (b_{v\alpha} - s\cos^2 x)\psi_{v\sigma} = 0 \quad .....(7.16)$$

where

$$b_{v\sigma} = 4E/9F, \quad .....(7.17)$$

$$s = 4V_3/9F \quad .....(7.18)$$

s is the dimensionless parameter known as the reduced barrier, b is an eigenvalue of equation (7.16), v is the torsional level quantum number and σ the torsional sublevel index.

The energy levels for restricted internal rotation are given by equation (7.19) and the observed torsional frequency is the difference between two energy levels, (7.20).

$$E_{v\sigma} = 2{\cdot}25 F b_{v\sigma} \quad .....(7.19)$$

$$\therefore \quad \Delta E = 2{\cdot}25 F(\Delta b_{v\sigma}) \quad .....(7.20)$$

For very high barriers the energy levels would be triply degenerate because of the three identical potential wells. However, quantum tunnelling alters this degeneracy in systems with medium barriers to two

levels, one singly degenerate A level caused by tunnelling and a doubly degenerate E level caused by rotation in two directions[72]. The splitting between the levels increases at higher torsional levels, as can be seen in diagram (7.1), but is negligible for the 0→1 transition.

If the torsional frequency ΔE is known for a particular torsional level than $\Delta b_{v\sigma}$ can be calculated. Using the solution of the Mathieu equation (7.16) the parameter s can be found and V_3 calculated using equation (7.18).

For simple cases where only the first torsional frequency has been assigned V_3 is calculated by interpolating into a table of Δb versus s values[79], using program THERM (see appendix). If higher torsions are observed then the data of D.R. Herschbach [80]is used which is shown graphically in diagram (7.2) and indicates the large splitting of A and E torsions at lower s values.

Table (7.1) gives the methyl barrier heights and calculation parameters of some compounds studied.

Asymmetric Twofold Barrier Height

The potential function for an asymmetric barrier is more complex than for a symmetric barrier. In this case the Fourier Expansion of the potential at angle α is

$$V_\alpha = \tfrac{1}{2}\Sigma_i V_i(1 - \cos i\alpha) \qquad .....(7.21)$$

and is normally truncated after i = 3. The summation of these curves is shown diagramatically in diagram (7.3) for the special case when the coefficients are all unity and α is taken as zero for the trans form. In this case the final potential represents a low energy trans conformer and two high energy gauche conformers.

If only the torsion of one conformer is observed then it is necessary to assume that the torsional oscillation is harmonic and

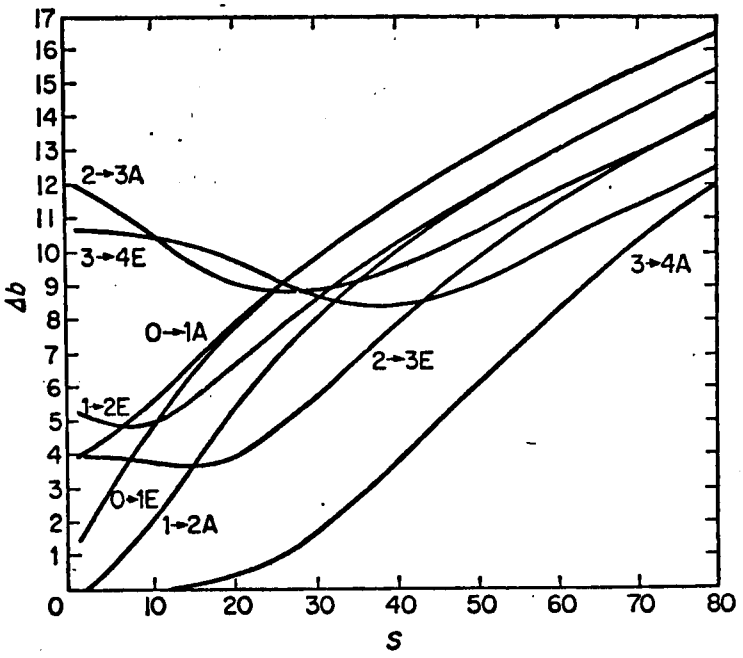

Diagram (7.2)
Graph of $\Delta b_{V\sigma}$ Versus s for Torsional Transitions of a Symmetric Threefold Barrier.

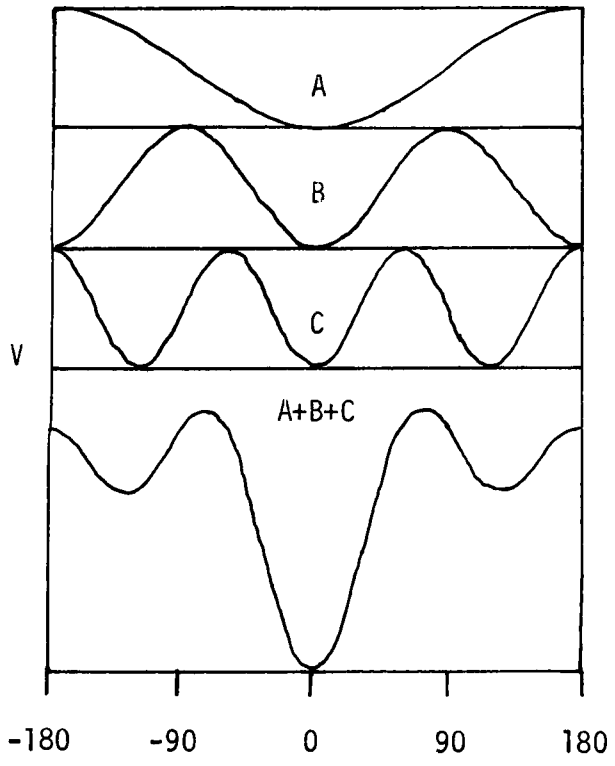

Diagram (7.3)
Components of the Potential Function
$V_\alpha = \frac{1}{2}\Sigma_i V_i(1 - \cos i\alpha)$.

hence for small values of α, cos α can be replaced by a power series in α of which only α^2 is important.

$$V_\alpha = (V_1 + 4V_2 + 9V_3)\alpha^2/4 \quad .....(7.22)$$

$$= V^*\alpha^2/4 \quad .....(7.23)$$

The equation (7.23) now has the form of a harmonic oscillator, because the curvature at the potential minimum has been matched to a cosine based function. In doing so an approximate barrier height V* has been introduced, which is related to the torsional frequency by F, given in equation (7.14).

$$V^* = \nu^2/F \quad .....(7.24)$$

The value of F is calculated by the method of K.S. Pitzer[103], using the reduced moment of inertia I_r. Details of the calculation of I_r are laid out in the section on the calculation of the twofold barrier height of crotonaldehyde.

Table (7.2) gives the results of such calculations for the compounds studied and gives values for the calculation parameters and V*. These calculations were performed using a well tested program CART.

C. Calculation of the Barrier Heights of Crotonaldehyde.

The threefold and twofold barrier heights of crotonaldehyde are calculated in full to illustrate the method used. The calculation of the principal moments of inertia and directional cosines has been done using the computer program CART, following the structure proposed by M. Suzuki and K. Kosima[56]. The calculation of the twofold barrier is simplified by defining the x axis along the aldehyde top axis and defining the origin at the aldehyde carbon as shown.

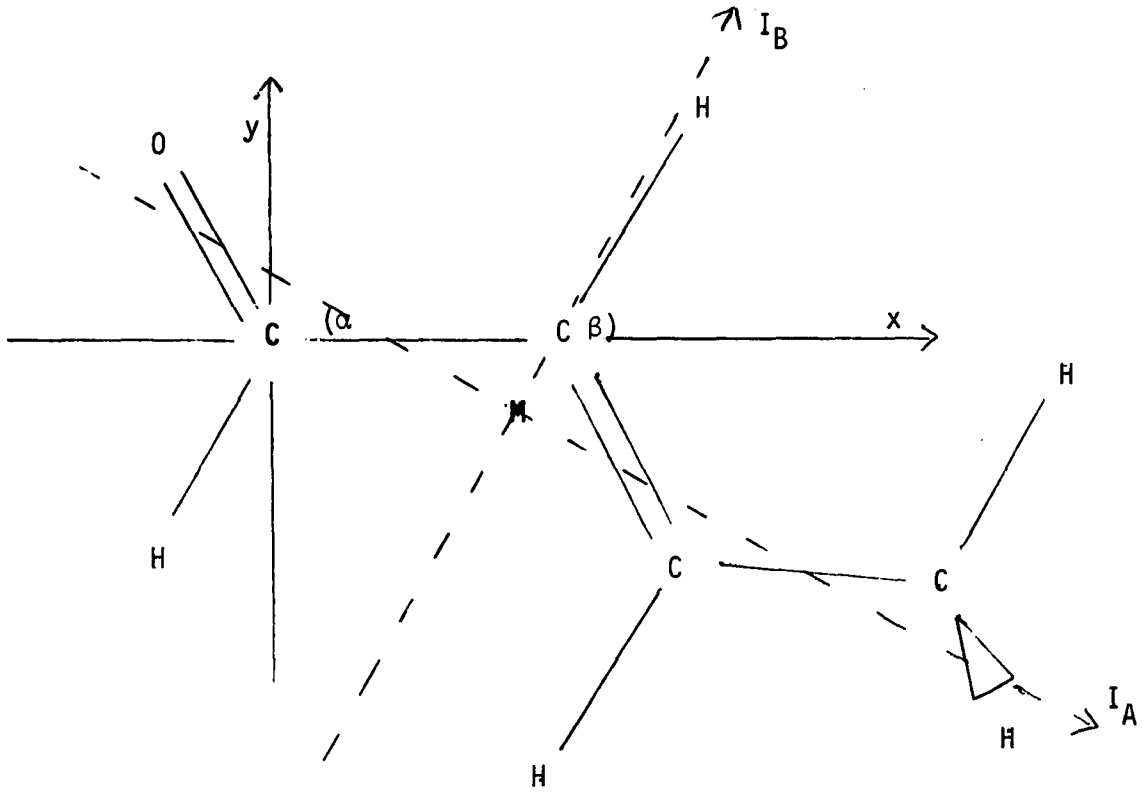

Diagram (7.4a)
Plot of the crotonaldehyde molecule such that the origin is at the aldehyde carbon.

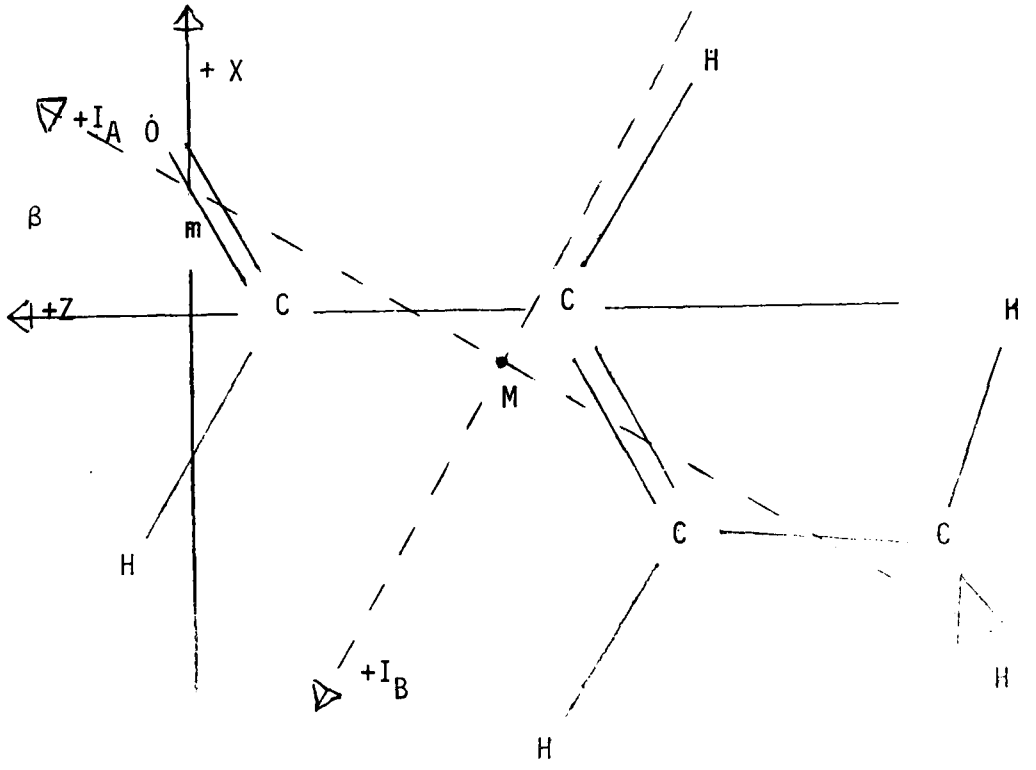

Diagram (7.4b)
Showing the definition of the new X,Y,Z axes and polarity of the principal moments of inertia.

With reference to the diagram (7.4a) the values of the principal moments of inertia are, in units of 10^{-39} gm cm^2.

$$I_A = 2{\cdot}57279$$

$$I_B = 38{\cdot}4470$$

$$I_C = 40{\cdot}48952$$

The directional cosines of the chosen x axis with the moments I_A, I_B and I_C are noted α, β and γ respectively.

α = 0·882336 angle α = 28·0745°

β = 0·470620 angle β = 61·9255°

γ = 0·0 angle γ = 90·0°

The centre of gravity of the molecule on the frame of reference used is (1·30457, -0·28241, 0·0).

Calculation of the Threefold Barrier Height

The moment of inertia of the methyl rotor about its own axis (z) is given by

$$I_\alpha = \Sigma_i m_i x_i^2 \qquad \text{.....(7.25}$$

and because the methyl carbon is on the axis this atom can be ignored.

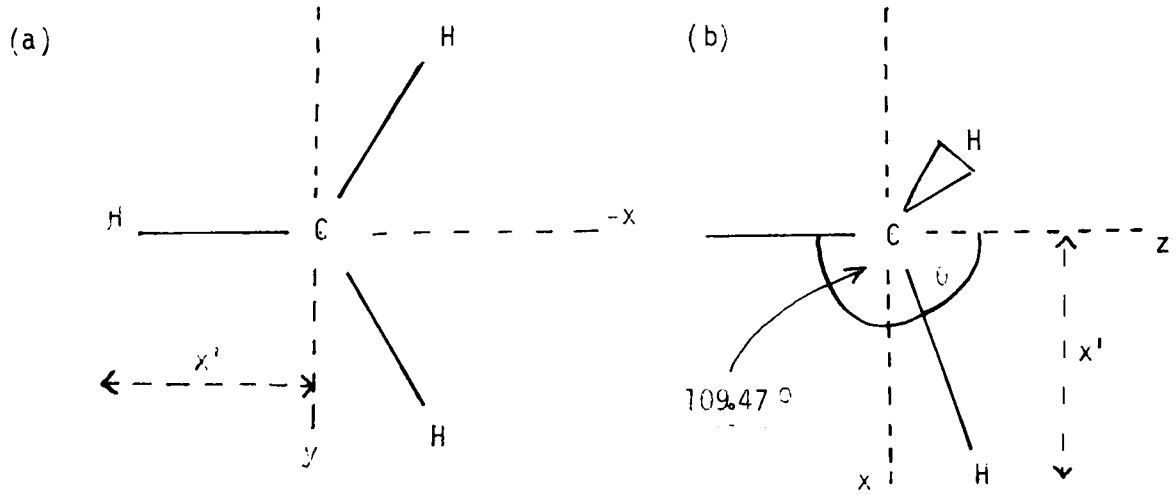

Diagram (7.5)

Figure (a) View of Methyl Top down z axis.

Figure (b) View of Top in xz plane.

From diagram (7.5) it can be seen that

$$x_i = 1{\cdot}090\sin\theta\ A^0$$

$$= 1{\cdot}090\sin(180^0 - 109{\cdot}47^0) \times 10^{-8}\text{cm}$$

taking the atomic weight of hydrogen as $0{\cdot}16738 \times 10^{-23}$g

$$I_\alpha = 3 \times 0{\cdot}16738(1{\cdot}090\sin 70{\cdot}53)^2 \times 10^{-39}$$

$$I_\alpha = \underline{0{\cdot}53031 \times 10^{-39}\ \text{gm cm}^2}$$

From diagram (7.4a) it can be seen that the directional cosines of the angles subtended by the principal moments on the rotation axis are easily calculated from α, β and γ as a, b and c.

a = 0·92547	angle α	=	$22{\cdot}26^0$
b = 0·37888	angle β		$67{\cdot}74^0$
c = 0·0	angle γ		$90{\cdot}00^0$

From equation (7.15), when λ_a = a etc.

$$I_r = 0{\cdot}53031\left[1 - 0{\cdot}53031\left(\frac{0{\cdot}92547^2}{2{\cdot}57279} + \frac{0{\cdot}37888^2}{38{\cdot}4470}\right)\right]$$

$$I_r = 0{\cdot}43564 \times 10^{-39}\text{gm cm}^2.$$

The value of F can now be calculated using equation (7.14), which by substituting values for constants becomes

$$F = 2{\cdot}79908 / 0{\cdot}43564\ \text{cm}^{-1}.$$

$$F = 6{\cdot}4252\ \text{cm}^{-1}.$$

J.R. Durig et.al.[63] assigned the solid phase torsional frequency at 173 cm^{-1}, which is used with F to calculate Δb .

$$\Delta b = 173 / 2{\cdot}25F$$

$$= 11{\cdot}97$$

This value of Δb gives a value of s, by interpolation into tables of Δb versus s, of 42·7. Because $V_3 = 2{\cdot}25Fs$

$$V_3 = 617{\cdot}3\ \text{cm}^{-1}$$

$$\therefore\quad V_3 = \underline{7{\cdot}38\ \text{KJ mol}^{-1}.}$$

Threefold barrier of crotonaldehyde using the solid phase torsional frequency compares well with the gaseous value calculated by M. Suzuki and K.Kozima[56] of 7·24 KJ mol^{-1}. J.R. Durig et.al.[63] calculated a value of 7·41 KJ mol^{-1} using the torsion of 173 cm^{-1}.

Calculation of the Twofold Barrier Height

The calculation has been simplified by choosing the aldehyde carbon as the centre of coordinates, with x axis along the top axis. Reference is made to diagram (7.4a).

1. Calculation of the centre of mass of the top.

The coordinates, diagram (7.4a) of the top atoms and mass in units of 10^{-39} gm cm^2 are

	x	y	z	m
C	0.0	0.0	0.0	1.99438
H	-0.47001	-1.00337	0.0	0.16737
O	-0.66890	1.01908	0.0	2.65660

Using equation (7.2) the centre of mass of the top can be calculated as (-0·38512, 0·52702, 0·0) in the above coordinate system.

2. Redefinition of the top coordinates.

The top coordinates and centre of molecular mass are now re-defined so that the top axis is now the Z axis and the X axis goes through the centre of mass of the top. The new axes are drawn in diagram (7.4b). This gives the top atoms the following coordinates:-

	X	y	Z	m
C	0.0	0.0	-0.38512	1.99438
H	-1.00337	0.0	0.08489	0.16737
O	1.01908	0.0	0.283778	2.65660

The centre of molecular mass has the new coordinates (-0.28241, 0.0, -1.68969). Due to the shift of axes the new directional cosines of I_A, I_B and I_C with the X axis are labelled α', β' and γ' respectively.

$$\alpha' = \beta, \quad \beta' = \gamma, \quad \gamma' = \alpha$$

3. Calculation of the vector from the centre of molecular mass to the new centre of coordinates.

This vector can be resolved into three components along the principal moments of inertia,

$$R = r_a + r_b + r_c$$

As the whole molecule is planar, $r_c = 0$. r_a and r_b can be calculated in two ways. Whichever method is used, the answer should always be checked by measuring the distance on the diagram.

(a) By simple Geometry.

The slope of R can be calculated using equation (7.26) and the angle between I_A and R calculated (7.27).

$$m = \frac{X_2 - X_1}{Z_2 - Z_1} = 0.16714 \qquad \text{.....(7.26)}$$

$$\phi = \alpha - \tan^{-1} m = 18.5860 \qquad \text{.....(7.27)}$$

The length of vector R is given by,

$$R = \sqrt{\{(X_2 - X_1)^2 + (Z_2 - Z_1)^2\}} \qquad \text{.....(7.28)}$$

$$= 1.71313$$

and .

$$r_a = R \cos \phi = 1.62378 \qquad \text{.....(7.29)}$$

$$r_b = R \sin \phi = 0.54602 \qquad \text{.....(7.30)}$$

(b) By Vector Analysis.

The coordinates of the new centre must be defined in the XYZ system, based instead on the centre of molecular mass. In this case X' = 0.28241, Z' = 1.68969. r_a and r_b are found by solving

$$\left| -X', Z' \right| \left| \begin{matrix} \cos\alpha & -\sin\alpha \\ \sin\alpha & +\cos\alpha \end{matrix} \right| = \left| r_b, r_a \right| \qquad .....(7.31)$$

Care must be taken to give -X' the correct sign because the +ve end of the X axis is defined arbitarily, the final sign of -X' is negative in this case.

$$r_a = -X'(-\sin\alpha) + Z'\cos\alpha = 1.62378$$

$$r_b = -X'\cos\alpha + Z'\sin\alpha = 0.54602$$

4. The array of directional cosines.

The following array must be filled in, where α^{ix} is the cosine of the angle subtended by I_i on the X axis.

$$\left| \begin{matrix} \alpha^{ax} & \alpha^{bx} & \alpha^{cx} \\ \alpha^{ay} & \alpha^{by} & \alpha^{cy} \\ \alpha^{az} & \alpha^{bz} & \alpha^{cz} \end{matrix} \right| = +1 \qquad .....(7.32)$$

The solution, equation (7.33) must be equal to +1 which ensures that all the axes are defined in the correct "right handed" system.

$$(\alpha^{ax}.\alpha^{by}.\alpha^{cz} + \alpha^{bx}.\alpha^{cy}.\alpha^{az} + \alpha^{ay}.\alpha^{bz}.\alpha^{cx}$$
$$-\alpha^{az}.\alpha^{by}.\alpha^{cx} - \alpha^{bz}.\alpha^{cy}.\alpha^{ax} - \alpha^{ay}.\alpha^{bx}.\alpha^{cz}.)$$
$$= +1 \qquad .....(7.33)$$

To do this the polarities of the X and Z axes are selected as desired, and the polarities of I_A and I_B are selected to make r_a and r_b positive, as in diagram (7.6)

I_C and Y remain to be defined and this is done according to expression (7.33). Note that, because the molecule is planar,

$$\alpha^{ay} = \alpha^{by} = \alpha^{cz} = \alpha^{cx} = 0$$

and $\alpha^{cy} = \pm 1$, depending on how the axes have been named.

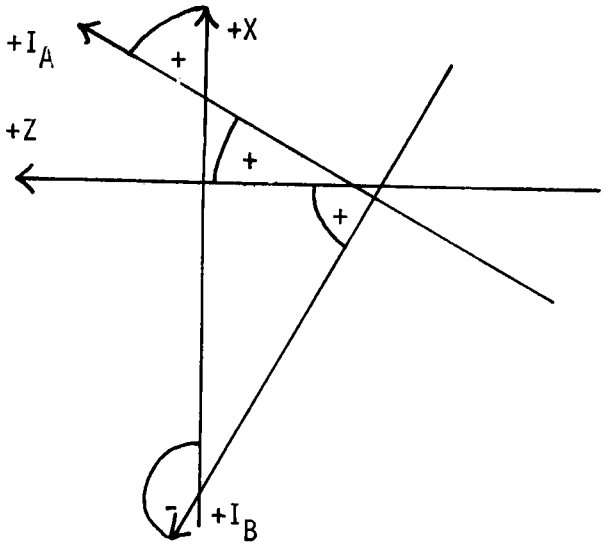

Diagram (7.6)
Illustration of the Method of Calculating the Signs of the Directional Cosines between Principal Moments and Selected Axes.

Diagram (7.6) shows the selected polarities for Z, X, I_A and I_B and the signs of the cosines. To find the sign rotate the +ve end of X or Z to the +ve end of I_A or I_B, if the angle is $>90^0$ then the cosine is -ve, if $<90^0$ then the cosine is +ve. From the diagram it can be seen that α^{bx} is negative whilst α^{ax}, α^{az} and α^{bz} are all positive, hence α^{cy} must be negative so that

$$\alpha^{az}.\alpha^{bx}.\alpha^{cy} - \alpha^{ax}.\alpha^{bz}.\alpha^{cy} = +1$$

Hence the directional cosines are:-

$$\begin{vmatrix} +0.47062 & -0.88234 & 0.0 \\ 0.0 & 0.0 & 0.0 \\ +0.88234 & +0.47062 & 0.0 \end{vmatrix} = +1$$

5. Calculation of the reduced moment of inertia.

The reduced moment of inertia of the top, I_r, can now be calculated[103]. With reference to the top coordinates calculated in section 2,

$$A_m = \Sigma_i m_i (X_i^2 + Y_i^2) = 2.92744 \times 10^{-39} \text{gm cm}^2$$

$$B_m = \Sigma_i m_i X_i Z_i = 0.75402 \times 10^{-39} \text{gm cm}^2$$

$$C_m = \Sigma_i m_i Y_i Z_i = 0.0$$

$$U_m = \Sigma_i m_i X_i = 2.53935 \times 10^{-39} \text{ gm cm}^2$$

where A_m, B_m and C_m are moments of inertia of the top and U_m is the off balance factor.

$$I_r = A_m - \sum_i \left[\frac{(\alpha^{iy} U_m)}{M} + \frac{(\beta_m^i)^2}{I_i} \right] \qquad \text{.....(7.35)}$$

where M is the molecular weight,

$$\beta_m^i = \alpha^{iz} A_m - \alpha^{ix} B_m - \alpha^{iy} C_m + U_m(\alpha^{i-1,y} r_{i+1} - \alpha^{i+1,y} r_{i-1}) \qquad \text{.....(7.36)}$$

and where i-1 and i+1 refer to cyclic shifts of axes so that i+1 = 1 when i=3 and i-1=3 when i=1.

$$\beta_m^a = \alpha^{az} . A_m - \alpha^{ax} . B_m + U_m . r_b . \alpha^{cy}$$
$$= 0.88234 . A_m - 0.47062 . B_m - 0.54602 . U_m$$
$$= 0.84161 \times 10^{-39} \text{ gm cm}^2$$

$$\beta_m^b = \alpha^{bz} A_m - \alpha^{bx} . B_m - U_m . r_a . \alpha^{cy}$$
$$= 0.47062 . A_m + 0.88234 . B_m + 1.62378 . U_m$$
$$= 6.16636 \times 10^{-39} \text{ gm cm}^2.$$

From equation (7.35)

$$I_r = A_m - \left[\frac{U_m^2}{M} + \frac{\beta m^{a^2}}{I_a} + \frac{\beta m^{b^2}}{I_b} \right]$$

$$= 2.92744 - \frac{2.53935^2}{11.6383} + \frac{0.84161^2}{2.57279} + \frac{6.16636^2}{38.4470}$$

$$= 1.1091 \times 10^{-39} \text{ gm cm}^2.$$

From equation (7.14), the value of the internal rotation constant is given by

$$F = 2.79908 \times 10^{-39} / I_r \text{ cm}^{-1}$$

$$F = 2.5238 \text{ cm}^{-1}$$

The twofold barrier parameter V* is given by equation (7.24) as

$$V^* = \nu^2/F$$

J.R. Durig et.al.[63] assigned the aldehyde torsion at 121 cm^{-1} which leads to the value for V* of 68.6 KJ mol^{-1} using a slightly different structure. Using this torsional frequency and the value of F calculated above,

$$V^* = 5801\ cm^{-1}$$

$$\therefore \quad \underline{V^* = 69.40\ KJ\ mol^{-1}}$$

D. Results

Methyl Barrier Heights. The calculated values for the barrier height of the methyl torsion, shown in table (7.1) are similar for all the methyl substituted butadienes. The barrier for s-trans isoprene was measured by microwave spectroscopy[40] as 10.96 ± 0.41 KJ mol^{-1} and the value obtained using the i.r. torsional frequency is 11.33 KJ mol^{-1} which is in reasonable agreement, although it is not possible to calculate the error limits of the i.r. value. The calculated value for s-cis isoprene, 10.80 KJ mol^{-1}, is lower than for the s-trans conformer. Molecular models show steric hindrance to methyl rotation in the s-trans conformer which is absent in the s-cis conformer, which is consistent with a higher barrier in the s-trans conformer.

The methyl barrier heights were also measured by microwave spectroscopy[42] for trans and cis pentadiene as 7.55 and 3.10 KJ mol^{-1} respectively. A theoretical study[104] of methyl barrier heights indicated that the barrier in cis-pentadiene would be low compared with trans-pentadiene, and gave a value for the isoprene barrier as 13.6KJ mol^{-1}.

These values are significantly different from the values calculated for the pentadienes from i.r. torsional frequencies in the present

work, 10.38 and 12.25 KJ mol^{-1} for trans and cis-pentadiene respectively.

	I_r	F	ν	V_3
	(gm cm^2)	(cm^{-1})	(cm^{-1})	(KJ mol^{-1})
Crotonaldehyde	0.4356	6.425	173	7.38
S-trans-isoprene	0.5310	5.272	199.3	11.33
S-cis-isoprene	0.5170	5.414	196.7	10.80
Trans-pentadiene	0.4515	6.199	205	10.38
Cis-pendadiene	0.5087	5.502	212	12.25

Table (7.1)
Values for the Parameters used in Calculation of the Barrier Height To Internal Rotation of the Methyl Group and the Resulting values of V_3.

J.R. Durig et.al. measured the methyl barrier heights in trans and cis crotonitrile[105] as 7.36 and 12.9 KJ mol^{-1}, and the crotonitriles have similar methyl environments to the pentadienes. Molecular models show that the cis-pentadiene methyl group is sterically hindered whereas no hindrance is observed in trans-pentadiene. This steric hindrance and the evidence of a larger barrier in cis-crotonitrile than in trans-crotonitrile is consistent with the present relative values in the pentadienes but is not in accord with the microwave values[42]. Also the methyl groups in cis-pentadiene and s-trans isoprene are in similar environments and so it is reasonable to expect similar barrier heights in the two compounds. The values given in table (7.1) are approximately the same, and so the value previously reported[42] for cis-pentadienes must be held in doubt, as it is much smaller, and the experimental results merit reinvestigation.

Twofold Barrier Heights. It can be seen, from table (7.2), that substitution for a hydrogen by a methyl or chlorine increases the barrier V*. This increase is lowest for trans-pentadiene and highest for isoprene. As noted before[78], the large difference in electroneg-

ativity between a chlorine and methyl group makes only a small change in V*, and it appears that the position of substitution is more important than other factors, as fluoroprene, chloroprene and isoprene all have similar V* values[78].

Substitution of a methyl group for a hydrogen alters V* according to the substitution position. Substitution at the trans position has little effect as the methyl group does not interfere with the internal rotation, but cis substitution or substitution at position 2 (isoprene) increases the value V* more. This is associated with steric hindrance to internal rotation of the asymmetric rotor.

Replacement of a $=CH_2$ group by =O lowers V* in the case of chloroprene and acryloyl chloride. This has been noted previously for butadiene and acrolein[78] (88.7 KJ mol^{-1}) and has been associated with the greater double bond character of the central C-C bond in butadiene than acrolein. A theoretical study on the barrier, V*, in substituted butadienes[106] concludes that substitution decreases the barrier and that isoprene has a lower barrier than butadiene. The poor correlation between this theoretical study and experimental results casts doubt on the validity of the similar study on methyl barriers[104] mentioned above by the same author, and shows the difficulty in calculating barriers accurately.

Values for the Parameters used in Calculation of the Twofold Barrier Parameter V*

	I_A	I_B	I_C	α^{ax}	α^{bx}	I_m	F	ν	V*
	(gm cm^2)					(gm cm^2)	(cm^{-1})	(cm^{-1})	(KJ mol^{-1})
Butadiene	2.011	18.904	20.915	0.5553	0.8316	1.050	2.665	163.7	100.6
Isoprene	9.735	20.136	29.325	0.3976	0.9176	1.437	1.948	152.7	143.2
Cis-Pentadiene	5.368	31.535	36.373	0.7620	0.6476	1.594	1.757	140	133.4
Trans-Pentadiene	2.982	38.782	41.234	0.4514	0.8923	1.242	2.253	150	119.5
Crotonaldehyde	2.572	38.447	40.490	0.4706	0.8823	1.109	2.524	122	70.55
Chloroprene+	15.853	22.254	38.107	0.0618	0.9981	1.409	1.987	144	124.8
Acryloyl Chloride+	15.177	22.133	37.311	0.1784	0.9840	1.461	1.916	106	70.14

+ Based on Isotopic Mixture

Table (7.2)

CHAPTER VIII

Calculation of the Gas Phase Thermodynamic Functions of Compounds Existing as a Mixture of Conformers by Statistical Mechanics.

A. Introduction.

B. Thermodynamic Contributions due to a Mixture of Conformers.

C. Results.

CHAPTER VIII

Calculation of the Gas Phase Thermodynamic Functions of Compounds Existing as a Mixture of Conformers by Statistical Mechanics

A. Introduction

Thermodynamic data on chemical compounds is important both theoretically and practically, but unfortunately the available information has not been tabulated for many compounds. Statistical calculation of data for the gaseous phase is comparatively straight forward for simple systems if a full vibtational assignment is available for a compound, and the calculated results agree with measured results. A review of the statistical calculations was given [107] by S.G. Frankiss and J.H.S. Green, where the following statistical formulae for the Gibbs Free Energy, Enthalpy, Heat Capacity and Entropy (all units of $JK^{-1}mol^{-1}$) are given:-

$$u = 1{\cdot}43879\ \omega_i/T$$

$$D = I_A{\cdot}I_B{\cdot}I_C{\cdot}\ 10^{117}\ gm\ cm^2$$

$$-\left(\frac{G^\theta - H_0^\theta}{T}\right) = 12{\cdot}4715\ \ln W + 33{\cdot}2573\ \ln T + 4{\cdot}15717\ \ln D - 8{\cdot}31433\ \ln \sigma - 43{\cdot}0867 - 8{\cdot}31433\sum_{i=1}^{i=j} \ln\left(1 - e^{-u}\right) \quad .....(8.1)$$

$$\left(\frac{H^\theta - H_0^\theta}{T}\right) = 33{\cdot}2573 + 8{\cdot}31433\sum_{i=1}^{i=j} u/(e^u - 1) \quad .....(8.2)$$

$$C_p^\theta = 33{\cdot}2573 + 8{\cdot}31433\sum_{i=1}^{i=j} u^2e^u/(e^u - 1)^2 \quad .....(8.3)$$

$$S^\theta = \left(\frac{H_0^\theta - H_0^\theta}{T}\right) - \left(\frac{G^\theta - H_0^\theta}{T}\right) \quad .....(8.4)$$

In the above expression, W is the molecular weight in grams per mole, σ is an integer depending on the symmetry of the molecule (1 for C_s molecules and 2 for C_{2h} molecules), and ω_i is the i^{th} fundamental frequency. The integer i runs from 1 to j if all vibrations can be considered as harmonic oscillators (including the torsions with a high barrier) j has the value 3N-6 where N is the number of atoms in the molecule. However, if a torsion with a medium barrier is present then this vibration is treated separately and j has the value 3N-7.

Several molecules have a methyl group undergoing hindered internal rotation due to the medium barrier. In this case the increase in thermodynamic functions is calculated from tables, using the partition function

$$Q_f = 2{\cdot}7930\ (10^{38}\ I_r T)^{\frac{1}{2}} / n \qquad .....(8.5)$$

where n is the symmetry of the barrier, 3 for a methyl group, and I_r is the reduced moment of inertia in gm cm^2.

Tables of V/RT against $1/Q_f$ are available for each thermodynamic function,[108,109] interpolation into these tables gives the contribution to the functions at each temperature due to the hindered rotation.

The above method of calculating thermodynamic functions of gases has several inherent assumptions. All vibrations except the torsion of a hindered rotation are assumed to be harmonic oscillations, also interactions between vibrational modes and between vibrations and rotation are ignored. At relatively low temperatures vibrations are reasonably harmonic but at higher temperatures anharmonicity can be calculated for diatomic molecules, but the complexity of a polyatomic molecule makes this difficult. Other possible high temperature effects are the change in molecular structure, force constants, barrier heights and moments of inertia due to higher rotational states and higher

vibrational states. As has been demonstrated hot bands and vibration rotation coupling are common in the compounds studied, but no correction terms for the partition functions can be made. The electronic partition function for most polyatomic molecules reduces to the degeneracy of the groundelectronic state which is 1, as the excited states are so high in energy that they can be ignored, and this results in reducing the electronic contributions to the functions to zero. At very high temperatures population of the excited electronic states is sufficient to give slow polymerisation of conjugated compounds and so the functions cannot be considered very accurate at these high temperatures.

Any interaction between rotating tops is ignored in molecules containing more than one top. This interaction is quantifiable between similar tops but is probably negligible between tops of such different nature as a methyl and vinyl group.

In this work all of the thermodynamic functions for the conformers of each compound were calculated using Program THERM on the IBM 1130. This uses moments of inertia, σ, molecular weight and full vibrational assignment for a conformer to calculate the functions at specified temperatures. Contributions to the functions by a methyl top are calculated using subroutine INTER, a rewritten version of the standard routine POLRG, which in turn uses other special rewritten 1130 subroutines MULDC, MINDC, GDADC and ORDDC. INTER computes the polynomial regression slope of each column of the V/RT versus $1/Q_f$ tables[108,109] and interpolates using the values of V/RT; then uses these results in rows to interpolate at the correct $1/Q_f$ values to obtain the final values of the thermodynamic contribution. During this process columns or rows which are not fitted to a tolerance of ± 2% are skipped to keep accurate results. The complete tables are fed in on punch cards

before the other data for each computer run.

The program was tested using the data of crotonaldehyde. Thermodynamic functions for the gas phase of the s-trans conformer of crotonaldehyde have been published by J.R. Durig et.al.,[63] and the values calculated by THERM agree to within the limits of computational error.

A listing of program THERM is given in the Appendix.

B. Thermodynamic Contributions Due To A Mixture of Conformers

The statistical calculations in part A above compute the thermodynamic functions for rigid molecules or molecules with internal rotation of a group across a medium or low barrier. Many of the compounds studied have conformers which can be identified as having different structures for a finite time due to the high barrier to rotation. In this case the torsion can be treated as a harmonic oscillator but the thermodynamic functions show an increase due to the mixture of conformers.

To calculate the functions for compounds existing as a mixture of conformers the functions are first calculated for each conformer separately using program THERM, and then if the enthalpy difference between conformers, ΔH^{θ}, is known then the contribution to the thermodynamic functions by mixing of the conformers can be calculated. Conversely, if accurate values of the gas phase thermodynamic functions are available, then a value of ΔH^{θ} can be calculated so that the calculated and measured functions agree. Because statistical mechanics can only calculate the enthalpy at temperature T relative to that at absolute zero, $(H_T^{\theta} - H_0^{\theta})/T$, the difference in enthalpy between conformers at absolute zero, ΔH_0^{θ}, must be calculated. An approximate relationship between ΔH^{θ} and ΔH_0^{θ} is given by equation (8.6), but due to the relatively

high experimental error in the calculation of ΔH^{θ} any approximation is negligible.

$$\Delta H^{\theta} = \Delta H_0^{\theta} + T\Delta C_p^{\theta} \qquad .....(8.6)$$

To calculate ΔH_0^{θ} the average value of ΔC_p^{θ} over the temperature range that ΔH^{θ} is determined must be calculated. The calculated values of ΔH_0^{θ} are given in Table (8.1), along with the moments of inertia of each conformer used in the calculations.

The method of calculation given refers to the general case of conformational equilibrium where a value for ΔH^{θ} is available and m equivalent types of low energy conformer A are in equilibrium with n types of conformer B; i.e. $\{A\} \rightleftharpoons \{B\}$ where $\{A\}$ is the total concentration of all types of conformer A. The entropy change of the equilibrium must take into account the statistical weights of conformers A and B, and is given by equation (8.7)

$$\Delta S^{\theta} = S_B^{\theta} - S_A^{\theta} + R \ln (n/m) \qquad .....(8.7)$$

The free energy change of the equilibrium is calculated in equation (8.9) from the statistical values by including the enthalpy difference between conformers at absolute zero, ΔH_0^{θ}.

$$\Delta G^{\theta} = \Delta H^{\theta} - T\Delta S^{\theta} \qquad .....(8.8)$$

$$\Delta G^{\theta} = T\left[\left(\frac{H_B^{\theta} - H_{0,B}^{\theta}}{T}\right) - \left(\frac{H_A^{\theta} - H_{0,A}^{\theta}}{T}\right) - S_B^{\theta} + S_A^{\theta} - R \ln(n/m)\right] + \Delta H_0^{\theta}$$

$$= T\left[\left(\frac{G_B^{\theta} - H_{0,B}^{\theta}}{T}\right) - \left(\frac{G_A^{\theta} - H_{0,A}^{\theta}}{T}\right) - R \ln(n/m)\right] + \Delta H_0^{\theta} \qquad .....(8.9)$$

$$= -RT \ln K \qquad .....(8.10)$$

From the free energy change the concentration of high energy conformer, X_B, can be calculated by equation (8.10) and (8.11)

$$X_B = K/(1 + K) \qquad .....(8.11)$$

Values of X_B calculated are given in table (8.4) over a range of temperatures.

Using the value of X_B calculated at any temperature the final values for the thermodynamic functions of the mixture, given in tables (8.5) - (8.7), are calculated by equations (8.12) - (8.15), first reported by J.G. Aston et.al[25].

$$S^{\theta} = X_A S^{\theta}_A + X_B S^{\theta}_B - R\left[X_A \ln (X_A/m) + X_B \ln (X_B/n)\right] \quad .....(8.12)$$

$$C_P = X_A C_{P,A} + X_B C_{P,B} + \left(\frac{X_A X_B}{R}\right)\left[\frac{\Delta H^{\theta}_0}{T} + \left(\frac{H^{\theta}_B - H^{\theta}_{0,B}}{T}\right) - \left(\frac{H^{\theta}_A - H^{\theta}_{0,A}}{T}\right)\right]^2 \quad .....(8.13)$$

$$\left(\frac{H^{\theta} - H^{\theta}_0}{T}\right) = X_A\left(\frac{H^{\theta}_A - H^{\theta}_{0,A}}{T}\right) + X_B\left[\left(\frac{H^{\theta}_B - H^{\theta}_{0,B}}{T}\right) + \frac{\Delta H^{\theta}_0}{T}\right] \quad .....(8.14)$$

$$-\left(\frac{G^{\theta} - H^{\theta}_0}{T}\right) = \left(\frac{H^{\theta} - H^{\theta}_0}{T}\right) - S^{\theta} \quad .....(8.15)$$

If accurate values of the gas phase thermodynamic functions of a compound have been measured by calorimetric methods, then ΔH^{θ} can be calculated by fitting statistical values to the experimental values using equations (8.12) to (8.15). Firstly the entropy is fitted by assuming a molecular model, and hence values for n and m, and varying X_B. Then using this value of X_B the C_P values are fitted by varying ΔH^{θ}_0. These calculations are performed over the range of temperatures that the calorimetric data is available, and if the fit is good X_B will increase regularly with temperature but ΔH^{θ}_0 will remain constant. ΔH^{θ} can then be evaluated from the average value of ΔH^{θ}_0 using equation (8.6).

In this method the calorimetric values for the entropy and heat capacity are fitted with preference to other functions as the enthalpy is difficult to measure by calorimetric methods.

C. Results

Butadiene Accurate values of the gas phase thermodynamic functions were calculated over the temperature range -100 to 150°C by R.B. Scott et.al.[110]. Attempts to fit this data to an equilibrium of conformers by statistical methods were made by J.G. Aston et.al.[25] , and L.M. Sverdlov and E.N. Bolotina[111]. The latter work used a method formulated by I. Godnev and V. Morozov[112] which was examined here and found to be inadequate.

J.G. Aston et.al.[25] formulated equations (8.12) to (8.15) used here. In their work they assumed that the high energy conformer was s-cis, and calculated ΔH_0^θ to be about 9·6 KJ mol^{-1}.

Recently L.A. Carriera calculated ΔH^θ to be 10·5 KJ mol^{-1} by observing torsional overtones in the Raman Spectrum and calculating the torsional potential[21].

Statistical values of the thermodynamic functions using more accurate vibrational assignments than J.G. Aston[25] were calculated for s-trans and s-cis conformers, and it was assumed that gauche conformers would have values very close to those of the s-cis conformer. In these calculations the s-trans structure postulated by K. Kuchitsu[22] and a suitable s-cis structure were used to calculate the moments of inertia given in table (8.1). All fundamental frequencies given in table (4.3) were considered as harmonic oscillators.

The calorimetric values of the entropy[110] at each temperature were fitted assuming firstly an s-cis high energy conformer (n=1) and secondly using gauche conformers (n=2). The resultant values of X_B calculated differed according to n, and these values were used to fit the heat capacity data by postulating values for ΔH_0^θ. It was found that the values of ΔH_0^θ between conformers were 10·4 and 11·4 KJ mol^{-1}

assuming s-cis and gauche forms respectively. Over the temperature range studied $T\Delta C_p^\theta$, equation (8.6), is negligible (i.e. less than 50 J mol^{-1}) and so ΔH^θ takes these values. Because L.A. Carriera[21] calculated ΔH^θ to be 10·5 KJ mol^{-1}, the value of 10·4 calculated assuming an s-cis conformer is in good agreement whilst the value of 11·4 assuming gauche conformers is not. Hence it is concluded that the high energy conformer of butadiene is s-cis. The results of the calculations assuming the s-cis conformer are given in table (8.2). This shows that the room temperature concentration of butadiene is less than 3% which explains why no evidence for the s-cis conformer was observed in Chapter IV. At this low concentration any errors due to the assumed structure or vibrational frequencies of the s-cis conformer will be negligible.

Isoprene J.E. Kilpatrick et.al.[113] gave values for the thermodynamic functions of isoprene and cis and trans-pentadiene which were calculated from other compounds. An attempt was made to fit these values, as was done for butadiene, by postulating a value for ΔH_0^θ but the fit was poor and it was necessary to postulate a higher value of ΔH^θ, equation (8.6), than observed in chapter IV. The thermodynamic functions have been recalculated using the experimental value of ΔH^θ which gives ΔH_0^θ as 4·9 KJ mol^{-1}. In the calculations the s-trans structure observed by microwave spectroscopy[40] was used and the high energy conformer assumed to be s-cis like butadiene. All the vibrational frequencies, table (4.3), were assumed to be harmonic oscillators except for the methyl torsion and contributions to the functions due to this torsion were calculated as explained in section B. Values of the thermodynamic functions are given in tables (8.5) to (8.7).

Cis- and Trans-Pentadiene No evidence has been found in this study of a high energy conformer of either compound, and so the thermodynamic

functions of the s-trans conformers only are presented in tables (8.5) - (8.7). These values are significantly different from those present in the literature [113,114], which were calculated from other compounds. The entropy and heat capacity data for trans-pentadiene are both larger than the literature values, as is the heat capacity data for cis-pentadiene below 400K. The entropy values of cis-pentadiene are lower than those presented in the literature.

In the calculations the s-trans structures of the pentadienes proposed by microwave spectroscopy[42] and the fundamental vibrations in table (5.3) were used.

Chloroprene Accurate calculations on the thermodynamic functions of gaseous chloroprene have not been made. It is reasonably accurate, however, to calculate the functions of a chloro compound R-X from its methyl analogue[109], R-Me. To do this for chloroprene the functions for isoprene were modified by allowing for the change from methyl to chlorine by equation (8.16), where F is a general thermodynamic function.

$$F(\text{chloroprene}) = F(\text{isoprene}) + F(\text{chloroethene}) - F(\text{propene}) \quad \ldots\ldots(8.16)$$

These calculated values are given in table (8.3). Data for chloroethene and propene was that selected by Stull et.al.[109]. The calculated values were fitted, in the same manner as butadiene, by assuming a high energy s-cis conformer as the calculated values for the s-trans conformer alone are too low, and both butadiene and acryloyl fluoride[15] probably have a planar high energy conformer. The average value of ΔH_0^θ necessary to fit the data is 8.7 KJ mol^{-1}. In the calculations, the s-trans structure proposed by P.A. Akishin[93] and a suitable s-cis structure were used to calculate moments of inertia, and the vibrational assignment given in table (6.3) was used.

Crotonaldehyde Thermodynamic functions have recently been reported[63]

for the s-trans conformer of crotonaldehyde in the gaseous phase. In the same work a full assignment was given for the s-trans conformer. Bands at 395 and 1690 cm^{-1} in the liquid Raman spectrum were assigned as s-cis bands, leading to a value of ΔH^{θ} of 1·7 cal mol^{-1}.

The structure of crotonaldehyde was shown to be s-trans by microwave spectroscopy[56,115], but no evidence for a high energy conformer was given. Both studies gave similar values for the moments of inertia and methyl torsion barrier height. The values of M. Suzuki and K. Kozima[56] were used for this calculation, and their value of 1730 cal mol^{-1} for the methyl barrier leads to a value of 171 cm^{-1} for the torsion in the gaseous phase. The s-cis structure was assumed present, as for acrolein[116].

The calculations show that a low concentration of s-cis crotonaldehyde is present (about 7% at room temperature) which explains why no evidence for this was found in the microwave spectra.

Acrolein E.A. Cherniak and C.C. Costain[33] examined the microwave spectrum of acrolein and ten isotopically substituted molecules and assigned peaks to s-trans conformers in each case, giving principal moments of inertia. They searched for evidence of a high energy conformer (either s-cis or gauche) but could find none, indicating a higher energy conformer concentration probably well below 10%, if at all.

L.A. Carriera examined the Raman spectrum of gaseous propenal and assigned weak peaks as torsional overtones of both the s-trans and high energy conformer[116]. The torsional potential function was calculated and this led to assignment of the high energy conformer as s-cis, 584 ± 180 cm^{-1} above the s-trans.

A complete vibrational assignment for s-trans acrolein was given by A.J. Bowles et.al.[34], using low frequency data reported by R.K. Harris[18],

but no evidence for a high energy conformer was found. Recently Krantz et.al. observed the i.r. spectrum using matrix isolation techniques[117], and noted weak bands which increased in intensity on photoradiation of the matrix. These bands were assigned to the s-cis conformer as redeposition of the matrix gave the original spectrum.

Acryloyl Chloride. The microwave spectrum of acryloyl chloride[59] located only peaks due to the s-trans conformer. Moments of inertia for molecules containing both Cl^{35} and Cl^{37} isotopes were given, and the values in table (8.1) are a mean value using the isotopic ratio 0.755 : 0.245. Moments were calculated for the s-cis conformer, as for acryloyl fluoride[57]. Microwave peaks were also observed for molecules in the first torsional excited state and an estimate for the torsional frequency of the s-trans molecule calculated as 94 cm^{-1} from equation (8.17). Δ_0 and Δ_1 are the inertia defects in ground state

$$\Delta_1 - \Delta_0 = -4(h/8\pi^2 c)(1/\nu) \qquad .....(8.17)$$

and first excited state respectively. This value of ν is close to the observed frequency of 106 cm^{-1}.

A value of ΔH^{θ} of 600 cal mol^{-1} was calculated over the temperature range 276-361K from the i.r. spectrum[60].

The vibrational frequencies of both conformers used in the calculations are those selected in table (6.3).

Acryloyl Fluoride. A microwave study assigned peaks to two conformers which were shown to be both planar[57]. The extra enthalpy of the s-cis conformer was calculated to be 90 ± 100 cal mol^{-1}. Peaks due to molecules in excited torsional states of both conformers were observed. Using equation (8.17) and the microwave data presented by J.J. Keirns and R.F. Curl[57], values for the torsional frequencies of s-trans and s-cis acryloyl fluoride are calculated as 93 and 85 cm^{-1} respectively for the gaseous phase.

A complete vibrational assignment was made by G.L. Carlson et.al.[58] and a value of ΔH^{θ} for a solution of acryloyl fluoride in CS_2 of 150 cal mol^{-1} was calculated by measuring the small temperature dependence of bands at just below 1000 cm^{-1}. R.L. Redington[118] studied the i.r. spectrum of matrix isolated acryloyl fluoride and gave complete updated assignments. The s-trans and s-cis torsions were assigned to very weak gas bands at 115 and 195 cm^{-1} respectively, which indicates a large energy difference between conformers. The s-cis value disagrees with the microwave prediction of 85 cm^{-1}, which is closer to the 83 cm^{-1} calculated in chapter VI for s-cis acryloyl chloride.

A recent study of a range of unsaturated compounds[37] has shown that there are two strong out-of-plane vibrations just below 1000 cm^{-1} in s-trans acryloyl fluoride, at about 996 cm^{-1} (trans wag) and 980 cm^{-1} ($=CH_2$ wag). These were the peaks assigned previously as a conformer pair[58], and so the i.r. ΔH^{θ} value cannot be used.

The frequencies used in this study are those selected by R.L. Redington[118] except for the following fundamentals:- trans wag, 986 cm^{-1} for both conformers, $=CH_2$ wag, 977 cm^{-1} for both conformers, cis wag, 805 (s-trans) and 800 (s-cis). These values are taken from the high resolution spectra of R.L. Redington [118], and it is interesting to note that the cis wag shows hot bands for both conformers, like the similar bands for acryloyl chloride. The s-cis torsion is given a value of 85 cm^{-1}.

Glyoxal The s-trans conformer of glyoxal has a centre of symmetry and therefore exhibits no microwave spectrum, whereas a high energy conformer will give a spectrum due to lower symmetry. J.R. Durig et.al.[37] examined the microwave spectrum and assigned peaks to a high energy conformer which had only a small inertia defect and so was determined to be

the planar s-cis form. The s-cis torsion was assigned a value of 114 ± 8 cm^{-1}.

An electron diffraction study[22] assigned the predominant conformer as s-trans and moments of inertia have been calculated from their proposed structure.

G.N. Currie and D.A. Ramsay[38] examined an electronic band of glyoxal at 488 nm under high resolution and measured the rotational spacings which they assigned to the s-cis conformer. They obtained a value of ΔH^{θ} of 1125 ± 100 cm^{-1}.

Fundamental frequencies were assigned by Harris[18], and Cole and Osbourne[39] have given more accurate values.

The concentration of s-cis glyoxal calculated is only ablut 0.5% at room temperature which explains why neither vibrational spectroscopy nor electron diffraction gave evidence of the s-cis conformer. In the electronic study[38]it was noted that the band due to the s-cis conformer was about 1000 times weaker than a similar s-trans band, which points to a very low concentration. It is interesting to note that even such low concentration of s-cis raises the entropy and heat capacity relative to the pure s-trans conformer by 0.3 and 1.2 JK^{-1} mol^{-1} respectively.

Oxalyl Chloride. The vibrational spectrum of oxalyl chloride was examined in gas, liquid and solid states using i.r. and in liquid states using Raman by J.R. Durig and S.E. Hannum[65]. Complete vibrational assignements were given for both s-trans and s-cis conformers except for the s-cis torsion, and a value of ΔH^{θ} given as 2.2 ± 0.2 Kcal mol^{-1} for the liquid state. However, no reason for selecting s-cis as the high energy form instead of gauche was given.

An electron diffraction study of ethanedioyl chloride in the gas was carried out by K. Hagen and K. Hedberg[67], who concluded that the molecule existed predominantly as the s-trans conformer, but the high

energy conformer was gauche , some 55° off the s-cis structure. This conclusion was verified qualitatively by a recent theoretical study on oxalyl chloride[119] which concluded that the high energy conformer is gauche, although a higher value of ΔH^{θ} (2.8 Kcal mol^{-1}) was given. They[67] calculated the concentration of gauche conformer at 0, 80°, and 190°C to be 0·324, 0·487 and 0·576 respectively, from which they calculated ΔH^{θ} as 1380 cal mol^{-1} and ΔS^{θ} as 2·3 cal mol^{-1} deg^{-1}. They gave proposed structures for both conformers and these were used to calculate the values of the moments of inertia given in table (8.1).

The calculations in this work gave results which agreed well with those of K. Hagen and K. Hedberg[67]. The values of ΔS^{θ} (measured statistically at 298K) and the concentration of gauche form at 273 K are 11·3 (+ 5·8) JK^{-1} mol^{-1} and 0·33, compare well with their values of 9·6 and 0·32 respectively.

Oxalyl Bromide The vibrational spectrum of oxalyl bromide was examined by J.R. Durig et.al.[66], in the gas, liquid and solid states using i.r. and the liquid and solid states using Raman. A complete assignment was given for the predominant s-trans conformer and nearly all the high energy conformer bands were assigned, and a value of ΔH^{θ} of 2·9 ± 0·1 Kcal mol^{-1} was obtained for the liquid state.

K. Hagen and K. Hedberg[68] studied oxalyl bromide in the gas phase using electron diffraction. They concluded that the high energy form was gauche like oxalyl chloride, but that ΔH^{θ} was only 0·63 Kcal mol^{-1} and ΔS^{θ} 1·1 (+ 1·376) cal deg^{-1} mol^{-1}. These results contrast greatly with those reported by J.R. Durig et.al.[66] and cannot be easily explained by difference between gas and liquid states.

In this work the vibrational assignment given by J.R. Durig et.al.[66] was used and moments of inertia were calculated from the results of

K. Hagen and K. Hedberg[68]. The calculated concentration of gauche conformer was 74% at room temperature which cannot be correct, as the vibrational spectrum indicates s-trans predominating. The s-trans conformer has a centre of symmetry which results in application of the mutual exclusion rule for vibrations due to this conformer. Bands which disappear on freezing are due to the asymmetric gauche form and are present in both Raman and i.r. whereas bands which remain in the solid are due to the centrosymmetric s-trans conformer and so are found in either Raman or i.r., but not both. However, at room temperature the s-trans bands are strongest and this would indicate that the concentration of gauche is less than 50%.

Because the calculations give results which are clearly inconsistent, the thermodynamic values are not tabulated. It appears that the electron diffraction study[68] gave a low ΔH^{θ} value, and that the liquid value[66] is probably more realistic.

It can be seen that this method of calculating thermodynamic functions can also be a useful method for checking experimental values of ΔH^{θ} and pointing out discrepancies.

Selected Values for the Principal Moments of Inertia of Conformers and the Enthalpy Differences between Conformers

	Low Energy Conformer				High Energy Conformer				Enthalpy Difference †	
		I_A^*	I_B^*	I_C^*		I_A^*	I_B^*	I_C^*	ΔH^θ	ΔH_0^θ
Butadiene	s-trans	2.0031	18.906	20.909	s-cis	4.1914	13.695	17.886	10400	10400
Isoprene	s-trans	9.7353	20.137	29.326	s-cis	8.7009	21.680	29.835	4590	4900
Trans-Pentadiene	s-trans	2.9724	38.852	41.287	-	-	-	-	-	-
Cis-Pentadiene	s-trans	5.3635	31.568	36.401	-	-	-	-	-	-
Chloroprene	s-trans	15.853	22.254	38.107	s-cis	9.9214	32.466	42.388	8800	8700
Crotonaldehyde	s-trans	2.5713	38.437	40.476	s-cis	4.5436	31.390	35.403	7110	6880
Acrolein	s-trans	1.7727	18.016	19.785	s-cis	3.7854	12.989	16.775	6990	6810
Acryloyl Chloride	s-trans	15.182	22.061	37.248	s-cis	8.8068	33.458	42.265	2510	2440
Acryloyl Fluoride	s-trans	7.9440	18.854	26.798	s-cis	7.6913	19.954	27.639	380	550
Glyoxal	s-trans	1.5125	17.529	19.042	s-cis	3.1403	13.533	16.642	13450	13460
Oxalyl Chloride	s-trans	16.786	55.725	72.512	gauche	26.212	44.200	60.210	5780	4780
Oxalyl Bromide	s-trans	17.221	144.44	161.66	gauche	36.300	98.295	118.27	2640	1940

* Units:- 10^{-39} gm cm^2

Units:- J mol^{-1}

Table (8.1)

Thermodynamic Functions of Butadiene in units of J K^{-1} mol^{-1}

T	S^{θ}		C_P^{θ}		$-(G^{\theta}-H_0^{\theta})/T$		X_{cis}	ΔH_0^{θ}
	A	B	A	B	A	B		
173.15	243.85	243.86	52.04	52.03	200.40	203.61	0.0007	10400
223.15	258.28	258.32	62.37	62.35	211.97	214.20	0.0066	10500
233.15	261.06	261.08	64.59	64.52	214.12	216.14	0.0080	10600
243.15	263.82	263.85	66.91	66.87	216.22	218.05	0.0105	10500
253.15	266.56	266.56	69.18	69.12	218.29	219.89	0.0125	10500
263.15	269.29	269.31	71.56	71.58	220.31	221.72	0.016	10400
273.15	272.01	272.02	73.89	73.89	222.30	223.51	0.019	10300
283.15	274.71	274.70	76.27	76.29	224.11	225.26	0.022	10400
298.15	278.73	278.73	79.89	79.88	227.10	227.83	0.028	10300
323.15	285.41	285.38	85.90	85.86	231.70	231.99	0.039	10300
353.15	293.35	293.33	93.04	93.09	236.96	236.80	0.056	10400
373.15	298.60	298.59	97.64	97.69	240.30	239.92	0.069	10400
423.15	311.54	311.52	108.24	108.26	248.09	247.49	0.106	10300

A:- Calorimetric Values Measured by R. B. Scott et.al.[110], B:- Fitted Values

Table (8.2). Average value of ΔH_0^{θ} is 10400 J mol^{-1}

Thermodynamic Functions of Chloroprene in J K^{-1} mol^{-1}.

T	S^{θ}		C_P^{θ}		$-(G^{\theta} - H_0^{\theta})/T$		X_{cis}	ΔH_0^{θ}
	A	B	A	B	A	B		
298.15	312.98	312.99	92.59	92.54	255.58	255.66	0.026	9800
300.0	313.50	313.55	92.97	92.93	255.86	256.02	0.026	9800
400.0	343.30	343.31	113.97	113.96	274.21	274.32	0.064	8300
500.0	370.62	370.61	130.98	131.01	290.77	290.95	0.094	8200
600.0	395.75	395.75	144.61	144.60	306.20	306.43	0.121	8100
700.0	418.88	418.88	155.72	155.72	320.54	320.90	0.140	8200
800.0	440.29	440.29	165.05	165.04	334.27	334.51	0.156	8400
900.0	460.12	460.13	172.99	172.99	347.10	347.34	0.165	8800
1000.0	478.75	478.76	179.77	179.76	359.45	359.59	0.180	8900

A:- Values calculated by equation (8.16). B:- Fitted Values

Average value of ΔH_0^{θ} is 8700 J mol^{-1}.

Table (8.3)

Concentration of High Energy Conformer Calculated in Percent

T	273.15	298.15	300.0	400.0	500.0	600.0	700.0	800.0	900.0	1000.0
Isoprene	9.7	11.3	11.3	17.0	21.3	24.4	26.8	28.7	30.1	31.4
Crotonaldehyde	5.3	6.7	6.9	13.1	18.8	23.6	27.6	30.8	33.5	35.7
Acrolein	5.9	7.5	7.6	14.2	20.3	25.3	29.3	32.6	35.3	37.6
Acryloyl Chloride	29.9	32.0	32.1	38.2	42.2	44.8	46.7	48.2	49.2	50.2
Acryloyl Fluoride	49.3	49.8	49.8	51.1	51.8	52.3	52.6	52.8	53.0	53.1
Glyoxal	0.47*	0.56	0.58	2.20	4.8	8.0	11.4	14.7	17.7	20.5
Oxalyl Chloride	32.8	38.1	38.5	54.4	54.0	70.0	74.8	76.9	78.9	80.5

* 289K

Table (8.4)

Values of Entropy, S^{θ}, at each Temperature, in $JK^{-1}\ mol^{-1}$.

T	273.15	298.15	300.0	400.0	500.0	600.0	700.0	800.0	900.0	1000.0
Isoprene	307.3	316.0	316.6	349.9	381.1	410.4	437.8	463.6	487.8	510.7
Trans-Pentadiene	312.8	321.8	322.4	356.2	387.8	417.3	444.9	470.7	495.0	517.9
Cis-Pentadiene	301.6	309.6	310.2	341.7	371.7	400.1	426.9	452.0	475.8	498.2
Crotonaldehyde	309.9	318.0	318.6	349.0	376.8	402.5	426.4	448.7	469.6	489.2
Acrolein	275.6	281.7	282.1	304.9	325.7	344.9	362.7	379.1	394.5	408.9
Acroloyl Chloride	310.0	317.1	317.7	343.7	366.9	388.0	407.2	424.8	441.1	456.2
Acryloyl Fluoride	296.5	302.6	303.0	325.9	347.2	366.9	385.2	402.2	418.0	432.8
Glyoxal	270.5*	272.4	272.7	291.9	309.1	324.9	339.3	352.6	364.9	376.2
Oxalyl Chloride	334.7	343.5	344.1	374.4	398.8	419.4	437.3	453.2	467.4	480.3

* 289K

Table (8.5)

Values of Heat Capacity, C_p^{θ}, at Each Temperature in $JK^{-1}\ mol^{-1}$.

T	273.15	298.15	300.0	400.0	500.0	600.0	700.0	800.0	900.0	1000.0
Isoprene	96.1	102.8	103.2	128.8	151.1	170.1	186.1	199.9	211.8	222.1
Trans-Pentadiene	98.7	105.1	105.5	130.4	162.4	171.2	187.0	200.6	212.4	222.6
Cis-Pentadiene	88.9	95.9	96.4	123.0	146.1	165.5	181.7	195.5	207.4	217.7
Crotonaldehyde	90.2	95.4	95.8	115.8	133.5	148.7	161.7	172.7	182.3	190.5
Acrolein	67.5	71.5	71.8	87.0	99.9	110.6	119.6	127.3	133.8	139.4
Acroloyl Chloride	79.2	83.1	83.4	98.0	110.3	120.3	128.6	135.4	141.2	146.1
Acryloyl Fluoride	67.2	71.4	77.3	88.2	102.3	113.9	123.4	131.2	137.7	143.1
Glyoxal	59.9*	60.9	61.1	72.3	82.3	90.3	96.8	102.0	106.3	109.7
Oxalyl Chloride	99.8	102.1	102.2	107.6	111.4	114.7	117.6	120.0	121.9	123.5

* 289K

Table (8.6)

Values of Gibbs Free Energy, $-(G^{\theta}-H_0^{\theta})/T$, at Each Temperature in J K^{-1} mol^{-1}.

T	273.15	298.15	300.0	400.0	500.0	600.0	700.0	800.0	900.0	1000.0
Isoprene	247.4	252.8	253.2	273.3	291.8	309.2	325.6	341.2	356.2	370.5
Trans-Pentadiene	249.8	255.5	255.9	276.9	296.0	313.8	330.5	346.4	361.6	376.1
Cis-Pentadiene	245.7	250.7	251.0	269.8	287.2	303.7	319.4	334.4	348.8	362.6
Crotonaldehyde	249.6	255.0	255.4	275.1	292.7	308.9	323.9	338.1	351.5	364.3
Acrolein	228.5	232.7	233.0	248.2	261.6	273.9	285.4	296.1	306.2	315.7
Acryloyl Chloride	254.7	259.6	260.0	277.7	293.3	307.3	320.2	332.2	343.4	354.0
Acryloyl Fluoride	247.5	251.9	252.2	267.8	281.6	294.2	305.9	316.9	327.2	337.1
Glyoxal	225.0*	226.4	226.7	240.7	252.7	263.4	273.2	282.2	290.8	298.8
Oxalyl Chloride	268.4	274.4	274.8	296.1	314.2	330.1	344.1	356.8	368.3	378.9

* 289K

Table (8.7)

REFERENCES

References

1. J.D. Kemp and K.S. Pitzer, J.Chem. Phys., 1936, 4, 749.
2. J.M. Riveros and E.B. Wilson, J.Chem. Phys., 1967, 40, 4605.
3. W.O. George, D.V. Hassid and W.F. Maddams, J.C.S. Perkin II, 1972, 1029.
4. W.O. George, D.V. Hassid and W.F. Maddams, J.C.S. Perkin II, 1972, 1798.
5. R.F. Curl, J.Chem. Phys., 1959, 30, 1529.
6. H. Susi and T. Zell, Spectrochim.Acta., 1963, 19, 1933.
7. A.J. Bowles, W.O. George and D.B. Cunliffe-Jones, Chem.Comm., 1970, 103.
8. M. Ōki and H. Nakanashi, Bull.Chem.Soc. Japan, 1970, 43, 2558.
9. J. Bailey and A.M. North, Trans.Faraday Soc., 1968, 64, 1499.
10. H. Wennerström, S. Forsén and B. Roos, J.Phys.Chem., 1972, 76, 2430.
11. G. Williams, N.L. Owen and J. Sheridan, Trans. Faraday Soc., 1971, 67, 922.
12. V.M. Rao and R.F. Curl, J.Chem.Phys., 1964, 40, 3688.
13. M. Ōki and H. Nakanashi, Bull.Chem.Soc. Japan, 1971, 44, 3144.
14. R.S. Mulliken, Rev.Mod.Phys., 1942, 14, 265.
15. D.R. Lide, J.Chem.Phys., 1962, 37, 2074.
16. D.R. Lide and M. Jen, J.Chem.Phys., 1964, 40, 252.
17. D.J. Marais, N. Sheppard and B.P. Stoicheff, Tetrahedron, 1962, 17, 163.
18. R.K. Harris, Spectrochim.Acta, 1964, 20, 1129.
19. A.R.H. Cole, G.M. Mohay and G.A. Osborne, Spectrochim Acta, 1967, 23A, 909.
20. A.R.H. Cole, A.A. Green and G.A. Osborne, J.Mol.Spectrosc., 1973, 48, 212.

21. L. A. Carriera, J.Chem.Phys., 1975, 62, 3851.

22. K. Kuchitsu, T. Fukuyama and Y. Morino, J.Mol.Struct., 1968, 1, 463.

23. D. Craig, J.J. Shipman and R.B. Fowler, J.Amer.Chem.Soc., 1961, 83, 2885.

24. W.B. Smith and J.L. Massinghill, J.Amer.Chem.Soc., 1961, 83, 4301.

25. J.G. Aston, G.Szasz, H.W. Woolley and F.G. Brickwedde, J.Chem. Phys., 1946, 14, 67.

26. L. Radom and J.A. Pople, J.Amer.Chem.Soc., 1970, 92, 4786.

27. P.N. Skancke and J.E. Boggs, J.Mol.Struct., 1973, 16, 179.

28. E.B. Reznikova, V.I. Tyulin and V.M. Tatevskii, Optika i Spectrosk., 1962, 13, 364.

29. P.A. Bazhulin, Y.A. Lazarev and N.V. Desyatova, Optika i Spectrosk., 1962, 13, 75.

30. A.L. Segre and S. Castellano, J.Mag.Res., 1972, 1, 5.

31. A.L. Segre, L. Zetta and A.Di. Corato, J.Mol.Spec., 1969, 32, 296.

32. R.I. Lipnick and E.W. Garbisch, J.Amer.Chem.Soc., 1973, 95, 6370.

33. E.A. Cherniak and C.C. Costain, J.Chem.Phys., 1966, 45(1), 104.

34. A.J. Bowles, W.O. George and W.F. Maddams, J.Chem.Soc(B)., 1969, 810.

35. J.B. Bentley, K.B. Everand, R.J.B. Marsden and L.F. Sutton, J.Chem.Soc., 1949, 2957.

36. R.A. Pethrick and E. Wyn-Jones, Trans.Faraday Soc., 1970, 66, 2483.

37. J.R. Durig, C.C. Tong and Y.S. Li, J. Chem.Phys., 1972, 57(10), 4425.

38. G.N. Currie and D.A. Ramsay, Can.J.Phys., 1971, 49, 317.

39. A.R.H. Cole and G.A. Osborne, Spectrochim.Acta, 1971, 27(A), 2461.

40. S.L. Hsu, M.K. Kemp, J.M. Pochan, R. C. Benson, and W.F. Flygare, J.Chem.Phys., 1969, 50, 1482.

41. S.Dzhessati, V.I. Tyulin and Y.A. Pentin, Zhur.Struct.Khim., 1965, 6, 465.

42. S.L. Hsu and W.H. Flygare, J.Chem.Phys., 1970, 52(3), 1053.

43. J.R. Lide, J.Chem.Phys., 1962, 37, 2074.

44. R.K. Harris and R.E. Witkowski, Spectrochim.Acta, 1964, 20, 1651.

45. G.J. Szasz and N. Sheppard, Trans.Faraday Soc., 1953, 49, 358.

46. A.A. Bothnerby and D. Jung, J.Amer.Chem.Soc., 1968, 90, 2342.

47. R.A. Beaudet, J.Chem.Phys., 1965, 42(11), 3758.

48. V.A. Kuznetsov, S. Dzhessati, A.R. Kyazimova and V.I. Tyulin, Vestnik.Moskov Uni.Khim., 1971, 26, 45.

49. S. Dzhessati, A.R. Kyazimova, V.I. Tyulin and Y.A. Pentin, Vestnik Moskov Univ. Khim., 1968, 23, 19.

50. S. Novick, J.M. Lehn, W. Klemperer, J. Amer.Soc., 1973, 95, 8189.

51. C.R. Brundle and M.B. Robin, J.Amer.Chem.Soc., 1970, 92, 5550.

52. R.J. Hobgood and J.H. Goldstein, J.Mol.Spectr., 1964, 12,76.

53. H. Wynberg, A.de Groot and P.W. Davies, Tet.Lett., 1963, 1083.

54. E.A. Braude, Experientia, 1955, 11, 457.

55. K.O. Hartmann, G.L. Carlson, R.E. Witkowski and W.G. Fateley, Spectrochim.Acta, 1968, 24(A), 157.

56. M. Suzuki and K. Kozima, Bull.Chem.Soc.Japan, 1969, 42, 2183.

57. J.J. Keirns and R.F. Curl Jnr., J.Chem.Phys., 1968, 48(8), 3773.

58. G.L. Carlson, W.G. Fateley and R.E. Witkowski, J.Amer.Chem.Soc., 1967, 89, 6437.

59. R. Kewley, D.C. Hemphill and R.F. Curl, J.Mol.Spec., 1972, 44, 443.

60. J.E. Katon and Feairheller, J.Chem.Phys., 1967, 47(4), 1248.

61. R.L. Redington and J.R. Kennedy, Sprectrochim.Acta., 1974, 30A, 2197.

62. J. Ronayne, M.V. Sargent and D.H. Williams, J.Amer.Chem.Soc., 1966, 80, 5288.

63. J.R. Durig, S.C. Brown, V.F. Kalasinsky and W.O. George, Spectrochim.Acta, 1976, 32A, 807.

64. G. Williams, N.L. Owen and J. Sheridan, Trans.Faraday Soc., 1971, 67, 922.

65. J.R. Durig and S.E. Hannum, J.Chem.Phys., 1970, 52, 6089.

66. J.R. Durig, S.E. Hannum and F.G. Baglin, 1971, 54, 2367.

67. K. Hagen and K. Hedberg, J.Amer.Chem.Soc., 1973, 95, 1003.

68. K. Hagen and K. Hedberg, J.Amer.Chem.Soc., 1973, 95, 4796.

69. W.O. George and A.J. Porter, J.C.S. Perkin II, 1973, 954.

70. W.O. George and A.J. Porter, J.Mol.Structure, 1973, 17, 152.

71. S. Mizushima, T. Shimanouchi, K. Kuratani and T. Miyazawa, J. Amer.Chem.Soc., 1952, 74, 1378.

72. T.M. Sugden and C.N. Kennedy, Microwave Spectroscopy of Gases, Published by Van Nostrand, London, 1965.

73. G. Herzberg, Molecular Spectra and Molecular Structure Part II, Van Nostrand, New York, 1945.

74. R.K. Thomas, E.C. Leisegang and Sir. H. Thompson, Proc.Royal Soc.Lond. A, 1972, 330, 15.

75. M. Kingsland and H. Spedding, Chem. and Ind., 1971, 507.

76. D.F. Koster, T.P. Vasilef and G.L. Carlson, Spectrochim.Acta, 1971, 27A, 1633.

77. W.O. George, D.V. Hassid, W.C. Harris and W.F. Maddams, J.C.S. Perkin II, 1975, 392.

78. W.G. Fateley, R.K. Harris, F.A. Miller and R.E. Witkowski, Spectrochim.Acta. 1965, 21, 231.

79. J.R. Durig, S.M. Craven and W.C. Harris, Vibrational Spectra and Structure, Vol. 1, Dekker, New York, 1972.

80. D.R. Hersbach, J.Chem.Phys., 1959, 31, 91.

81. Yu. N. Panchenko, Spectrochim.Acta. 1975, 31A, 1201.

82. Yu. N. Panchenko. I.A. Gagina, O.T. Nikitin, R. Aroca Munoz, Yu. A. Pentin and V.K. Matveev, Vestn.Mosk.Univ.Khim., 1972, 27, 518.

83. N. Sheppard and P. Simpson, Quart.Rev., 1952, 6, 1.

84. R. Torkington and H.W. Thompson, Proc.Roy.Soc.A, 1945, 184, 35.

85. N.B. Colthup, L.H. Daly and S.E. Wiberley, Introduction to Infrared and Raman Spectroscopy, 1964, Academic Press.

86. J.F. Ogilvie and K.C. Cole, J.Mol.Spectrosc. 1970, 35, 332.

87. P. Albriktsen, A.V. Cunliffe and R.K. Harris, J.Mag.Res., 1970, 2, 150.

88. M. Bacon and G.E. Maciel, Mol.Phys., 1971, 21, 257.

89. R.S. Rasmussen and R.R. Brattain, J.Chem.Phys., 1947, 15, 131.

90. N.V. Tarasova and L.M. Sverdlov, Opt.Spektrosk., Akad.Nauk. SSSR, Otd. Fiz.-Mat.Nauk. St. Statei, 1967, 3, 140.

91. V.T. Aleksania and E.V. Sobolev, Zhur.Struct.Khim, 1963, 4, 527.

92. E.G. Treschova, V.M. Tatevskii, R.Y. Lebina, A. Buktorova, Zhur.Struct.Khim., 1952, 26, 1266.

93. P.A. Akishin, L.V. Vilkov and V.M. Tateskii, Doklady Akad.Nauk. SSSR, 1958, 118, 117.

94. R.A. Munos and Y.N. Panchenko, Vestnik Mosk.Univ.Khim., 1971, 26, 35.

95. N.V. Tarasova and L.M. Sverdlov, Zhur.Fiz.Khim., 1968, 42, 1602.

96. A.A. Bothnerby and R.K. Harris, J.Amer.Chem.Soc., 1965, 87, 3445.

97. J.R. Cowles, W.O. George and W.G. Fateley, J.C.S. Perkin II, 1975, 396.

98. M.L. Evans and H.E. Hallam, J.Mol.Structure, 1976, 32, 133.

99. A.J. Barnes and G.C. Whittle, Molecular Spectroscopy of Dense Phases Proceedings of the 12th European Congress on Molecular Spectroscopy, 1976, Elsevier Scientific Publishing Co., Amsterdam.

100. J.O. Herschfelder, J.Chem.Phys,. 1940, 8, 431.

101. W.G. Fateley and F.A. Miller, Spectrochim.Acta, 1963, 19, 611.

102. W.J. Orville Thomas (Editor), Internal Rotation in Molecules, 1974, John Wiley.

103. K.S. Pitzer, J.Chem.Phys., 1946, 14, 239.

104. H. Dodziuk, J.Mol.Structure, 1971, 10, 275.

105. J.R. Durig, C.K. Tong, C.W. Hawley and J. Bragin, J.Phys.Chem., 1971, 75, 44.

106. H. Dodziuk, J.Mol.Structure, 1974, 20, 317.

107. S.G. Frankiss and J.H.S. Green, 'Chemical Thermodynamics', 1973 Chem.Soc.Specialist Report, Vol.1, Ch.8.

108. G.N. Lewis and M. Randall, 'Thermodynamics', rev. by K.S. Pitzer and L. Brewer, McGraw-Hill, New York, 1961.

109. Stull, Westram and Sinke, 'Chemical Thermodynamics of Organic Compounds', Wiley, New York, 1969.

110. R.B. Scott, C.H. Meyers, R.D. Rands, F.G. Brickwedde and N. Bekkedahl, J.Res.Nat.Bur.Stand., 1945, 35, 39.

111. L.M. Sverdlov and E.N. Bolotina, Russ.J.Phys.Chem., 1962, 36, 1502.

112. I. Godnev and V. Morosov, Zhur.Fiz.Khim, 1947, 21, 799.

113. J.E. Kilpatrick, C.W. Beckett, E.J. Prozen, K.S. Pitzer and F.D. Rossini, J.Res.Nat.Bur.Stand., 1949, 42, 225.

114. J.F. Messerley, S.S. Todd, and G.B. Guthrie, J.Chem.Eng. Data, 1970, 15, 227.

115. S.L. Hsu and W.H. Flygare, Chem.Phys. Letters, 1969, 4, 317.

116. L.A. Carriera, J.Phys.Chem., 1976, 80, 1149.

117. A. Krantz, T.D. Goldfarb, and C.Y. Lin, J.Amer.Chem.Soc., 1972, 94, 4022.

118. R.L. Redington, J.Chem.Phys., 1975, 62, 4927.

119. J. Tyrrell, J.Amer.Chem.Soc., 1976, 98, 5456.

APPENDIX

A. Spectra.

B. Calculation of a Far-Infrared Spectrum From an Interferogram.

C. Computer Programs.

D. Courses Attended.

A. Spectra. Spectrum 1

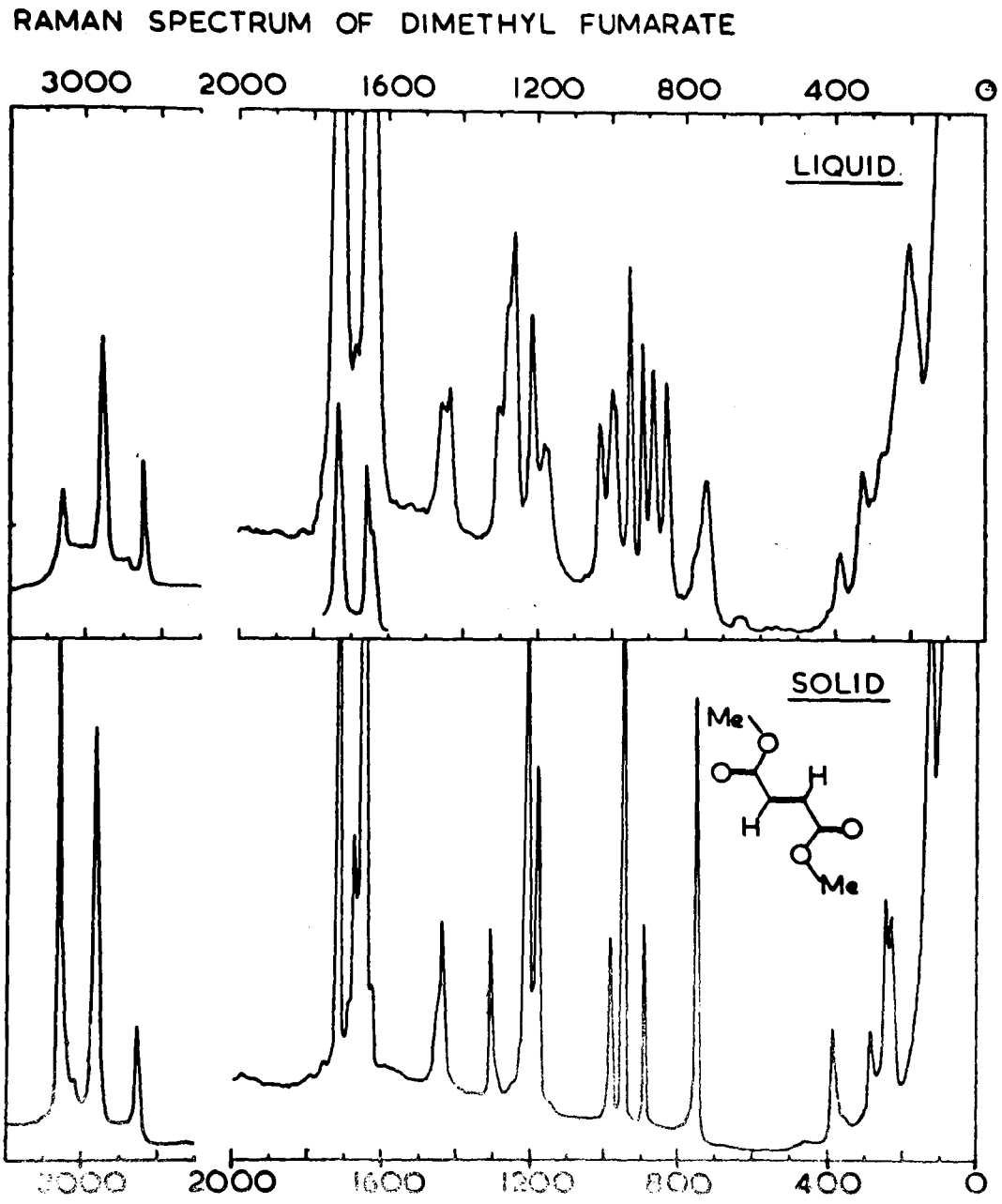

Spectrum 2

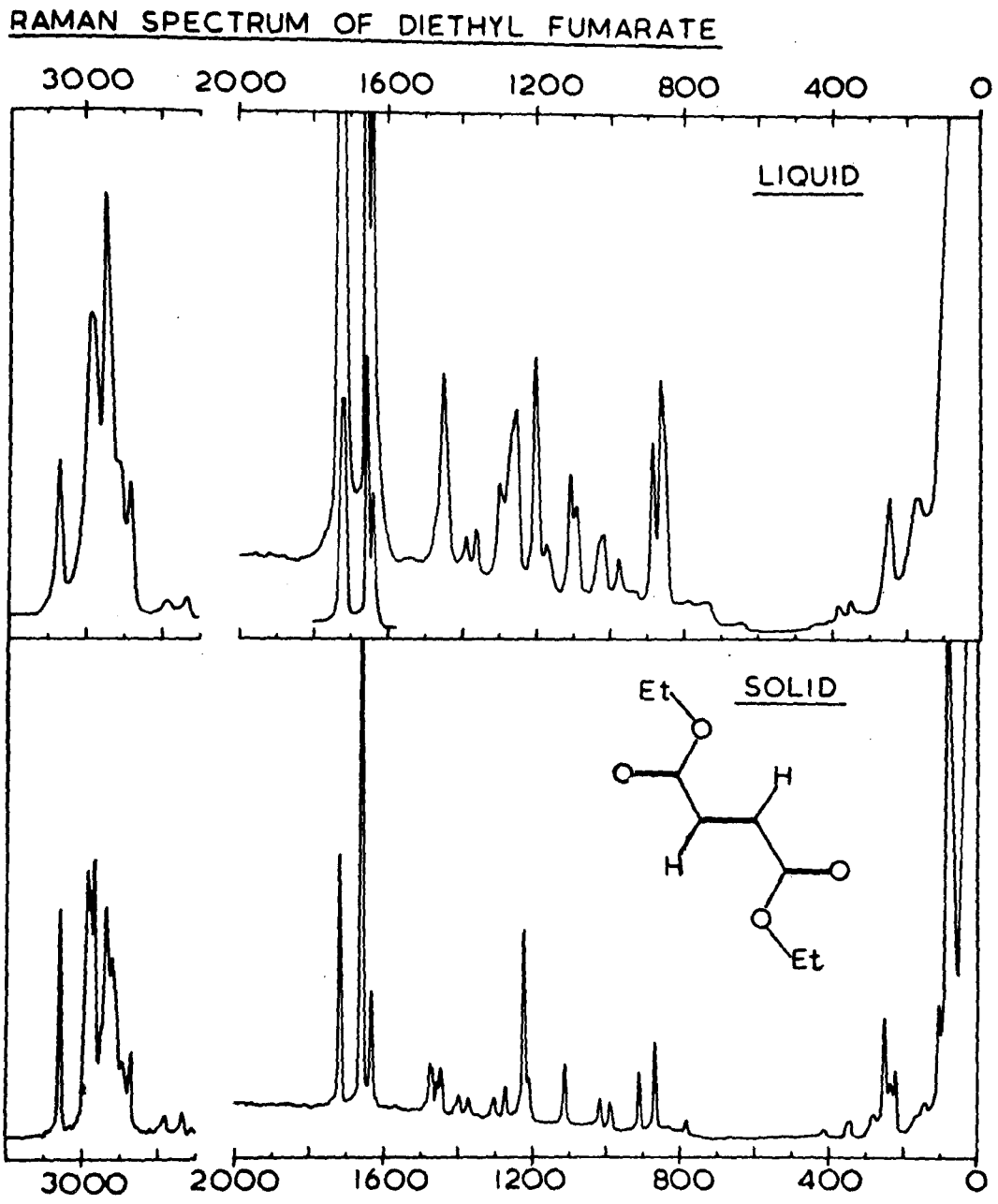
RAMAN SPECTRUM OF DIETHYL FUMARATE
3000
2000
1600
1200
800
400
0
LIQUID
SOLID
Et
H
H
Et

Spectrum 3.

RAMAN SPECTRUM OF Di-n-BUTYL FUMARATE

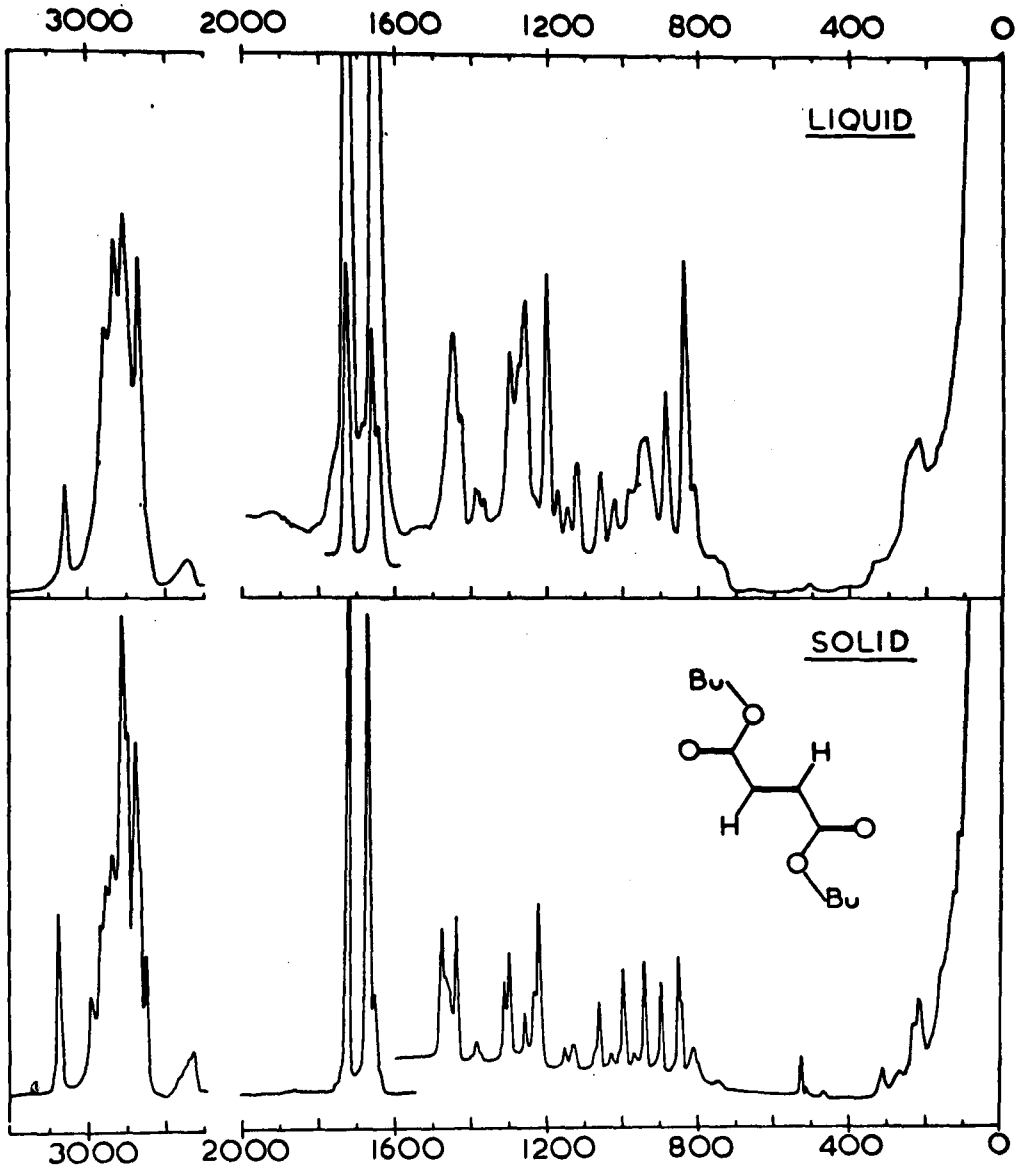

Spectrum 4

RAMAN SPECTRUM OF DIMETHYL MALEATE

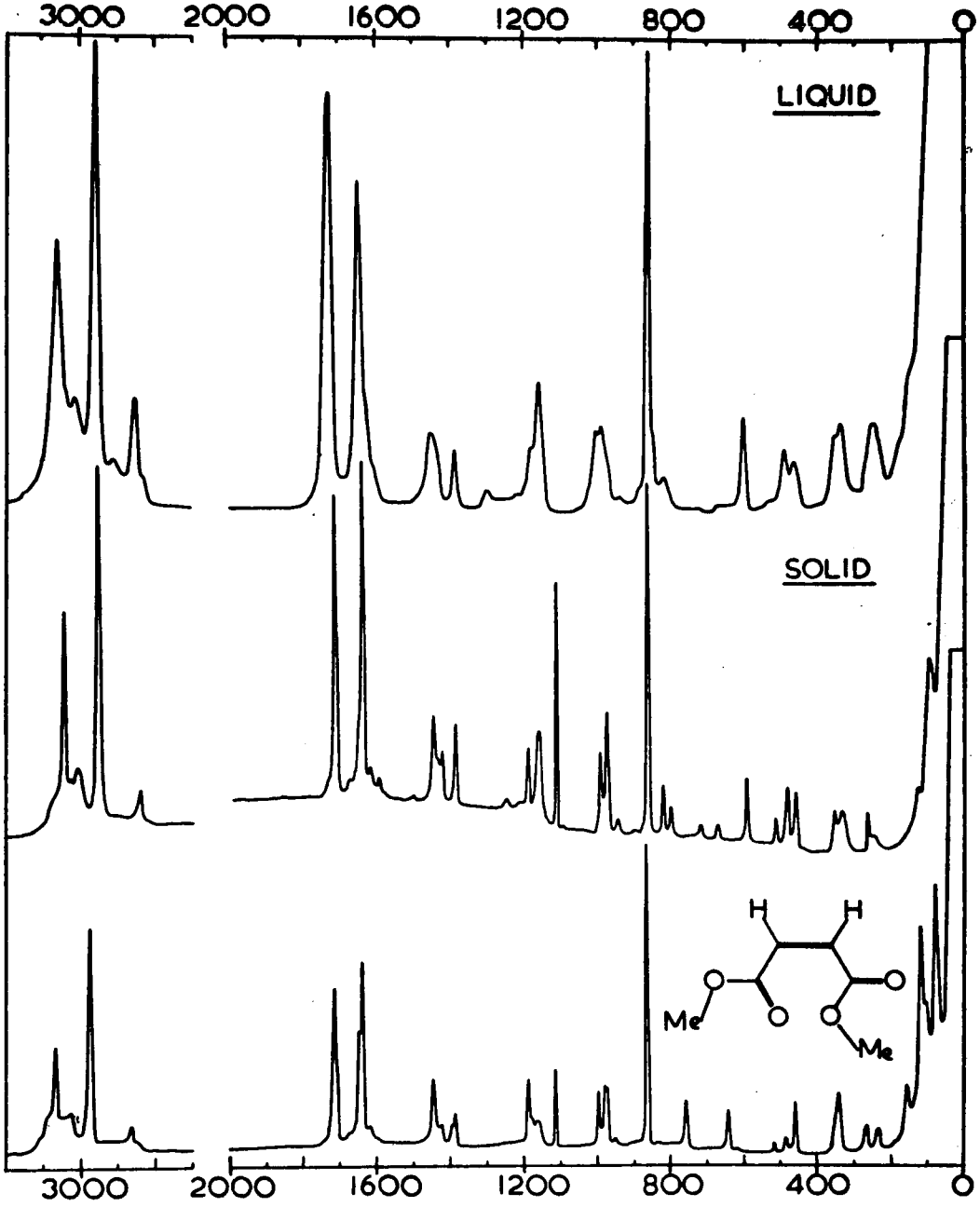

Spectrum 5

RAMAN SPECTRUM OF DIETHYL MALEATE

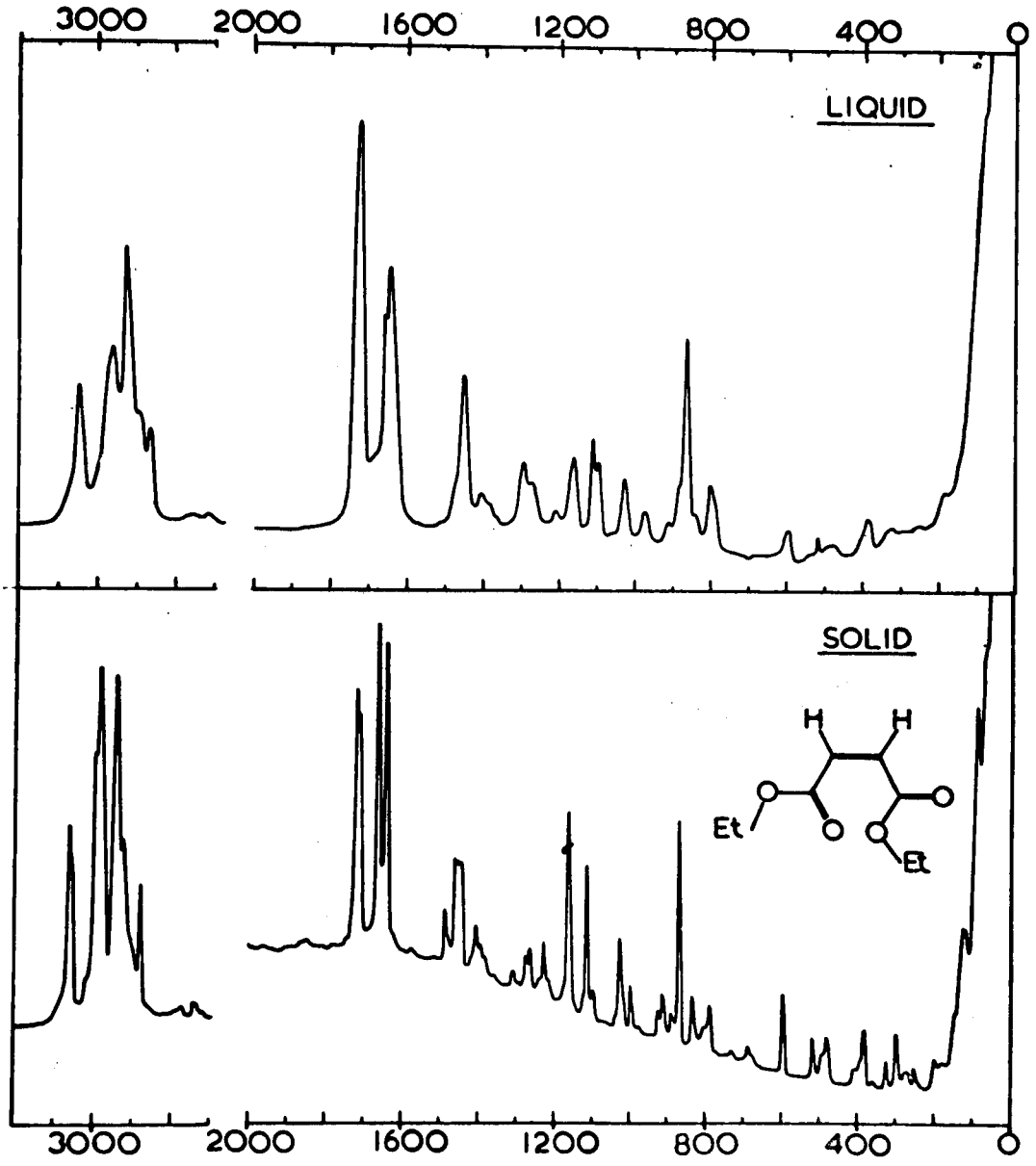

Spectrum 6

RAMAN SPECTRUM OF Di-n-BUTYL MALEATE

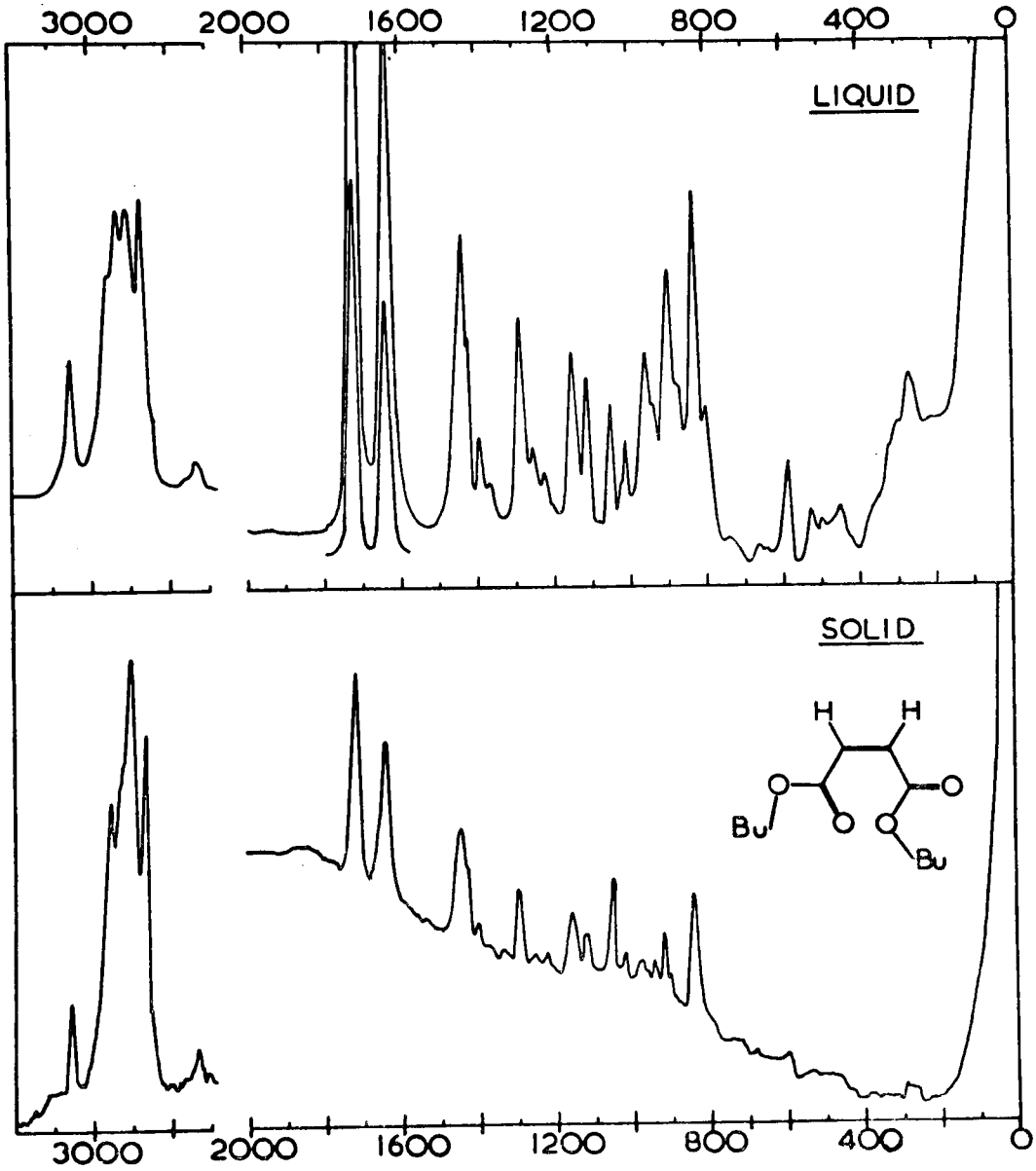

Spectrum 7

RAMAN SPECTRUM OF ISOPRENE

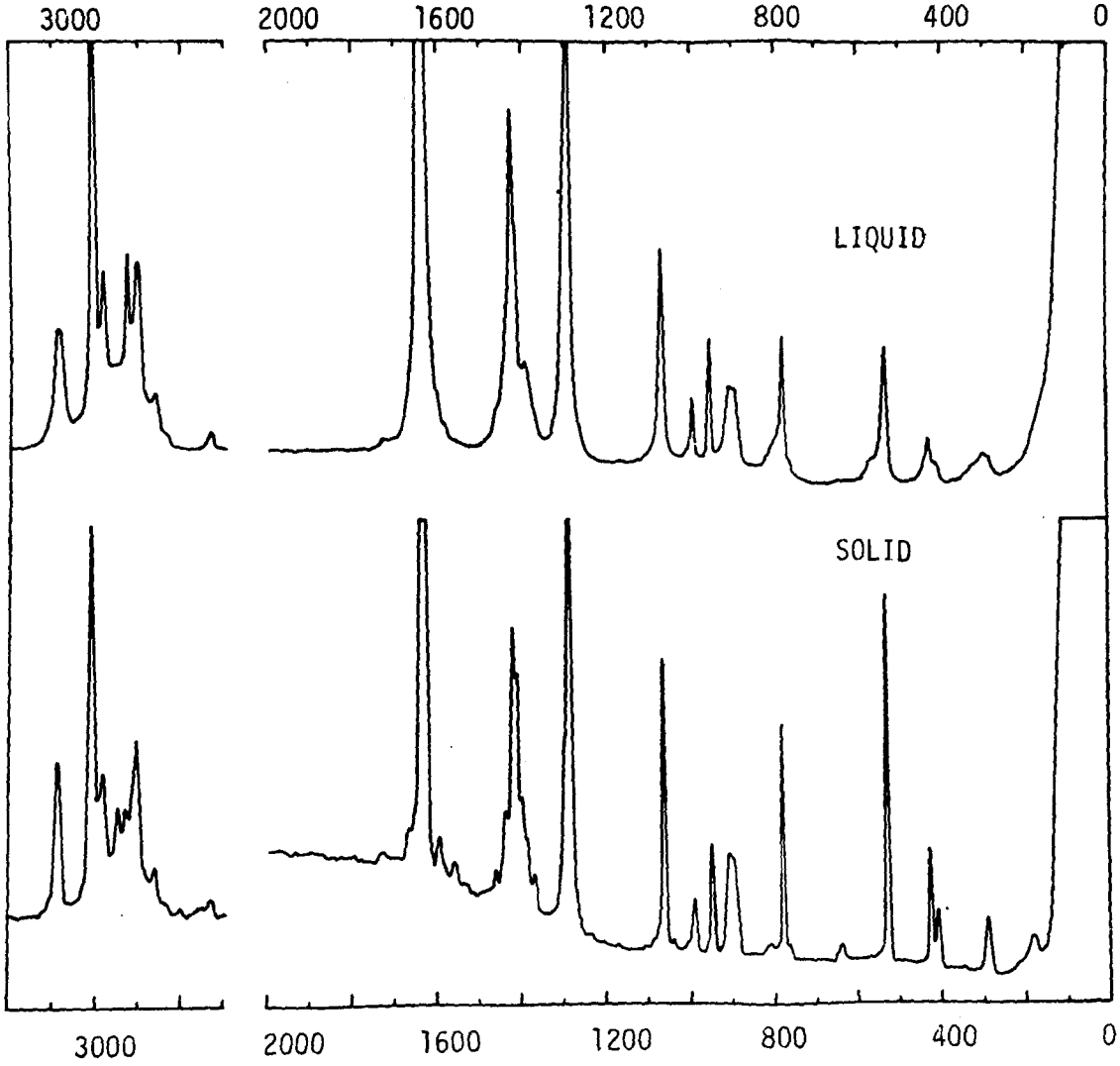

B. Calculation of A Far-Infrared Spectrum From an Interferogram

1. Theory. If a monochromatic source giving radiation of frequency ν_0 is used on a Michelson Interferometer, the intensity of the light falling on the Golay detector varies with a difference in pathlength achieved by a moving mirror and is given by

$$I_{(x)} = I_0 (1 + \text{Cos } 2\pi\nu_0 x) \qquad .....(A.1)$$

The source normally used is a mercury lamp which emits broad band radiation and so expression (A.1) is altered to account for this, resulting in

$$I_{(x)} = \int_{-\infty}^{+\infty} I_{(\nu)} (\text{Cos } 2\pi\nu x)dx \qquad .....(A.2)$$

the intensity at frequency ν can be calculated by the Fourier Transform of expression (A.2), which is equation (A.3)

$$I_{(\nu)} = \int_{-\infty}^{+\infty} I_{(x)} (\text{Cos } 2\pi\nu x)dx \qquad .....(A.3)$$

Hence the intensity of radiation frequency can be calculated by performing the above integration on the interferogram; the mirror path difference, x, from dead centre is altered stepwise and the intensity noted at each step. To simplify the integration it can now be changed to a summation because of the stepwise accumulation of data:-

$$I_{(\nu)} = \sum_{-\infty}^{+\infty} I_{(x)} (\text{Cos } 2\pi\nu x)dx \qquad .....(A.4)$$

and as data cannot be calculated with x changing from $+\infty$ to $-\infty$ the data is truncated, from +x to -x. The effect of this truncation is to give finite resolution, depending on x, and also to produce subsidary maxima on the spectrum. A smoothing function (apodisation) is used to overcome this at the expense of some resolution, which is given by 1/2x (no apodisation) or 1/x (apodisation present).

In an ideal situation the interferogram is symmetrical about zero

path difference, when a 'single sided' interferogram can be used requiring less data sampling and computing time. In practice this is only possible if the machine can 'find' the centre of the interferogram, like the Digilab FTS 15, which uses a laser beam to locate dead centre. To minimise computing time a 'double sided' interferogram is recorded by the Beckmann-RIIC FS 720 system, and the computer 'folds' this to a 'single sided' interferogram by locating the central (highest) number and averaging outwards. This method is useful in that it minimises the effect of a noise spike, but the central number located is never exactly on the peak maximum.

Calculation of the spectrum is performed using Ratiospec 3. This program is a completely rewritten version of Ratiospec 1 as used at Portsmouth Polytechnic on an ICL 4100 series computer. Ratiospec 2 runs on the Kingston Polytechnic 4100 and includes special graph plotting routines to give a conventional spectrum.

2. The Processing of Data From the FS 720 Interferometer on the Computer Via the Program Ratiospec 3.

The program is designed specifically for use with the Beckmann RIIC FS 720. This instrument produces an interference pattern punched onto paper tape as numbers between 0 and 9999. The data is terminated by a zero punched by the 720 operator.

These numbers are processed by Ratiospec to produce a far-infared spectrum. The resulting spectrum may be background, ratioed or single beam.

The Program. This is written in 1900 Algol. Input is by paper tape and output is via line printer and paper tape. There are two procedures, "Binread" for input and "output" for output.

Binread Procedure. This checks that input numbers are within the normal range 1000-9999, if not, error messages are output and the program continues. It also checks that the amount of data fed in before zero is found is enough to process. If not enough data is found then more numbers are generated using the opposite end of the symmetrical interferogram, and a warning message is printed.

Output Procedure. This produces a line printer listing of wavenumber values versus arbitrary intensities and then gives the following options:

Line printer - graphical output

Paper tape - output

The Main Program. This accepts the data after input of control data and declares suitable core for storage of the data. If more than 2600 numbers are read in then backing disc store is called up to accommodate the extra data. The 'Resolution' available without discs is slightly better than 1 wavenumber and with discs about 0.4 wavenumber.

The spectrum is then computed according to the control data, and procedure "output" prints in the required format.

Header Tape. A library of header tapes are available which all contain:-

(1) Job heading

(2) Magnetic tape call up

(3) Control data

Job Heading/Magnetic Tape Call up. These operations document the job and load the program from magnetic tape into the computer processor. Examples of this may be seen on printouts of specimen header tapes.

Control Data. After the Data Document is opened the first data to be input must be:-

(1) SPEC - This governs the mode of computation

2 for BACKSPEC

6 for RATIOSPEC

8 for SINGLESPEC

10 for TOTALSPEC (this is when a ratioed spectrum is produced using the raw BACKSPEC interferogram which is computed first to give the background, and then the spectrum to be ratioed is fed in after, in the same run).

(2) Q - This governs resolution. Typical values are:-

499 - 5.0 cm^{-1} resolution

799 - 3.125 cm^{-1} resolution

2499 - 1.0 cm^{-1} resolution

from the relationship:-

$$\text{resolution} = 1250/\{(Q-1)/2+1\}$$

(N.B. Q must be an odd number)

(3) MIN and (4) MAX - These are the limits of the spectrum in cm^{-1}.

(5) SAM - This is the sampling interval in microns, normally 8 as set on the instrument.

(6) D - This represents points per unit of resolution (e.g 2 when Q = 499 will plot out a point on the spectrum every 2.5 cm^{-1}.

(7) RAN - This is the number of runs to be averaged for one spectrum

(8) SET - This is the number of different spectra (e.g. 1 for BACKSPEC, 2 for TOTALSPEC.

(9) PLOT - Governs line printer output

1 gives a normal plot for all spectra

3 gives a log plot

2 gives a plot for ratioed spectra, but no back groud spectrum.

0 gives no plot

(10) PNCH - 7 gives output tape for all spectra

2 gives output tape for ratioed spectrum, but not for background spectrum.

0 gives no tape output.

If a high resolution tape (Q > 2600) is made but only needs to be run at low resolutions then RAN must be set to 100 and Q set to its required value below 2600. This is necessary to call up discs to store all the data.

Tape Order. This must be written out for the operators to follow:-

BACKSPEC OR SINGLESPEC	Tape (1) (Header Tape)
	Backspec (s)
	**** (end data marker)

RATIOSPEC Tape (1)

Output from Backspec

Ispec (s)

****

TOTAL SPEC Tape (1)

Backspec

Ispec (s)

****

Tape Handling. The interferogram must be punched with 8" of blank tape at end. The first number on each tape is read as the spectrum number which is to be hand punched on:-

Newline

Spectrum No.

Newline

Data

The end of every interferogram (more than one can be on one tape) must be terminated by:-

Newline

Zero

Newline

Halt - (Control D) at end of tape

Output tapes must have any 1900 'George' output information at beginning and end removed, and a new line punched at the beginning and a halt code at the end.

C. Computer Programs.

1. Program RATIOSPEC 3

This program is written in Algol 60 for the Kingston Polytechnic ICL 1903 Computer. Procedures labelled 'External' are standard procedures for handling data on discs. The main program commences at statement 236, and calls 'Binread' and 'Help' to input the interferogram tape. The results are produced by 'Output' on the line printer or tape punch.

```
0
0
0       'PROGRAM'(RATIOSPEC3)
0
0       'INPUT'  1=TP1
0       'OUTPUT' 2=LP1
0       'OUTPUT' 3=TP0
0
0
0       'BEGIN'
1
1       'REAL'AR,BR,CR,DR,ED,FD,GD,HR,IC,JC,KC,LC,MC,NC,OC,PC,QC,RC,SC,
            SD,SE,SF,MIN,MAX,PI,RES,OUT;
1       'INTEGER'A,B,C,D,E,F,G,H,I,J,K,O,U,Y,AV1,AV2,DACC,CYCLE,LOT,PLOT,PNCH,
2           POINT,PAN,RUN,LVMC,SAM,SET,SPEC,START,STR,SUM1,SUM2;
2
2       'PROCEDURE' OUT(N);'VALUE' N;'INTEGER' N;'EXTERNAL';
6       'PROCEDURE' DISSTORE(N,S,T,G,L);'VALUE'N,L,G;'INTEGER'N,L,G;
10                              'STRING'S,T;'EXTERNAL';
11      'PROCEDURE' PUTARRAY(N,K,A);'VALUE'N;'INTEGER'N,K;'ARRAY'A;'EXTERNAL';
16      'PROCEDURE' GETARRAY(N,K,A);'VALUE'N;'INTEGER'N,K;'ARRAY'A;'EXTERNAL';
21      'PROCEDURE' PUTPART(N,K,A,X,Y);'VALUE'N;'INTEGER'N,K;'REAL'X,Y;'ARRAY'A;'EXTERNAL';
27      'PROCEDURE' READTRAP(P);'PROCEDURE'P;'EXTERNAL';
30      'PROCEDURE' HELP(CRUD);'INTEGER'CRUD;
33      'BEGIN'
33        'COMMENT' CRUD IS CODED VALUE OF ERRONEOUS INPUT CHARACTER WHICH WOULD
33                  NORMALLY CAUSE A HALT STATEMENT. HELP WILL REPLACE THIS BY A
33                  NEWLINE, AND BINREAD CHECKS THE RESULTS;
33        WRITETEXT('('('C')'HELP%WAS%NEEDED%AT%AA[')'); PRINT(A+1,4,0);
36        WRITETEXT('('1'('C')'CRUD%PRESENT%WAS%')'); PRINTCH(CRUD);
38        CRUD:=CODE('('EL')')
39      'END';
39
39      'PROCEDURE' BINREAD(AA);
41      'INTEGER' 'ARRAY' AA;
42      'BEGIN'
42        A:=1;
44      REALAGAIN:AA[A]:=READ;
45        'IF'AA[A]=0'THEN'LOT:=A-1 'ELSE''BEGIN'
45          'IF'AA[A]>100,0 'OR'AA[A]<1000 'THEN''BEGIN'
46            WRITETEXT('('('2C')'AA[')'); PRINT(A,4,0);
49            WRITETEXT('('1%=%')'); PRINT(AA[A],6,0);
51            WRITETEXT('('('C')'NUMBER%OF%RUN%=%')'); PRINT(RUN,1,0);
53          'END';
54          'IF'AA[A]>100,0 'THEN''BEGIN'
54            AR:=AA[A]/1,000;
56            AR:=AR-ENTIER(AR);
57            AA[A]:=AR*1,000;
58          'END';
59          A:=A+1;
60          'GOTO'REALAGAIN;
61        'END';
```

```
62          POINT:=1;
63          'FOR'A:=2'STEP'1'UNTIL'LOT'DO''IF'AA[A]>AA[POINT]'THEN'POINT:=A;
65          START:=POINT-(D-1)/2;
66          'IF'START<1 'OR' (START-1+D)>LOT'THEN''BEGIN'
66        WRITETEXT('('('30')'NOT%ENOUGH%POINTS%TAKEN%RUN%MODIFIED.')');
68        WRITETEXT('('('C')'THE%HIGHEST%POINT%=')'); PRINT(POINT,4,0);
70        WRITETEXT('('('C')'THE%NUMBER%OF%POINTS%SAMPLED%=')'); PRINT(LOT,4,0);
72        WRITETEXT('('('C')'THE%NUMBER%OF%RUN%MODIFIED%=')'); PRINT(RUN,1,0);
74        WRITETEXT('('('C')'THE%NUMBER%OF%SUBSTANCE%=')'); PRINT(F,4,0);
76            SELECT OUTPUT(3);
77            NEWLINE(1);
78            SUM1:=SUM2:=AV1:=AV2:=0;
79            'IF'START<1'THEN''BEGIN'
79              B:=2*POINT;
81              'IF'POINT>21'THEN''BEGIN'
81                'FOR'A:=1'STEP'1'UNTIL' 20 'DO' SUM1:=SUM1+AA[A];
84                'FOR'A:=B'STEP'-1'UNTIL'B-19'DO'SUM2:=SUM2+AA[A];
86                AV1:=AV1/20;
87                AV2:=AV2/20;
88              'END';
89              PRINT(F,4,0); NEWLINE(1);
91              'FOR'A:=LOT'STEP'-1'UNTIL'B+1'DO''BEGIN'
92                PRINT(AA[A]+(AV1-AV2),4,0); NEWLINE(1);
95              'END';
96            'END';
97            'IF'(START-1+D)>LOT'THEN''BEGIN'
97              B:=2*POINT-LOT;
99              'IF'(LOT-POINT)>21'THEN''BEGIN'
99                'FOR'A:=LOT'STEP'-1'UNTIL'LOT-19'DO'SUM1:=SUM1+AA[A];
102               'FOR'A:=B  'STEP'1 'UNTIL'B+19  'DO'SUM2:=SUM2+AA[A];
104               AV1:=AV1/20;
105               AV2:=AV2/20;
106             'END';
107             'FOR'A:=B-1'STEP'-1'UNTIL'1'DO''BEGIN'
108               PRINT(AA[A]+(AV1-AV2),4,0); NEWLINE(1);
111             'END';
112             B:=0;
113             PRINT(B,1,0); NEWLINE(1);
115           'END';
116           SELECT OUTPUT(2);
117         'END';
118         B:=START;
119         'FOR'A:=0'STEP'1'UNTIL'D'DO''BEGIN'
120           AA[A]:=AA[B];
122           B:=B+1;
123         'END';
124       'END' OF PROCEDURE BINREAD;
124
124       'PROCEDURE' OUTPUT(DA,FA);
126       'REAL''ARRAY' DA,FA;
127       'BEGIN'  NEWLINE(6);
129         HR:=CR;  R:=0;
131         'FOR'I:=1'STEP'1'UNTIL'OUT'DO''BEGIN'
132           'IF'H=6'THEN''BEGIN'
133             NEWLINE(1);
135             H:=0;
136           'END';
137           'IF'SPEC=6'OR'SPEC=10'AND'F'NE'0'THEN'DA[I]:=DA[I]/FA[I];
138           SPACE(5); PRINT(HR*RES,5,3);
140           SPACE(1); PRINT(DA[I],5,3);
```

```
142           HR:=PR+FOR;
143           H:=H+1;
144         'END' OF RESULT LOOP FOR NUMERICAL OUTPUT ON LINEPRINTER;
145         'IF' PNCH=2 'OR' PNCH=2'AND' F'NE'0 'THEN''BEGIN'
146           SELECT OUTPUT(3); NEWLINE(1);
148           PRINT(E,7,0); NEWLINE(3);
150           'FOR'I:=1'STEP'1'UNTIL'OUT'DO''BEGIN'
151             PRINT(DA[I],4,3); NEWLINE(1);
154           'END';
155           RUNOUT;
156           SELECT OUTPUT(2);
157         'END' OF RESULT LOOP FOR BINARY OUTPUT ON PAPERTAPE;
158         SD:=SE:=DA[1];
159         'FOR'I:=2'STEP'1'UNTIL'OUT'DO''BEGIN'
160           'IF'DA[I]>SD'THEN'SD:=DA[I];
162           'IF'DA[I]<SE'THEN'SE:=DA[I];
163         'END';
164         'IF'PLOT=3'THEN''BEGIN'
164           SF:=100/LN(100);
166           'FOR'I:=1'STEP'1'UNTIL'OUT'DO''BEGIN'
167             'IF'SD=DA[I]'THEN'DA[I]:=100
168             'ELSE'DA[I]:=(LN(100)-LN((SD-DA[I])*100/SD))*SF;
169           'END;
170         'END''ELSE''BEGIN'
170           SF:=100/SD;
172           'FOR'I:=1'STEP'1'UNTIL'OUT'DO'DA[I]:=DA[I]*SF;
174         'END';
175       NEWLINE(6);
176         'IF'SPEC=2'OR'SPEC=10'AND'F=0'THEN'WRITETEXT('('BACKGROUND%')');
177         'IF'SPEC=6'OR'SPEC=10'AND'F'NE'0'THEN'WRITETEXT('('RATIOED%')');
178         'IF'SPEC=2'THEN'WRITETEXT('('SINGLE%BEAM%')');
179       WRITETEXT('('INTERFEROSPECTRUM')');
180       WRITETEXT('('('10S')'KINGSTON%POLYTECHNIC%')');
181       WRITETEXT('('('C')''('9S')'ES%720')');
182       WRITETEXT('('('4')'SPECTRUM%NUMBER%')'); PRINT(E,4,0);
184         'IF'SPEC=6'OR'SPEC=10'AND'F'NE'0 'THEN''BEGIN'
184           WRITETEXT('('RATIOED%AGAINST%BACKSPEC%')'); PRINT(F,4,0);
187         'END';
188       WRITETEXT('('('20')'RUNS%AVERAGED%')'); PRINT(RAN,1,0);
190       WRITETEXT('('('C')'RESOLUTION%')'); PRINT(RES,2,3);
192       WRITETEXT('('('C')'LIMIT%FREQUENCIES%ARE%')'); PRINT(MIN,3,0);
194       WRITETEXT('(',')'); PRINT(MAX,3,0); WRITETEXT('('CM-1')');
197       WRITETEXT('('('C')'NUMBER%OF%OUTPUT%POINTS%')'); PRINT(OUT,4,0);
199       WRITETEXT('('('C')'SCALE%FACTOR%')'); PRINT(SF,3,5);
201       WRITETEXT('('('C')'SAMPLING%INTERVAL%')'); PRINT(SAM,2,0);
203       WRITETEXT('('('C')'POINTS%PER%UNIT%OF%RESOLUTION%')'); PRINT(D,1,0);
205       WRITETEXT('('('20')'INPUT%POINTS%PROCESSED%')'); PRINT(Q,4,0);
207       WRITETEXT('('('C')'NUMBER%OF%POINTS%SAMPLED%')'); PRINT(LOT+1,4,0);
209       WRITETEXT('('('C')'HIGHEST%POINT%')'); PRINT(POINT,4,0);
211         'IF'PNCH=2'OR'PNCH=2'AND'F'NE'0'THEN'
211       WRITETEXT('('('C')'OUTPUT%TAPE%GIVEN%FOR%THIS%SPECTRUM.')');
212         'IF'PLOT=3'THEN'
212       WRITETEXT('('('C')'LOGARITHMIC%PLOT.')');
213       NEWLINE(5);
214           'IF'PLOT'NE'0'THEN''BEGIN'
214             'IF'PLOT=2'AND'F=0'THEN''GOTO' MISS;
216             PR:=CR;
217             H:=0;
218             'FOR'I:=1'STEP'1'UNTIL'OUT'DO''BEGIN'
219               'IF'I=H+1'THEN''BEGIN'
```

RATIOSPEC 3 contd.

```
220                 PRINT(RES*HR,3,3);
222                 HR:=HR+DR*4;
223                 I:=I+4;
224                 STR:=DA[I];
225                 'FOR'J:=1'STEP'1'UNTIL'STR'DO'SPACE(1);
227                 WRITETEXT('('*'('C')')');
228               'END' 'ELSE''BEGIN'
228                 STR:=DA[I]+10;
230                 'FOR'J:=1'STEP'1'UNTIL'STR'DO'SPACE(1);
232                 WRITETEXT('('*'('C')')');
233               'END';
234             'END';
235         MISS:'END' OF RESULT LOOP FOR GRAPHICAL OUTPUT ON LINEPRINTER;
236         'END' OF PROCEDURE OUTPUT;
236
236
236           SELECT INPUT(1);  SELECT OUTPUT(2);  ON(23);
240           READTRAP(PSEUDO);
241         'COMMENT' 'AS' ENSURES NO GAPS IN LINEPRINTER GRAPH OF SPECTRUM;
241           SPEC:=READ; D:=READ; MIN:=READ;
244           MAX:=READ; SAM:=READ; D:=READ;
247           RAN:=READ; SET:=READ; PLOT:=READ; PNCH:=READ;
251           'COMMENT' BACKSPEC=2,PLOTSPEC=4,RATIOSPEC=6,SINGLESPEC=8,TOTALSPEC=10,
251             Q(NO. OF BINREAD NOS. TAKEN) MUST BE AN ODD NO. ,
251             SAM=SAMPLING INTERVAL, D=POINTS PER UNIT OF RESOLUTION,RAN=NO. OF
251             RUNS ON ONE TAPE TO BE AVERAGED PER SPECTRUM, MIN AND MAX ARE
251             LIMITS OF SPECTRA, SET = NUMBER OF SPECTRA, PLOT GOVERNS LINEPRINTER
251             OUTPUT-- 1 GIVES NORMAL PLOT, 3 GIVES LOG PLOT, 0 GIVES NO PLOT, 2
251             GIVES NO PLOT FOR BACKGROUND BUT PLOT FOR RATIOED SPECTRA. PNCH
251             GOVERNS TAPE OUTPUT, 7 GIVES TAPE, 0 GIVES NO TAPE, 2 GIVES NO TAPE
251             FOR BACKGROUND BUT TAPES FOR RATIOED SPECTRA;
251           PI:=3.1415927;
252           C:=(Q-1)/2;
253           DR:=PI/(C+1);
254           RES:=10000/SAM/(C+1);
255           CR:=MIN/RES;
256           DR:=1/D;
257           OUT:=ENTIER(D*(MAX-MIN)/RES+1);
258           'COMMENT' OUT IS NO. OF OUTPUT POINTS ON SPECTRUM;
258           'IF'Q>2000'THEN''GOTO'HIGHRES;
259           'IF'RAN=100'THEN''BEGIN'
259             RAN:=1;
261             'GOTO'HIGHRES;
262             'COMMENT' SET RAN=100 FOR LOW RESOLUTION RUN OF A VERY LONG TAPE,
262                       BUT BEWARE USING TOTALSPEC AS RAN IS RESET TO 1;
262           'END';
263           'BEGIN'
263             'REAL''ARRAY' BA,CATQ:C],DA,EA[1:OUT];
263             'INTEGER''ARRAY' AA[0:3000];
264             'IF'SPEC=6'THEN''BEGIN'
265               F:=READ;  'COMMENT' F IS BACKSPEC NO. ;
267               'FOR'I:=1'STEP'1'UNTIL'OUT'DO' EA[I]:=READ;
269             'END''ELSE'F:=0;
270             'FOR'CYCLE:=1'STEP'1'UNTIL'SET'DO''BEGIN'
271               F:=READ; 'COMMENT' F IS SPECTRUM NO.;
273               'FOR'I:=0'STEP'-1'UNTIL'0'DO' BA[I]:=CA[I]:=0;
275               'FOR'PUR:=1'STEP'1'UNTIL'RAN'DO''BEGIN'
276         FEED:   BINREAD(AA);
278               'FOR'I:=0'STEP'-1'UNTIL'1'DO''BEGIN'
279                 FD:=AA[C+1];
```

RATIOSPEC 3 contd.

```
281                 ED:=A/[L-1];
282                 GO:=(COS(PR*I)+1)/2;
283                 BA[I]:=(ED+ED)*GO+BA[I];
284                 CA[I]:=(ED-ED)*GO+CA[I];
285               'END';
286               BA[0]:=BA[C]+BA[0];
287               CA[0]:=0;
288             'END';
289         K=1K: 'IF'RAN>1'THEN''FOR'I:=C'STEP'-1'UNTIL'0'DO''BEGIN'
290               BA[I]:=BA[I]/RAN;
291               CA[I]:=CA[I]/RAN;
292             'END' OF DATA INPUT LOOP;
293             HR:=CP;
294             'FOR'I:=1'STEP'1'UNTIL'OUT'DO''BEGIN'
295               TC:=2*PR*HR;
296               JC:=COS(TC)*2;
297               KC:=SIN(TC);
298               MC:=NC:=PC:=QC:=0;
299               'FOR'A:=C'STEP'-1'UNTIL'0'DO''BEGIN'
300                 LC:=BA[A]+JC*MC-NC;
301                 QC:=CA[A]+JC*PC-QC;
302                 NC:=MC;     MC:=LC;
303                 QC:=PC;     PC:=QC;
304               'END';
305               RC:=BA-JC*NC/2;
306               SC:=KC*QC;
307               DA[I]:=SQRT(RC*RC+SC*SC);
308               HR:=HR+BR;
309             'END' OF CALCULATION OF RESULTS;
310             OUTPUT(9,FA);
311             'IF'SPEC=10'AND'F=0'THEN''BEGIN'
312               'FOR'I:=1'STEP'1'UNTIL'OUT'DO'FA[I]:=DA[I]/SF;
313               F:=F;
314             'END';
315         RECYCLE:'END';
316           'END';  'GOTO'HOME;
317         HIGHRES:USESTORE(9,'('FD')','('COS%WORKFILE')',2,0);
318           K:=1;
319           'IF'SPEC=4'THEN''BEGIN'
320             'REAL''ARRAY'FA[1:OUT];
321             F:=READ;'COMMENT' F IS BACKSPEC NO.
322             'FOR'I:=1'STEP'1'UNTIL'OUT'DO' FA[I]:=READ;
323             PUTARRAY(9,F,FA);
324           'END''ELSE'F:=0;
325           'FOR'CYCLE:=1'STEP'1'UNTIL'SET'DO''BEGIN'
326             C:=READ;
327             'BEGIN'
328               'REAL''ARRAY' BA,CA[0:1000];
329               'INTEGER''ARRAY' AA[0:20000];
330               READARRAY(AA);
331               BA[0]:=AA[C]; CA[0]:=0;
332               B:=5*60;
333               PUTARRAY(9,F,BA,BA[0],BA[B]);
334               PUTARRAY(9,F,CA,CA[0],CA[B]);
335               I:=1;
336         LOOP: 'BEGIN'
337               'FOR'K:=1'STEP'1'UNTIL'5'DO''BEGIN'
338                 'IF'I<C+1'THEN'GOTO'Z;
339                 TC:=BA[C+I];
340                 BA[C+I]
```

RATIOSPEC 3 contd.

```
350                 GD:=(COS(BR*I)+1)/2;
351                 BA[Y]:=(FD+ED)*GD;
352                 CA[Y]:=(FD-ED)*GD;
353                 I:=I+1;
354               'END';
355               PUTARRAY(9,K,BA);
356               PUTARRAY(9,J,CA);
357               'GOTO' LOOP;
358             'END';
359       ZAP:  PUTPART(9,K,BA,BA[1],BA[Y]);
360             PUTPART(9,J,CA,CA[1],CA[Y]);
361         'END' OF ARRAY BUILDING ON DISC;
362         'BEGIN'
362           'REAL''ARRAY'BA,CA[0:C+1];
362           'IF'SPEC=6'OR'SPEC=10'AND'F'NE'0'THEN'K:=OUT+1'ELSE'K:=1;
364           J:=5000;
365           GETARRAY(9,K,BA);
366           GETARRAY(9,J,CA);
367           HR:=PR;  J:=9000;  LVMC:=0;
370           'BEGIN'
370             'REAL''ARRAY'DA[1:100];
370       CALC: 'FOR'I:=1'STEP'1'UNTIL'100'DO''BEGIN'
372               IC:=2*BR*HR;
374               JC:=COS(IC)*2;
375               KC:=SIN(IC);
376               MC:=NC:=PC:=QC:=0;
377               'FOR'A:=C'STEP'-1'UNTIL'0'DO''BEGIN'
378                 LC:=BA[A]+JC*MC-NC;
380                 QC:=CA[A]+JC*PC-QC;
381                 NC:=MC;     MC:=LC;
383                 QC:=PC;     PC:=QC;
385               'END';
386               RC:=MC-JC*NC/2;
387               SC:=KC*QC;
388               DA[I]:=SQRT(RC*RC+SC*SC);
389               'IF'LVMC*100+I=OUT'THEN''GOTO'ZOOM;
390               HR:=HR+DR;
391             'END' OF CALCULATION OF RESULTS;
392             PUTARRAY(9,J,DA);
393             LVMC:=LVMC+1;
394             'GOTO'CALC;
395       ZOOM: PUTPART(9,J,DA,DA[1],DA[I]);
396           'END' OF RESULT BUILDING ON DISC;
397         'END';
398         'BEGIN'
398           'REAL''ARRAY'DA,EA[1:OUT];
398           K:=1;  J:=9000;
401           'IF'SPEC=6'OR'SPEC=10'AND'F'NE'0'THEN'
401           GETARRAY(9,K,EA);
402           GETARRAY(9,J,DA);
403           OUTPUT(DA,EA);
404           'IF'SPEC=10'AND'F=0'THEN''BEGIN'
404             'FOR'I:=1'STEP'1'UNTIL'OUT'DO'EA[I]:=DA[I]/SF;
407             F:=F;  K:=1;
409             PUTARRAY(9,K,EA);
410           'END';
411         'END';
412         'GOTO'RERUN;
413         'COMMENT'RATIOSPEC3 WRITTEN BY DACC DURING 1974. THIS EDITION
413                  COMPILED IN FEB 1975;

413       RERUN:'END';
414       HOME:'END';
```

2. Program THERM.

This program is written in FORTRAN IV for the IBM 1130 computer

```
**      THIS VERSION LOADED ONTO DISC 1900 ON 17/02/76
*ONE WORD INTEGERS
*EXTENDED PRECISION
C
C      PROGRAM THERM
C      THIS PROGRAM CALCULATES THE THERMODYNAMIC FUNCTIONS OF AN IDEAL
C      GAS OVER A RANGE OF SELECTED TEMPERATURES. THE FIRST CALCULATIONS
C      ASSUME THE MOLECULE IS A RIGID ROTOR, BUT A SECOND SET OF
C      CALCULATIONS CAN BE CARRIED OUT WITHOUT A SYMMETRIC TOP, IF THE
C      TORSION IS THE LAST VIBRATIONAL FREQUENCY ENTERED.
C      TORSIONAL BARRIER HEIGHTS AND THERMODYNAMIC CONTRIBUTIONS ARE THEN
C      CALCULATED BY CURVE FITTING AND INTERPOLATION
C
       DIMENSION TP(24),W(48),SA(22),DBA(22),GFE(24),S(24),H(24),HCP(24),
      1  ENTA(24,12),HCPA(24,12),HA(24,12),QF(24),RQF(24),VA(24),XA1(24),
      2  XA2(24),XA3(24),YA(24),RESA(24,12),DATA(24),VDA(24),GFET(24),
      3  ST(24),HT(24),HCPT(24)
       COMMON MX,MY
       READ(2,2)  (XA1(I),I = 1,24)
       READ(2,2)  (XA2(I),I = 1,24)
       READ(2,2)  (XA3(I),I = 1,24)
       READ(2,2)   (YA(I),I = 1,24)
     2 FORMAT(12F6.2)
       DO 3 I = 1,24
     3 READ(2,6) (HCPA(I,J),J=1,12)
       DO 4 I = 1,24
     4 READ(2,6)   (HA(I,J),J=1,12)
       DO 5 I = 1,24
     5 READ(2,6) (ENTA(I,J),J=1,12)
     6 FORMAT(12F6.4)
       DO 7 I = 1,22
     7 READ(2,8) DBA(I),SA(I)
     8 FORMAT(F6.3,F6.0)
       PI = 3.1415928
       MX # 5
       MY # 2
       READ(2,10) LOT
    10 FORMAT(I2)
    20 READ(2,30)
       READ(2,35)
       WRITE(5,31)
    31 FORMAT(1H1)
    30 FORMAT('   THIS    IS    THE    HEADER    LENGTH    EXPECTED  HERE ')
    35 FORMAT('  AND    THIS     IS     THE     SECOND     CARD       HERE ')
       WRITE(5,30)
       WRITE(5,35)
C
C      LOT IS TOTAL NUMBER OF RUNS AND IS PUNCHED IN COLUMNS 1-2
C      FOR EACH PROBLEM (PROBLEMS CAN BE STACKED) THERE FOLLOWS
C        CARD 1 USER INFORMATION
C        CARD 2 USER INFORMATION
C        CARD 3  MODE,1 FOR RIGID ROTOR, 2 IF TORSION PRESENT  (COLUMN) 1
C                ISIGMA, NUMBER OF EQUIVALENT ORIENTATIONS OF THE
C                              MOLECULE IN SPACE                    2-3
C                WT, MOLECULAR WEIGHT IN GRAMS          F12.6       4-15
C        CARD 4  PMS, SMALLEST PRINCIPLE MOMENT OF INERTIA           1-12
C                PMM, MEDIUM              ''            F12.6       13-24
C                PML, LARGEST             ''                        25-36
C                ALL IN UNITS OF 10**-39 GM.CM**2
C        CARD 5  NT,  NUMBER OF SPECIFIED TEMPERATURES               1-2
C                NW,  NUMBER OF VIBRATIONAL FREQUENCIES              3-4
C
C        CARDS 6 ONWARDS
C         TEMPERATURES IN F8.2 FORMAT     9 TO A CARD
C         FREQUENCIES IN F8.1 FORMAT      9 TO A CARD
C
```

```
      READ(2,40) MODE, ISIG1, WT
   40 FORMAT(I1,I2,F12.6)
      READ(2,45) PMS,PMM,PML
   45 FORMAT(3F12.6)
      READ(2,50) NT,NW
   50 FORMAT(2I2)
      READ(2,60) (TP(I),I=1,NT)
   60 FORMAT(9F8.2)
      READ(2,70) (W(I),I=1,NW)
   70 FORMAT(9F8.1)
      WRITE(5,80)
   80 FORMAT(//31HO PRINCIPAL MOMENTS OF INERTIA )
      WRITE(5,81)
   81 FORMAT(39HO               UNITS OF 10**-39 GM.CM**2)
      WRITE(5,85) PMS
      WRITE(5,85) PMM
      WRITE(5,85) PML
   85 FORMAT(5X,F12.6)
      WRITE(5,90)
   90 FORMAT(//31HO FUNDAMENTAL FREQUENCIES, CM-1)
      WRITE(5,100) (W(I),I=1,NW)
  100 FORMAT (8F10.1)
      WRITE(5,110) NW
  110 FORMAT (35HO NUMBER OF FREQUENCIES SUPPLIED = I2)
      IF(MODE-1) 140,120,140
  120 JOB = 1
      WRITE(5,130)
  130 FORMAT(//19HO RIGID ROTOR MODEL)
      GO TO 160
  140 JOB = 2
      WRITE(5,150)
  150 FORMAT(//33HO RIGID ROTOR MODEL MINUS TORSION)
      NW=NW-1
  160 WRITE(5,170)
  170 FORMAT (/9X'TEMP'8X'GIBBS F.E.'8X'ENTHALPY'7X'HEAT CAPACITY'7X'ENT
     1ROPY'/)
      D=PMS*PMM*PML
      SIG1=ISIG1
      DO 199 I=1,NT
      SH = 0.0
      SG = 0.0
      SC = 0.0
      DO 180 J=1,NW
       U = 1.43879*W(J)/TP(I)
       V = EXP(U)-1
      WW = 1-1/EXP(U)
      SH = SH+U/V
      SG = SG+ALOG(WW)
  180 SC = SC+(U*U*EXP(U))/(V*V)
      GFE(I) = 12.47150*ALOG(WT)+33.25732*ALOG(TP(I))+4.15717*ALOG(D)
     1       -8.31433*ALOG(SIG1)-43.0867-8.31433*SG
        H(I) = 33.25732+8.31433*SH
      HCP(I) = 33.25732+8.31433*SC
        S(I) = GFE(I)+H(I)
      WRITE(5,190) TP(I),GFE(I),H(I),HCP(I),S(I)
  190 FORMAT(7X,F7.2,4(7X,F10.6))
      GFEC = GFE(I)/4.184
        HC =   H(I)/4.184
      HCPC = HCP(I)/4.184
        SC =   S(I)/4.184
  199 WRITE(5,200) GFEC,HC,HCPC,SC
  200 FORMAT(21X,4(F10.6,7X))
      IF(JOB-2) 220,210,220
  210 NW=NW+1
      GO TO 240
  220 IF(MODE-1)910,910,240
  240 READ(2,250) NORM
  250 FORMAT (I1)
```

```
C
C     THE THREEFOLD METHYL BARRIER HEIGHT IS NOW CALCULATED. IF NORM IS
C     2 THEN OTHER VALUES OF AN3(H-C-C ANGLE OF METHYL GROUP) AND CH
C     (C-H BOND LENGTH) TO BE INPUT. AN4 IS ANGLE BETWEEN TOP AND
C     SMALLEST MOMENT PMS. ISIGMA2 IS ROTATION SYMMETRY OF TOP. RM IS
C     REDUCED MOMENT OF INERTIA
C
      IF(NORM-1) 270,260,270
  260 AN3 = 109.47
       CH = 1.090
      GO TO 290
  270 READ(2,280) AN3,CH
  280 FORMAT (F6.2,F6.3)
  290 READ(2,300) AN4
  300 FORMAT (F6.2)
      ISIG2 = 3
      AN5 = (180-AN3)*PI/180
      XMI = 3.0*0.16738*((CH*SIN(AN5))**2)
      RMI = XMI*(1-XMI*(COS(PI*AN4/180.0)**2)/PMS-XMI*(COS(PI*(AN4-90.0)
     */180.0)**2)/PMM)
        F =2.79907/RMI
      DB = W(NW)/(2.25*F)
      WRITE(5,310)
  310 FORMAT (///1X'PARAMETERS USED IN BARRIER HEIGHT CALCULATION')
      WRITE(5,320) CH,AN3
  320 FORMAT (1X'C-H BOND LENGTH = 'F5.3/1X'H-C-C BOND ANGLE = 'F6.2)
      WRITE(5,330) AN4
  330 FORMAT (1X'ANGLE BETWEEN SMALLEST MOMENT AND TOP = 'F6.2)
      WRITE(5,340) XMI,RMI
  340 FORMAT (1X'MI OF TOP = 'F8.6/1X'REDUCED MOMENT OF INERTIA = 'F8.6)
      WRITE(5,350) F
  350 FORMAT (1X'F VALUE IS = 'F9.6)
C
C     CALCULATION OF THE THREEFOLD BARRIER HEIGHT IS NOW PERFORMED USING
C     SUBROUTINE INTER.
C
      DATA(1)/ # DB
      DO 360 I = 2,24
  360 DATA(I) = 0.0
      CALL INTER(1,4,22,1,DBA,SA,RESA,DATA)
      SVAL = RESA(1,1)
      WRITE(5,380) DB
  380 FORMAT (1X'MATHIEU FUNCTION EIGENVALUE DB = 'F7.4)
      WRITE(5,390) SVAL
  390 FORMAT (1X'MATHIEU EQUATION PARAMETER  S  = 'F7.4)
C     THE ABOVE PROCEDURE IS BY LOG-LOG INTERPOLATION INTO DB VERSUS S
      V3 = 2.250*SVAL*F
      WRITE(5,400)
  400 FORMAT (/1X'THREEFOLD BARRIER HEIGHT')
      WRITE(5,410) V3
  410 FORMAT (10X'V3 = 'F9.4' CM-1')
      V3 = V3*0.01196255
      WRITE(5,420) V3
  420 FORMAT (10X'V3 = 'F9.4' KJ.MOL-1')
      V3 = V3/4.184
      WRITE(5,425) V3
  425 FORMAT (10X'V3 = 'F9.4' KCAL.MOL-1')
      WRITE(5,430)
  430 FORMAT (///5X'PARTION FUNCTION FOR FREE ROTATION')
      WRITE(5,440)
  440 FORMAT (6X'TEMP'12X'QF'11X'1/QF'11X'V/RT')
      DO 445 I=1,NT
       QF(I) = 0.9310*SQRT(RMI*TP(I)/10)
      RQF(I) = 1/QF(I)
      VA(I) = V3*1000.0/(TP(I)*1.9872)
  445 WRITE(5,450) TP(I),QF(I),RQF(I),VA(I)
  450 FORMAT (4X,F7.2,7X,F8.5,7X,F8.6,8X,F8.6)
C
C     CONTRIBUTIONS TO THERMODYNAMIC PARAMETERS DUE TO THE THREEFOLD
C     BARRIER ARE CALCULATED USING A SPECIAL INTERPOLATION SUBROUTINE
C     INTER DEVELOPED BY DACC WHICH IS USED TO INTERPOLATE VERTICALLY
C     INTO COLUMNS OF TABLES AND THEN AGAIN INTO THE RESULTING ROWS.
C     COLUMNS NOT FITTED TO LESS THAN + OR - 2 PERCENT TOLERANCE BY
C     INTER ARE SKIPPED BY THE (J-N) TEST.
C
```

```
      K = 1
      DO 466 J = 1,12
      DO 460 I = 1,24
  460 VDA(I) = HCPA(I,J)
      CALL INTER(K,7,24,NT,YA,VDA,RESA,VA)
      K = K + 1
  466 CONTINUE
      DO 490 I = 1,NT
      DO 480 J = 1,12
  480 VDA(J) = RESA(I,J)
      CALL INTER(I,7,12,1,XA1,VDA,RESA,RQF)
      HCPT(I)= RESA(1,I)*4.184
  490 HCP(I) = HCP(I) + HCPT(I)
      K=1
      DO 510 J = 1,11
      DO 500 I = 1,24
  500 VDA(I) =  HA(I,J)
      CALL INTER(K,7,24,NT,YA,VDA,RESA,VA)
      K = K + 1
  510 CONTINUE
      DO 530 I = 1,NT
      DO 520 J = 1,11
  520 VDA(J) =RESA(I,J)
      CALL INTER(I,5,11,1,XA2,VDA,RESA,RQF)
       HT(I) = RESA(1,I)*4.184
  530   H(I) =   H(I) + HT(I)
      K = 1
      DO 550 J = 1,11
      IF(J-3) 534,550,534
  534 IF(J-6) 535,550,535
  535 DO 540 I = 1,24
  540 VDA(I) =ENTA(I,J)
      CALL INTER(K,7,24,NT,YA,VDA,RESA,VA)
      K = K + 1
  550 CONTINUE
      DO 570 I = 1,NT
      DO 560 J = 1,9
  560 VDA(J) =RESA(I,J)
      CALL INTER(I,7,9,1,XA3,VDA,RESA,RQF)
       ST(I) = 8.31433*(0.5+ALOG(QF(I)))-RESA(1,I)*4.184
  570   S(I) =   S(I) + ST(I)
      DO 580 I = 1,NT
      GFET(I)=  ST(I) - HT(I)
  580 GFE(I) =   S(I) - H(I)
      WRITE(5,585)
  585 FORMAT(///10X' TORSIONAL CONTRIBUTIONS')
      WRITE(5,170)
      DO 586 I = 1,NT
  586 WRITE(5,190) TP(I),GFET(I),HT(I),HCPT(I),ST(I)
      WRITE(5,590)
  590 FORMAT(//54HO RIGID ROTOR MODEL WITH TORSIONAL CONTRIBUTIONS ADDED
     1)
      WRITE(5,170)
      DO 900 I = 1,NT
      WRITE(5,190) TP(I),GFE(I),H(I),HCP(I),S(I)
      GFEC = GFE(I)/4.184
        HC =   H(I)/4.184
      HCPC = HCP(I)/4.184
        SC =   S(I)/4.184
      WRITE(5,200) GFEC,HC,HCPC,SC
  900 CONTINUE
C
C     THIS PROVIDES OUTPUT ON CARDS IN S.I. UNITS SUITABLE FOR INPUT
C     INTO PROGRAM MIX
C
      READ(2,903)
  903 FORMAT(' DUMMY READ TO LOAD PUNCH  ')
      WRITE(2,30)
      WRITE(2,35)
      DO 905 I = 1,NT
  905 WRITE(2,906) TP(I),GFE(I),H(I),HCP(I),S(I)
  906 FORMAT(5F12.6)
  910 LOT = LOT - 1
      IF(LOT) 920,920,20
  920 CALL EXIT
      END
```

3. Program MIX

This program is written in FORTRAN IV for the IBM 1130 computer.

```
PAGE    2                  THIS VERSION COMPILED ON 14/09/76

C                                                       D.COMPTON     SCIENCE
C       PROGRAM MIX                                                              MIX   10
C       THIS CALCULATES THE THERMODYNAMIC FUNCTIONS OF A MIXTURE OF              MIX   20
C   CONFORMERS OVER A RANGE OF TEMPERATURES USING A MODEL WITH EITHER            MIX   30
C   S-CIS (MODE = 1) OR 2 GAUCHE CONFORMERS (MODE = 2) OR BOTH (MODE = 0)        MIX   40
C       1 REFERS TO THE LOW ENERGY (S-TRANS) CONFORMER.                          MIX   50
C                                                                                MIX   60
        DIMENSION TA(30),GA1(30),GA2(30),GA3(30),HA1(30),HA2(30),HA3(30),        MIX   70
       1  CA1(30),CA2(30),CA3(30),SA1(30),SA2(30),SA3(30)                        MIX   80
        R = 8.31433                                                              MIX   90
        READ (2,5) N                                                             MIX   91
      5 FORMAT(I2)                                                               MIX   92
        DO 180 J=1,N                                                             MIX   93
        WRITE(5,10)                                                              MIX  100
     10 FORMAT(1H1)                                                              MIX  110
        READ (2,20)                                                              MIX  120
        WRITE(5,20)                                                              MIX  130
     20 FORMAT('    THIS      IS     THE       TITLE          POSITION    HERE ') MIX  140
C                                                                                MIX  150
C       CARD 1 USER INFORMATION                                                  MIX  160
C       CARD 2 NT, NUMBER OF TEMPERATURES  USED                (COLUMN) 1-2      MIX  170
C              TYPE, 1 IF S-CIS FORM OR 2 IF GAUCHE                      3-4     MIX  180
C            DHO DIFFERENCE IN ENTHALPY BETWEEN CONFORMERS, ALLOWING FOR         MIX  190
C            CONTRIBUTION FROM DHO = DH - T*(CP2-CP1)          F12.6    5-17     MIX  191
C       CARD 3 ONWARDS   IN F12.6 FORMAT  T,G,H,C,S   ALL CARDS FOR              MIX  200
C              LOW ENERGY CONFORMER FIRST                                        MIX  210
C                                                                                MIX  211
        READ (2,30) NT,MODE,DH                                                   MIX  220
     30 FORMAT(2I2,F12.6)                                                        MIX  230
        DO 40 I=1,NT                                                             MIX  240
     40 READ (2,50) TA(I),GA1(I),HA1(I),CA1(I),SA1(I)                            MIX  250
     50 FORMAT(5F12.6)                                                           MIX  260
        DO 60 I=1,NT                                                             MIX  270
        READ (2,70) TEMP ,GA2(I),HA2(I),CA2(I),SA2(I)                            MIX  280
        IF (TEMP-TA(I)) 65,60,65                                                 MIX  281
     60 CONTINUE                                                                 MIX  282
        GO TO 71                                                                 MIX  283
     65 WRITE(5,66)                                                              MIX  284
     66 FORMAT(///'   ERROR IN DATA CARDS,   JOB ABANDONED  ')                   MIX  285
        GO TO 180                                                                MIX  286
     70 FORMAT(5F12.6)                                                           MIX  290
     71 WRITE(5,80)                                                              MIX  300
     80 FORMAT(///9X'TEMP'8X'GIBBS F.E.'8X'ENTHALPY'7X'HEAT CAPACITY'7X          MIX  310
       1'ENTROPY'11X'X2'/)                                                       MIX  320
        DO 90 I=1,NT                                                             MIX  330
        IF (MODE-1) 81,81,82                                                     MIX  331
     81 DG = DH - TA(I)*(GA2(I)-GA1(I))                                          MIX  341
        GO TO 83                                                                 MIX  342
     82 DG = DH - TA(I)*(GA2(I)-GA1(I))-R*TA(I)*ALOG(2.0)                        MIX  343
     83 EK = EXP(-DG/(R*TA(I)))                                                  MIX  350
        X2 = 1.0/(1.0/EK+1.0)                                                    MIX  360
        X1 = 1.0 - X2                                                            MIX  370
        IF (MODE-1) 84,84,85                                                     MIX  371
     84 SA3(I) = X1*SA1(I)+X2*SA2(I)-R*(X1*ALOG(X1)+X2*ALOG(X2))                 MIX  380
        GO TO 86                                                                 MIX  381
     85 SA3(I) = X1*SA1(I)+X2*SA2(I)-R*(X1*ALOG(X1)+X2*ALOG(X2/2.0))             MIX  382
     86 CA3(I) = X1*CA1(I)+X2*CA2(I)+(X1*X2/R)*(DH/TA(I)+HA2(I)-HA1(I))**2       MIX  390
        HA3(I) = X1*HA1(I)+X2*(DH/TA(I)+HA2(I))                                  MIX  400
        GA3(I) = SA3(I)-HA3(I)                                                   MIX  410
     90 WRITE(5,100) TA(I),GA3(I),HA3(I),CA3(I),SA3(I),X2                        MIX  420
    100 FORMAT(6X,F7.2,7X,4(F10.6,7X),F7.5)                                      MIX  430
        WRITE(5,110) DH                                                          MIX  440
    110 FORMAT(///'   ENTHALPY DIFFERENCE BETWEEN CONFORMERS WAS 'F7.1)         MIX  450
        IF(MODE-1) 120,120,140                                                   MIX  460
    120 WRITE(5,130)                                                             MIX  470
    130 FORMAT('    MODEL USED S-TRANS AND  S-CIS CONFORMERS')                   MIX  480
        GO TO 160                                                                MIX  481
    140 WRITE(5,150)                                                             MIX  490
    150 FORMAT('    MODEL USED S-TRANS AND GAUCHE CONFORMERS')                   MIX  500
    160 IF (MODE-1) 170,180,180                                                  MIX  510
    170 MODE = 2                                                                 MIX  515
        GO TO 71                                                                 MIX  520
    180 CONTINUE                                                                 MIX  530
        CALL EXIT                                                                MIX  531
        END                                                                      MIX  540
```

D. Courses Attended.

Courses and conferences attended by the Candidate as part fulfilment of the requirements for a C.N.A.A. higher degree.

1. M.Sc. course in Molecular Spectroscopy. Approximately 60 hours of the lecture program were attended.
2. Introduction to Algol Programming (8 hours).
3. Electronics and Instrumentation for Research Students (6 hours).
4. Seminars given by both external and internal speakers were attended at both colleges, and the candidate presented lectures on his work in both colleges. (50 hours).
5. The 4th International Conference on Raman Spectroscopy at Brunswick, Maine, U.S.A. was attended in August, 1974 (1 week).
6. The Candidate acted as experiment tutor on the Advanced Spectroscopy Course held at Kingston Polytechnic in June, 1975 (1 week.)
7. Meetings of the Infrared and Raman Discussion Group were attended at various colleges (30 hours). The programme for the 83rd I.R.D.G. meeting is shown overleaf.

INFRARED AND RAMAN DISCUSSION GROUP -

The 83rd meeting of the Group will be held at The Polytechnic of Wales, Pontypridd, on Monday 4 April and Tuesday 5 April 1977, in Room H 39.

Details of location are given overleaf. Members and guests may attend on either or both days by returning the enclosed form to Mr. I.A.Degen, Hon. Treasurer.

PROGRAMME

Monday 4 April - TRACE METHODS OF ANALYSIS

1100 - 1130 - C O F F E E

1130 - 1230 - W.G.Fateley (Kansas State University)
"Trace Methods by Interferometry"

1240 - 1245 - Group Business

1300 - 1415 - L U N C H

1430 - 1500 - W.O. George (The Polytechnic of Wales)
"Trace Methods by Infrared"

1510 - 1540 - R. Bent (Yarsley Testing Laboratories)
"Trace Analysis of Gases from Decomposition of Plastics"

1550 - 1620 - K. Golding (Wilks Scientific Limited)
"Analysis of Trace Contaminants in Aviation Breathing Oxygen using a Microcomputer Controlled Gas Analyser"

1630 - 1700 - J.K. Corbett (Chemical Inspectorate R.O.F.)
"Pressure Effects in Infrared Trace Gas Analysis"

Tuesday 5 April - STRUCTURE AND CONFORMATIONAL STUDIES

0900 - 0930 - C O F F E E

0930 - 1030 - R.D. Gillard (University College Cardiff)
"Aspects of Optical Rotatory Dispersion and Circular Dichroism"

1040 - 1110 - A.J. Barnes (University of Salford)
"Conformational Isomerism by Matrix Isolation"

1120 - 1150 - N.L. Owen (University College North Wales, Bangor)
"Infrared and Microwave Studies of Vinyl Mercaptan"

1200 - 1230 - D.A.C.Compton (The Polytechnic of Wales)
"Spectroscopic and Thermodynamic Studies of Substituted Butadienes

1240 - 1245 - Group Business

1300 - 1415 - L U N C H

1430 - 1500 - H. Elliott (The Polytechnic of Wales)
"The Vibrational Spectra of Silicon Nitride Ceramics"

1510 - 1540 - S. Wild (The Polytechnic of Wales)
"Infrared and X-ray Studies of β-Sialons"

1550 - 1620 - L.T.H. Ferris and T. Jenkins (University College Cardiff)
"Raman Spectra in Phase Transitions of Coloured Compounds"